STRUCTURAL GEOMETRY OF THRUST SYSTEM IN THE RED OAK AND TALIHINA QUADRANGLES, LATIMER AND LEFLORE COUNTIES, ARKOMA BASIN, SOUTHEASTERN OKLAHOMA

By

SYED YAWAR MEHDI
Bachelor of Science
University of Karachi
Karachi, Pakistan
1989

Master of Science
University of Karachi
Karachi, Pakistan
1991

Submitted to the Faculty of the
Graduate College of the
Oklahoma State University
In partial fulfillment of the
requirements for
the Degree of
MASTER OF SCIENCE
May, 1998

STRUCTURAL GEOMETRY OF THRUST SYSTEM IN THE RED OAK AND TALIHINA QUADRANGLES, LATIMER AND LEFLORE COUNTIES, ARKOMA BASIN, SOUTHEASTERN OKLAHOMA

Thesis Approved:

Dean of Graduate College

Acknowledgement

The completion of this work is a direct result of the love, inspiration and support of many people. Time and space prohibits the acknowledgement of them all by name.

I wish to express my sincere appreciation to my advisor, Dr. Ibrahim Cemen, for his consistent supervision, helpful guidance, encouragement, support, and genuine friendship throughout the graduate program. My heartfelt appreciation is also extended to my thesis committee members Dr. Zuhair Al-Shaieb and Dr. Gary Stewart for agreeing to serve in my thesis committee and for their indispensable assistance, friendship and encouragement during this study. Dr. Zuhair Al-Shaieb is due special appreciation for his extensive financial supports, assistance in interpretation of my petrographic data, and also for allowing me to use the facilities available in the geochemistry lab. I really enjoyed working with Dr. Al-Shaieb both as a research assistant and teaching assistant.

I wish to express gratitude to a few of my former fellow geology students, Catherine Price, Jeff Ronck and Justin Evans, and my current geology friends, Phebe Deyhim, Paul Blubaugh and Chin Fong Yang for always being there when I needed words of encouragement, a shoulder to lean on, a listening ear or an extra hand to assist.

This acknowledgement would be incomplete without mentioning special thanks to Dr. Jim Puckette for his non-stop help, encouragement, friendship and positive advice throughout my graduate studies. Thank you Jim.

Thanks are due to my elder brother Syed Arzoo Mehdi and his family for constant encouragement and guidance. I would also like to appreciate the love and encouragement

given to me by my entire family members. Thanks are also due for my roommate Asif Moyeen for the moral support he gave me in times of difficulties during this study.

Last and most importantly, my thanks to my mom and dad as without their continued support, encouragement, prayers, and love throughout my life this would not have been possible.

TABLE OF CENTENTS

LIST OF FIGURES

Figure Page

CHAPTER I

INTRODUCTION

The Arkoma basin and the Ouachita Mountains are located in southeastern Oklahoma and western Arkansas (Figure 1). They were formed during the Late Paleozoic Ouachita orogeny. The Arkoma Basin is considered a foreland basin that developed as a result of compressional tectonics that formed the Ouachita Mountains, and is marked by gentle folds with minor faulting, due to mild compressions. The Ouachitas, on the basis of structural geology and stratigraphy, are classified into three separate assemblages: the frontal belt, the central belt, and Broken Bow uplift.

The Frontal belt is bounded to the north by the surface exposure of the Choctaw Fault and to the south by the Winding Stair Fault. This belt is characterized by imbricately thrusted, folded and tilted shallow-water Morrowan sedimentary rocks to Atokan turbidite facies. The central belt is characterized by broad synclines separated by narrow anticlines. Mississippian and Lower Pennsylvanian turbidites are exposed almost throughout the belt. The Broken Bow Uplift is composed of Lower Ordovician to Lower Mississippian marine strata. Rocks are isoclinally folded as well as thrusted in this uplift (Suneson and others, 1990).

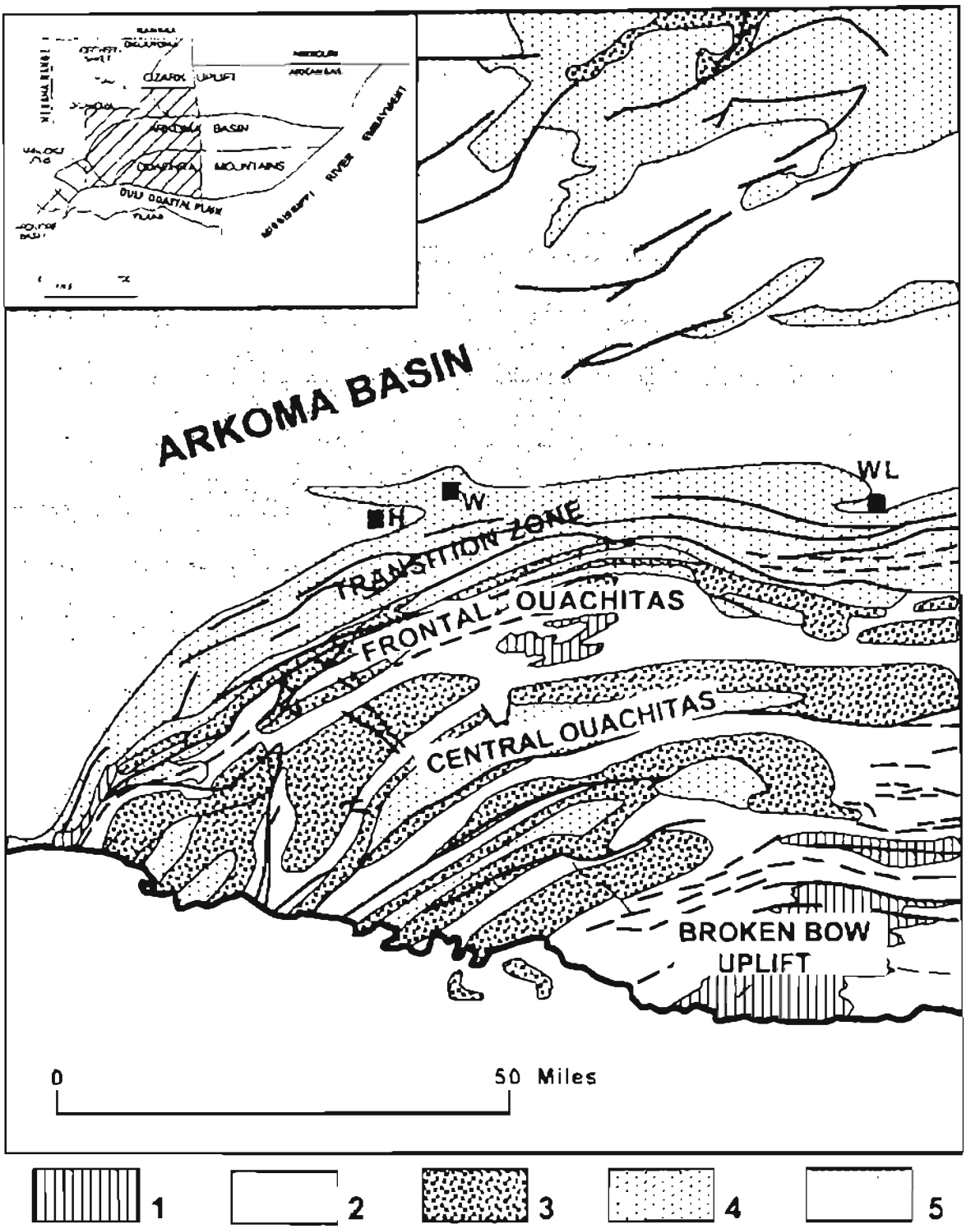

Figure 1: Simplified geologic map of the Ouachita Mountains in southeastern Oklahoma. Explanations: (1) Early and middle Paleozoic (Cambrian through Early Mississippian); (2) Middle and late Mississippian (Stanley Group of Ouachita facies); (3) Morrowan (Jackfork Group and Johns Valley Formations of Ouachita facies); (4) Atokan (Spiro/Wapanucka; and Atoka formation of the Frontal Ouachita and Arkoma basin); (5) Desmoinesian (Hartshorne, McAlester, Savana and Boggy Formations of the Krebs Group of the Arkoma basin. Simplified map on the upper left corner shows the location of the map area. Abbreviations: H=Hartshorne; W=Wilburton; and WL=Wister Lake.

The northern boundary of the Arkoma basin is the Ozark Uplift, whereas the southern boundary is defined by the surface trace of the Choctaw Fault. The eastern boundary lies in central Arkansas under the Cretaceous and Tertiary cover of the Gulf Coast and Mississippi Embayment.

STATEMENT OF PURPOSE

The study area covers the Red Oak and Talihina Quadrangles (U.S. Geological Survey, 1988 and 1989, respectively) (Figure 2), which includes parts of Latimer and LeFlore Counties (T3N-T6N, R21E-R22E). The main purpose of this study is to delineate the structural geometry of the Late Paleozoic thrust system present in Red Oak and Talihina quadrangles. This includes:

1. defining and illustrating the main detachment surfaces;
2. depicting the structural geometry of thrusting along the frontal edge of the Ouachita fold-thrust belt;
3. establishing the geometry and structural positioning of the duplex in the footwall of the Choctaw Fault zone;
4. characterizing the petrographic features of the lower Atokan Spiro Sandstone;
5. establish the relationship between the deformation bands and porosity within the lower Atokan Spiro Sandstone.

METHODS OF INVESTIGATION

In order to accomplish the main objective of this study, the following information was used to construct the balanced cross sections:

1. A simplified geological map of the study area is prepared from the surface geology mapped by Neil Suneson, C.A.Ferguson, and LeRoy Hemish.

2. Spontaneous potential (SP), gamma ray, induction, and resistivity/conductivity logs obtained from Oklahoma City Geological Society and Tulsa Log Libraries are examined to locate and understand the log signatures of the Spiro, Red Oak, Panola, and Cecil sandstones. These units are most widely recognizable and are important in delineating the thrust system of the study area, and were extensively used in constructing the balanced cross-sections.
3. Scout tickets obtained from the above mentioned log libraries as well as OSU Log Library were examined to corroborate the interpretations from the wire line well logs.
4. Reflection seismic lines donated by EXXON and AMOCO oil companies were used to understand the subsurface structural geology. Most seismic lines that are used in this study are at high angles to the axes of the major structural features of the area.
5. Five balanced cross-sections were constructed to delineate the thrust geometry in the study area (Plate I through V).
6. Restoration was performed to all the balanced cross-sections using the key-bed restoration method in order to establish the amount of shortening due to thrusting in the study area.
7. 29 thin-sections from two outcrops and one core were analyzed to determine sediment type, possible source, diagenetic changes, porosity and depositional environment.

In order to yield the most accurate geometry in the study area, all the structural cross-sections were constructed parallel to the tectonic transport direction which is assumed to be perpendicular to the axes of the major thrust faults. In the study area, this is approximately south to north. The horizontal scale of the cross-sections is 1"=2,000' and the vertical scale is 1"=1,000'.

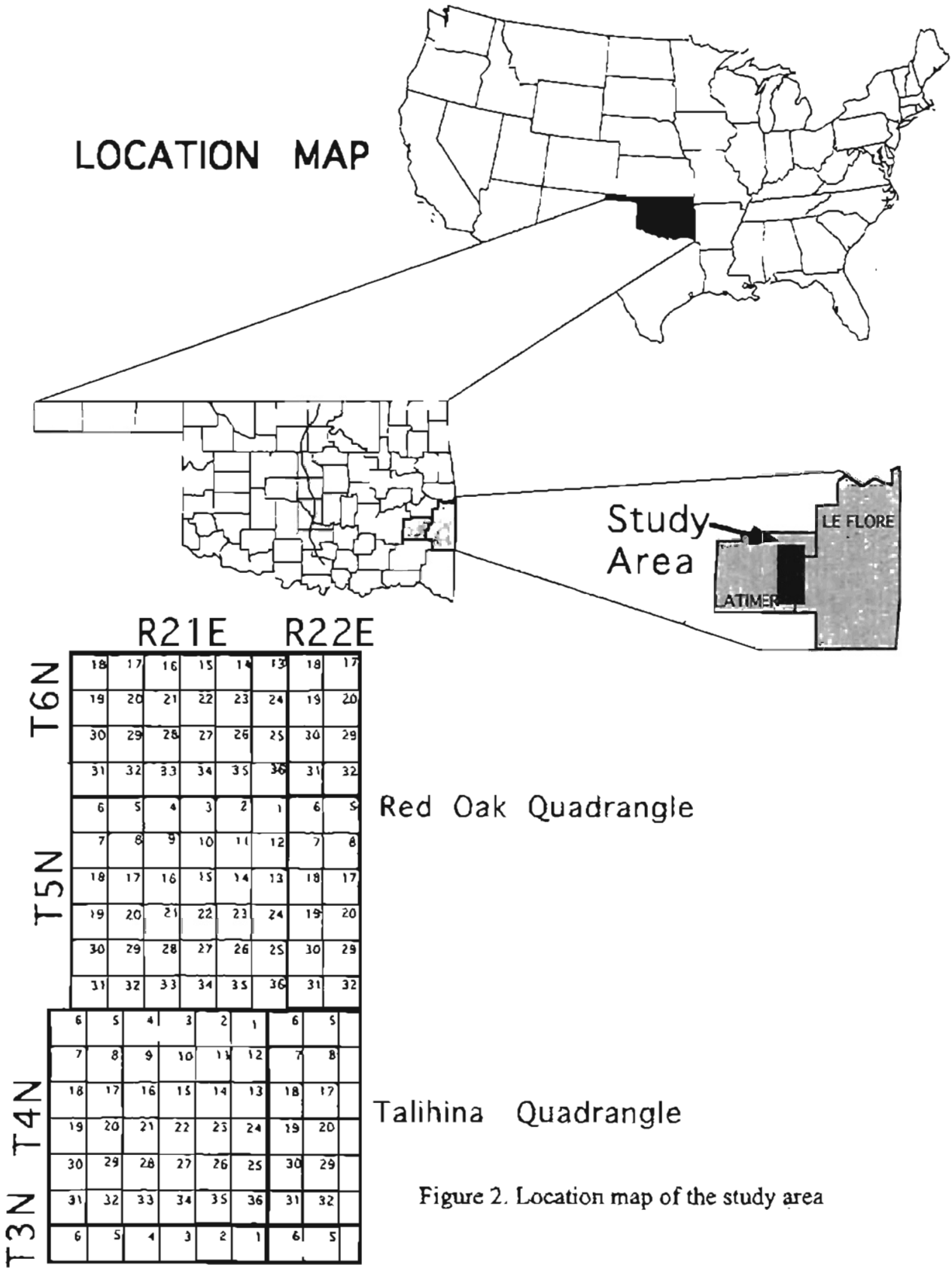

Figure 2. Location map of the study area

All the wells used during the study for the purpose of construction of cross-sections were assumed to be vertically drilled unless indicated otherwise by available data. Deviated wells were plotted to determine the surface and bottom hole locations. If no true vertical depths (TVD) conversions were given, then the approximate vertical depths to stratigraphic intervals within deviated borehole were deviated by simple geometry illustrated in Figure 3. Only structural "tops" were used in constructing the balanced cross-section. The Spiro Sandstone represented on the cross-sections includes the Morrowan Wapanucka Limestone.

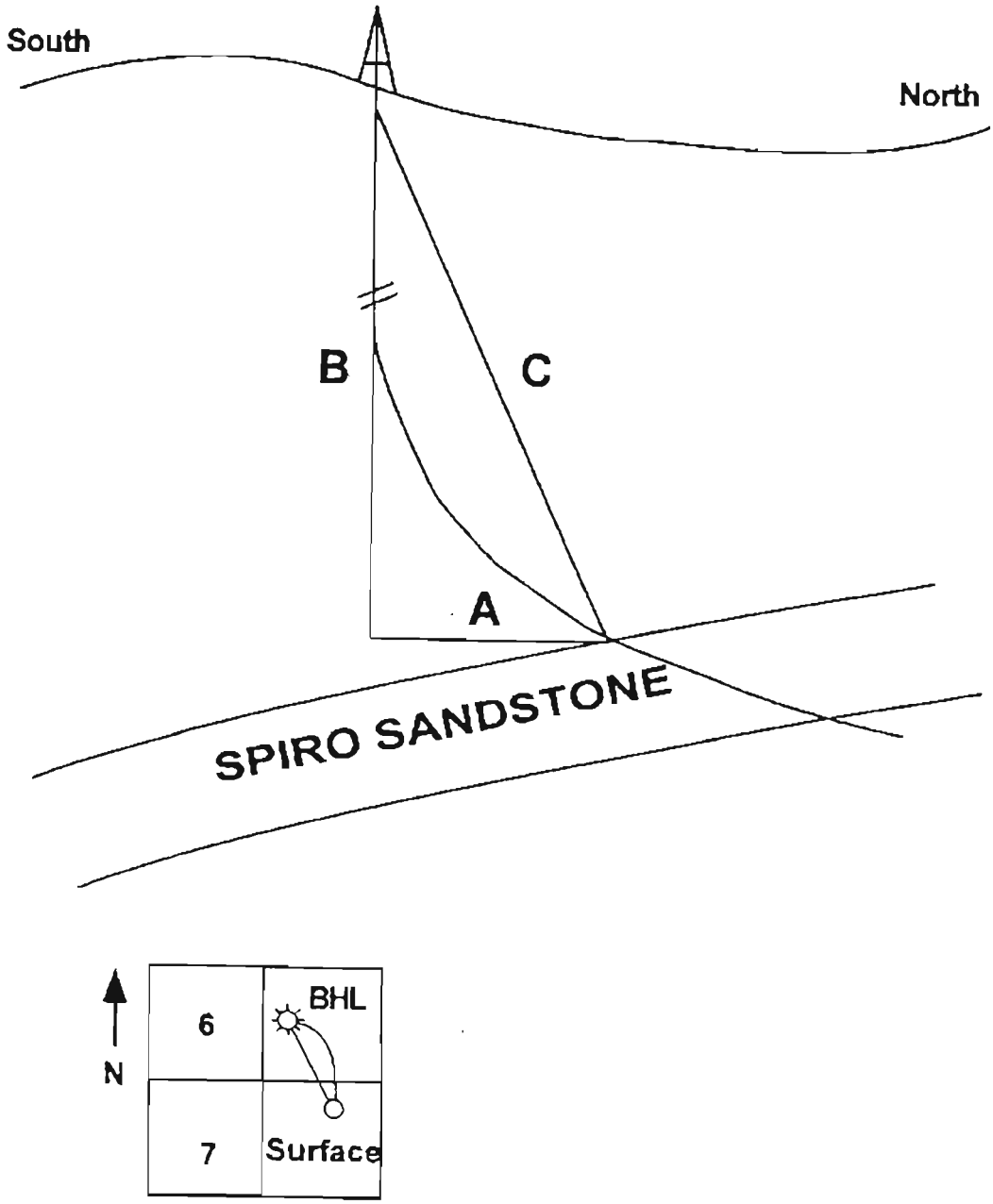

Figure 3. Simplified model for figuring depth in deviated wells.

CHAPTER II

GEOLOGICAL SETTING

Tectonics of Arkoma basin and Ouachita Mountains

The Arkoma basin (fig 1) has been referred to as the Arkansas-Oklahoma coal basin," the "Arkansas Valley basin," and the McAlester basin" (Branan, 1968). Geologists of the two states, over the years, have adopted the name "Arkoma basin" for the sake of clarity in the literature. Straddling the Arkansas-Oklahoma border, the Arkoma Basin extends about 100 miles east of Fort Smith, Arkansas, and curves another 120 miles southwest into Oklahoma. North to south, the basin ranges from 20-50 miles wide. The deepest part of this arcuate trough is adjacent to the Ouachita mountain system where the sedimentary column is estimated to be 30,000' thick (Branan, 1968).

The Arkoma basin formed during the Ouachita orogeny. Several plate tectonic models have been proposed for the formation of the Ouachita fold-thrust belt. Keller and Cebull (1973) proposed a cordilleran model suggesting a north-dipping subduction zone and presence of a mobile core. Roeder (1973) suggested a late orogenic flip of the subduction zone from north-dipping to south-dipping. The most widely accepted model, however, is a collision model with a south-dipping subduction zone. This model is supported by Morris (1974), Brigg and Roeder (1975), Graham and others (1976), Wickham, Roeder, and Briggs (1976), and Houseknecht and Kacena (1983) and appears

to fit the present geological data. Below is a summary of this model taken mainly from Houseknecht and Kacena (1983).

In late Proterozoic or early Paleozoic rifting occurred that resulted in the opening of a proto-Atlantic (Iapetus) ocean basin (Fig 4a). Following this initial rifting, the southern margin of the North American craton became a passive margin that continued to receive sediments through early and middle Paleozoic (Fig 4b). During that time interval, a classic shelf-slope-rise geometry evolved. Shelf facies are predominately carbonates with lesser amounts of shale and quartzose sandstone and are referred to as the Arbuckle facies. Off-the –shelf facies include dark colored shales with smaller amounts of limestone, sandstone, and bedded chert and are collectively called the Ouachita facies (Houseknecht, 1986).

In Devonian or Early Mississippian, a southward-dipping subduction developed and the ocean basin began to close (Fig 4c), however the continental margin remained stable. During early Atokan time (Figure 4d), the ocean basin was consumed and the subduction complex moved northward onto the continental margin. Due to the northward movement of the subduction complex and subduction of the continental margin, flexural bending of the continental crust resulted in the formation of normal faults. These faults, which offset both the basement and overlying rocks, mark the end of the stable shelf environment. They also created additional accommodation space for sedimentation in Early Mississippian to earliest Atokan times. Contemporaneous subduction and the deposition of lower through middle Atokan shales and sandstones resulted in marked variation in thickness across faults (Figure 5) (Hounseknecht and McGilvery, 1990).

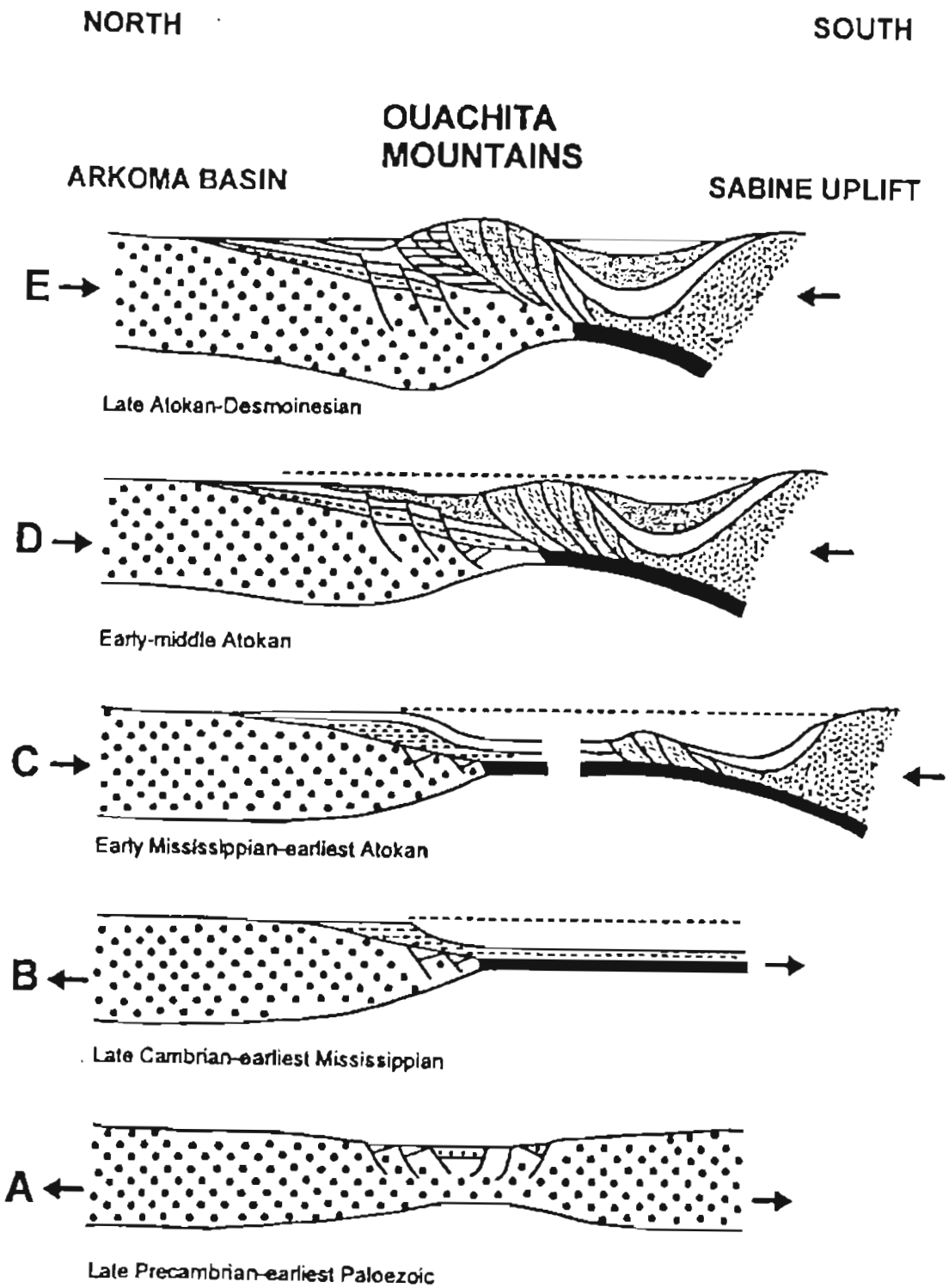

Figure 4. Diagrammatic evolution of southern margin of North America (From Houseknecht and Kacena, 1983)

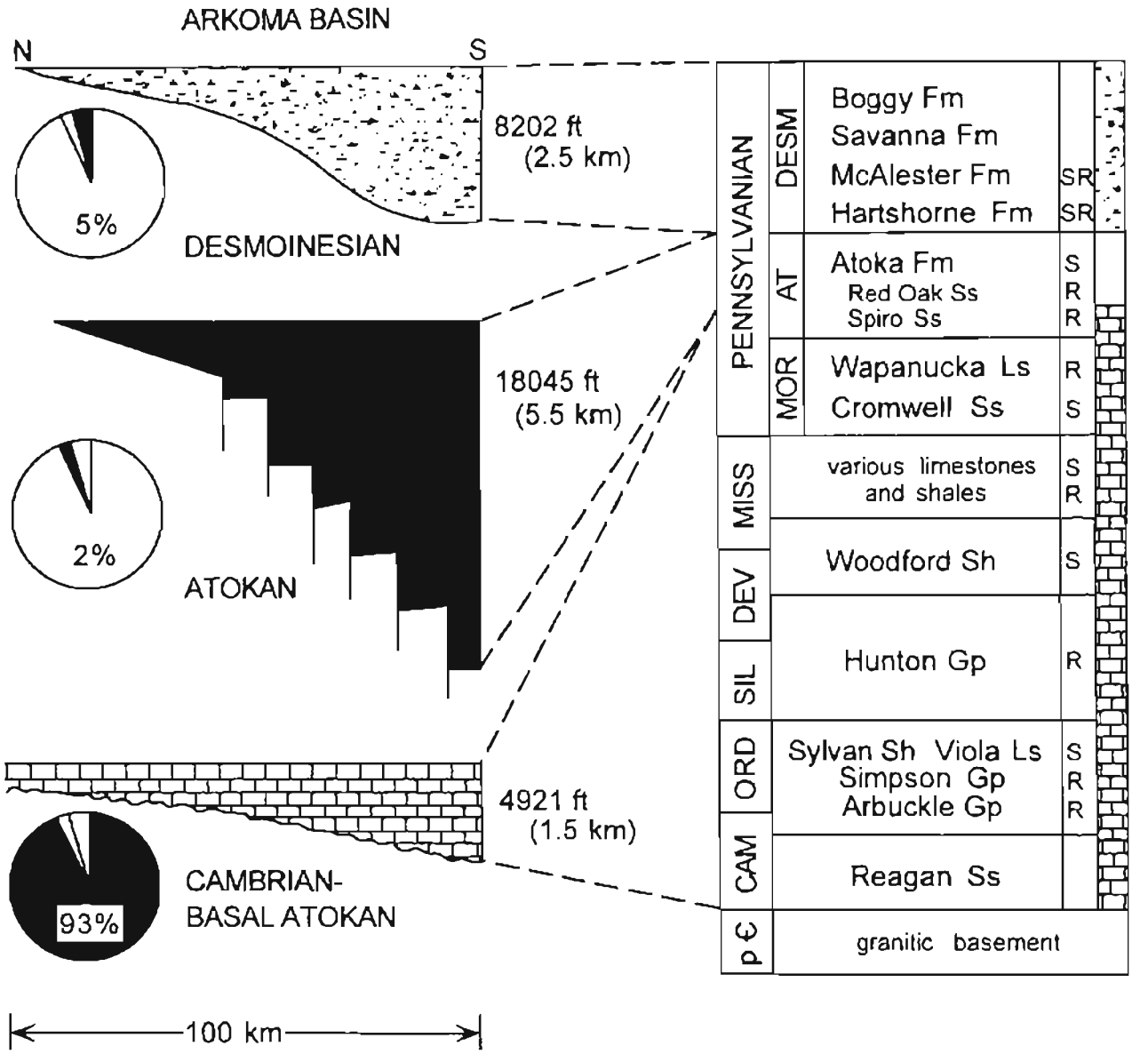

Figure 5. Stratigraphic framework of the ARkoma Basin in Oklahoma. Pie chart represent total time of deposition during the period. (From Houseknecht and McGilvery, 1990).

Near the end of the Atokan time, the advancing compressional front altered the stress distribution in the foreland. Thin-skinned thrusting within Atokan strata became the dominant structural style (Figure 4e)(Houseknecht and Kacena, 1983). The structural configuration of the Arkoma-Ouachita system has remained relatively undisturbed since the Desmoinesian, although minor thrusting and folding did occur after the Desmoinesian. After the Atokan time, shallow marine and fluvial sedimentation prevailed until the foreland basin, the Arkoma basin, was filled (Figure 6)(Houseknecht and Kacena, 1983).

Transition Zone Geometry

The debate over the imbricate fans and the presence of a triangle zone in the transition zone between Ouachita Mountains and the Arkoma Basin has been around for a considerable amount of time. Following is a brief description of Suneson (1995) summarized interpretations of the various models of transition zone proposed until the early 1990's (Figure 7):

Arbenz (1984) was the first to recognize south-dipping thrust faults, blind imbricate thrust branching from the exposed thrust system, and deep decollement surfaces that served as the floor thrust for the imbricate thrust that extend into the basin (Figures 8a & 8b). Arbenz interpreted the detachment surface as gradually rising towards north.

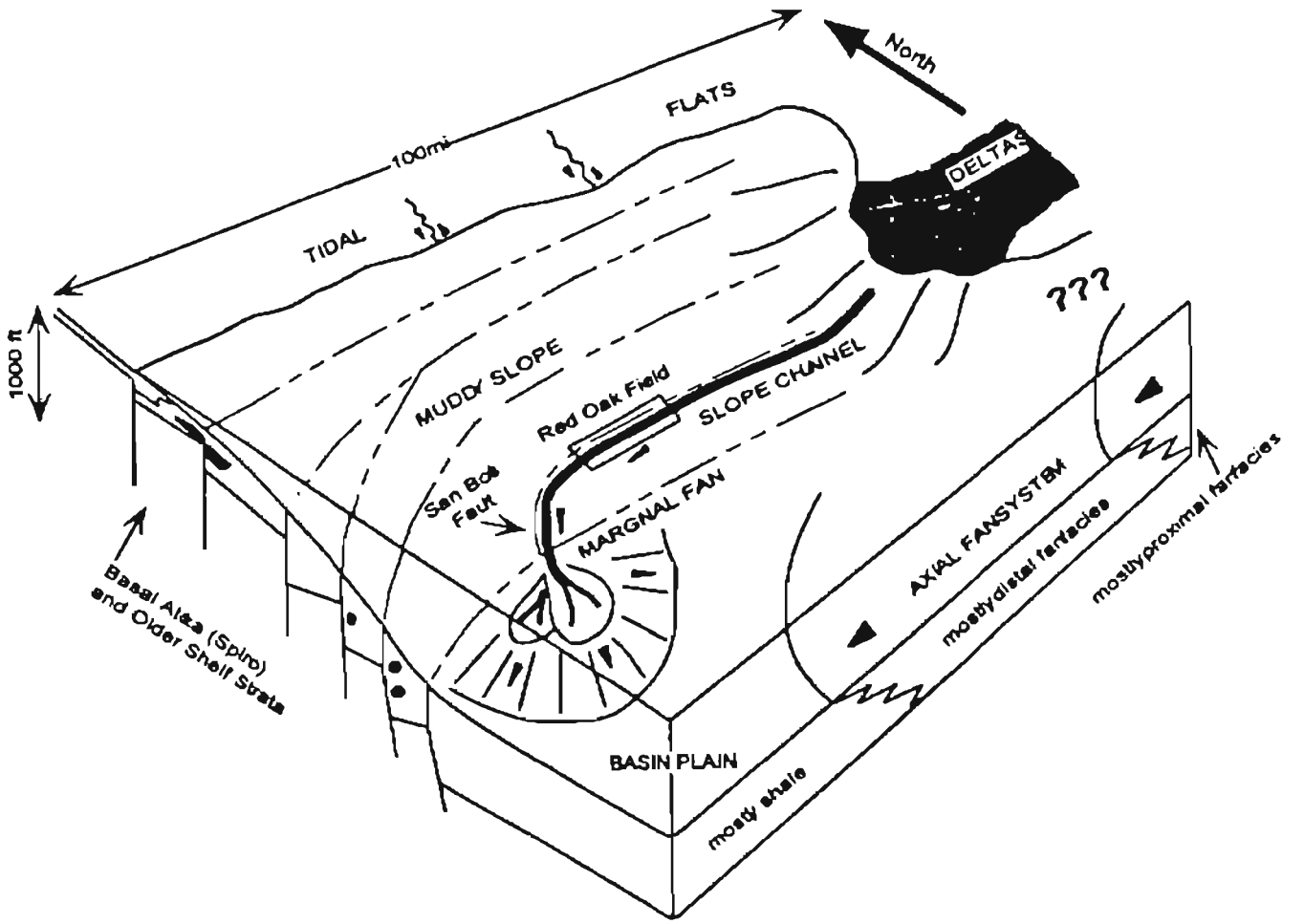

Figure 6. Reconstruction of depositional system in which Atoka strata were doposited in the Arkoma basin (from Houseknecht and McGilvery, 1990; modified from Houseknecht 1986)

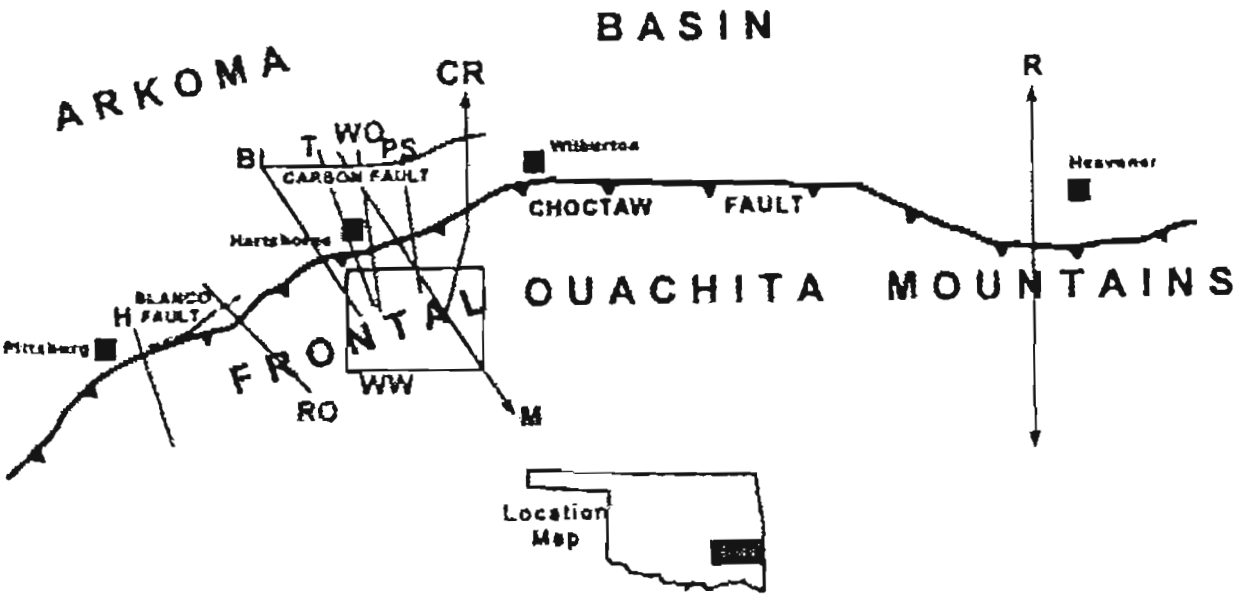

Figure 7. Location map for previous investigations described in the text. (From Suneson, 1995)

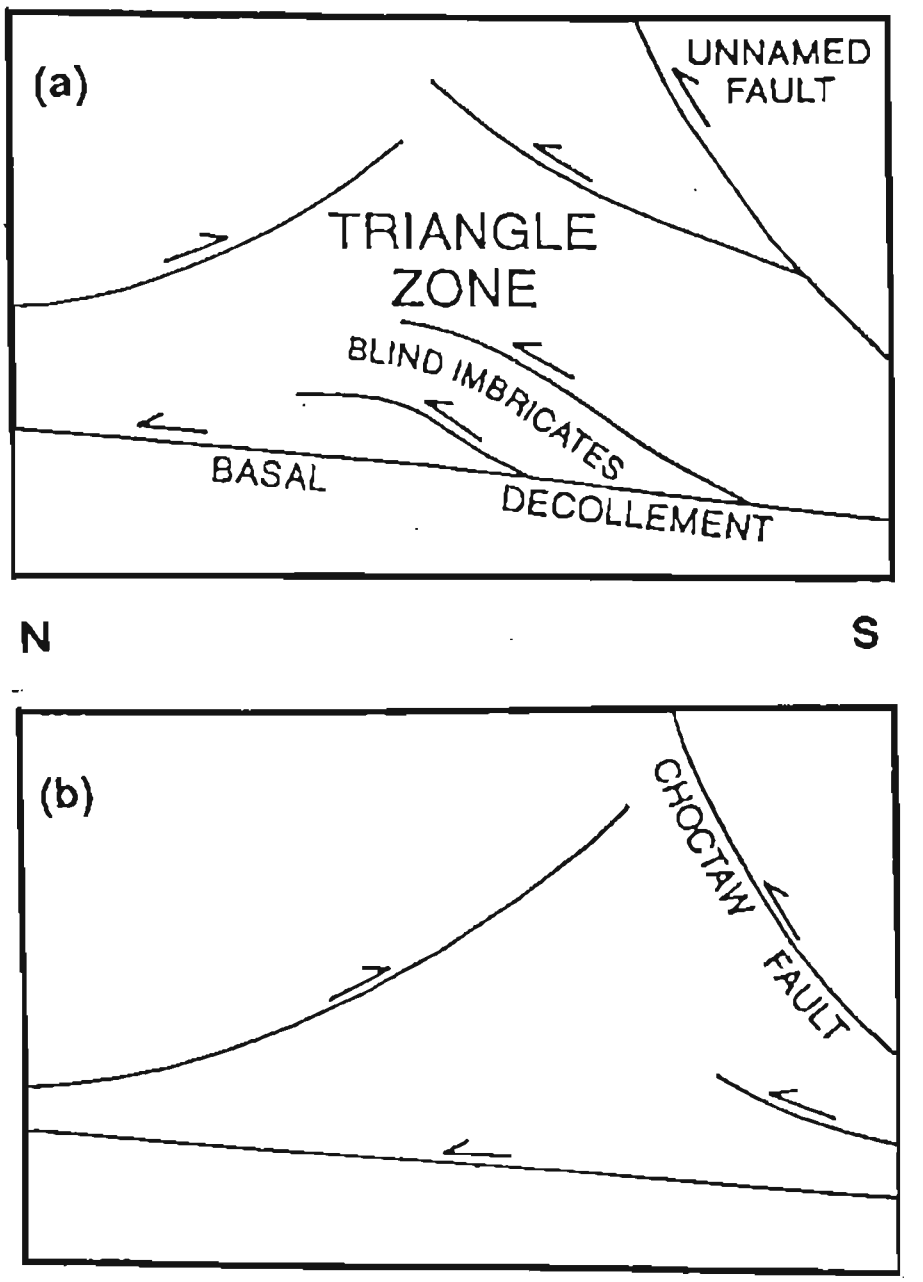

Figure 8. Sketch cross-section displaying the complex geometry of thrusting along the transition zone of the Arkoma Basin and Ouachita Mountains as proposed by (a) Arbenz (1984) and (b) Arbenz (1989). (From Suneson, 1995)

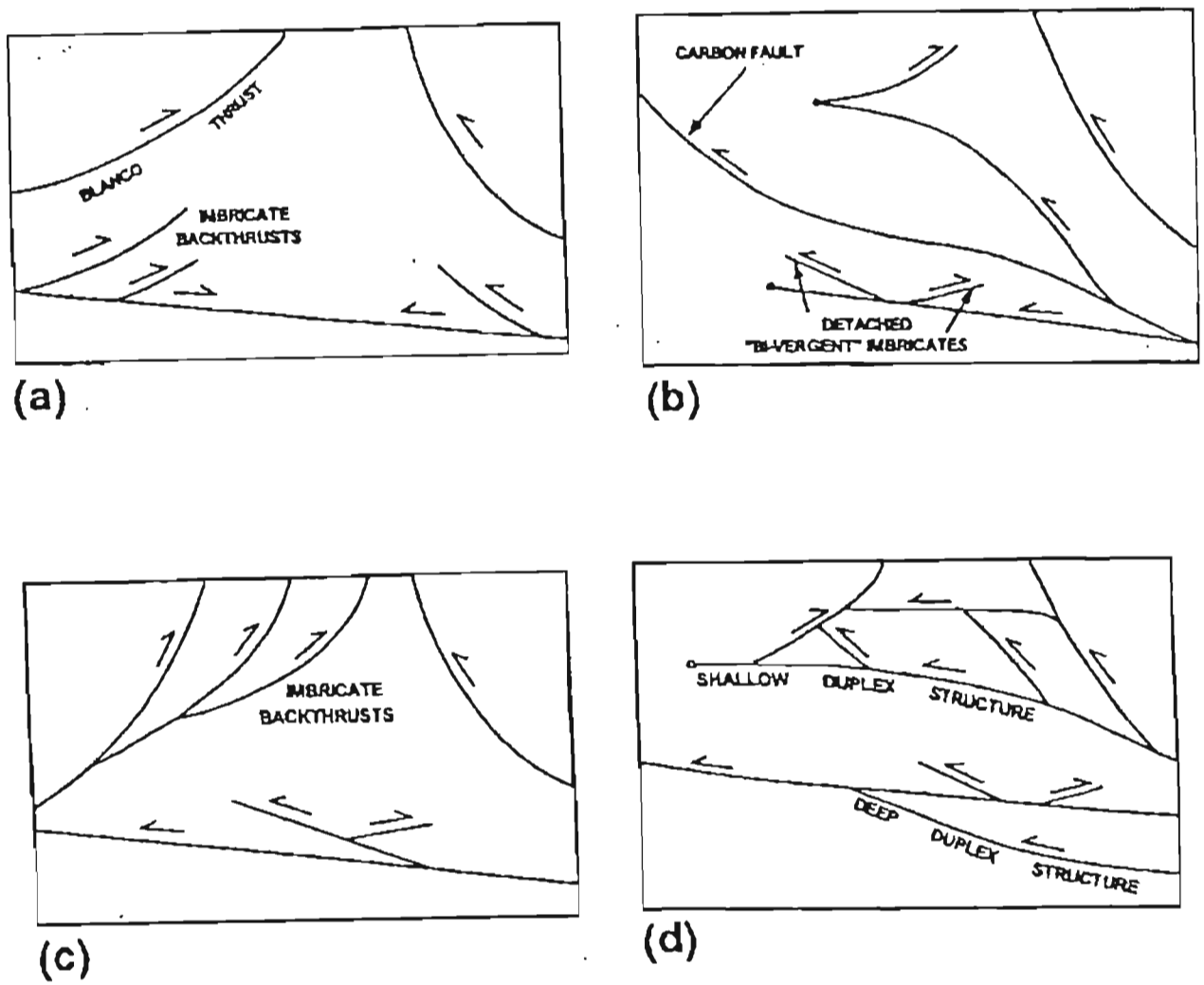

Figure 9. Sketch cross section of the transition zone geometry as proposed by : (a) Hardie (1988); (b) Milliken (1988); (c) Camp and Ratcliff (1989); and (d) Reeves, et. al., (1990). (From Suneson , 1995)

Hardie (1988), referring to the geometry of the basinward side of the transition zone (Figure 9a) first used the term "triangle zone". He proposed that the Blanco thrust, located to the southwest of Hartshorne, Oklahoma, serves as a "basinal roof of a relatively thick triangle zone." His cross section includes numerous back-thrusts and blind imbricates within the footwall of Choctaw Fault. A detachment surface along the bottom of the Pennsylvanian Springer Formation is also identified in Hardie's research mapping of the suggested area. Milliken (1988) introduced a term "bi-vergent" imbricate thrusts describing these thrust and suggested that they are floored by a deeper detachment (Figure 9b).

Camp and Ratliff (1989) published a computer-balanced cross-section across the transition zone near Wilburton, Oklahoma and identified a thick triangle zone floored by blind imbricate thrust faults and back thrusts and a deep north-directed decollement that climbs from Mississippian shales in the south to Middle Pennsylvanian strata beneath the folds of the Arkoma basin (Fig 9c). Their cross section also shows imbricate backthrusts splaying off the roof backthrust of the triangle zone.

Reeves and other (1990) proposed that a thin triangle zone is floored by two north-directed duplex structures, which is separated by a relatively shallow major decollement. They also suggested that the deep decollement is in Lower Atokan strata. (Figure 9d).

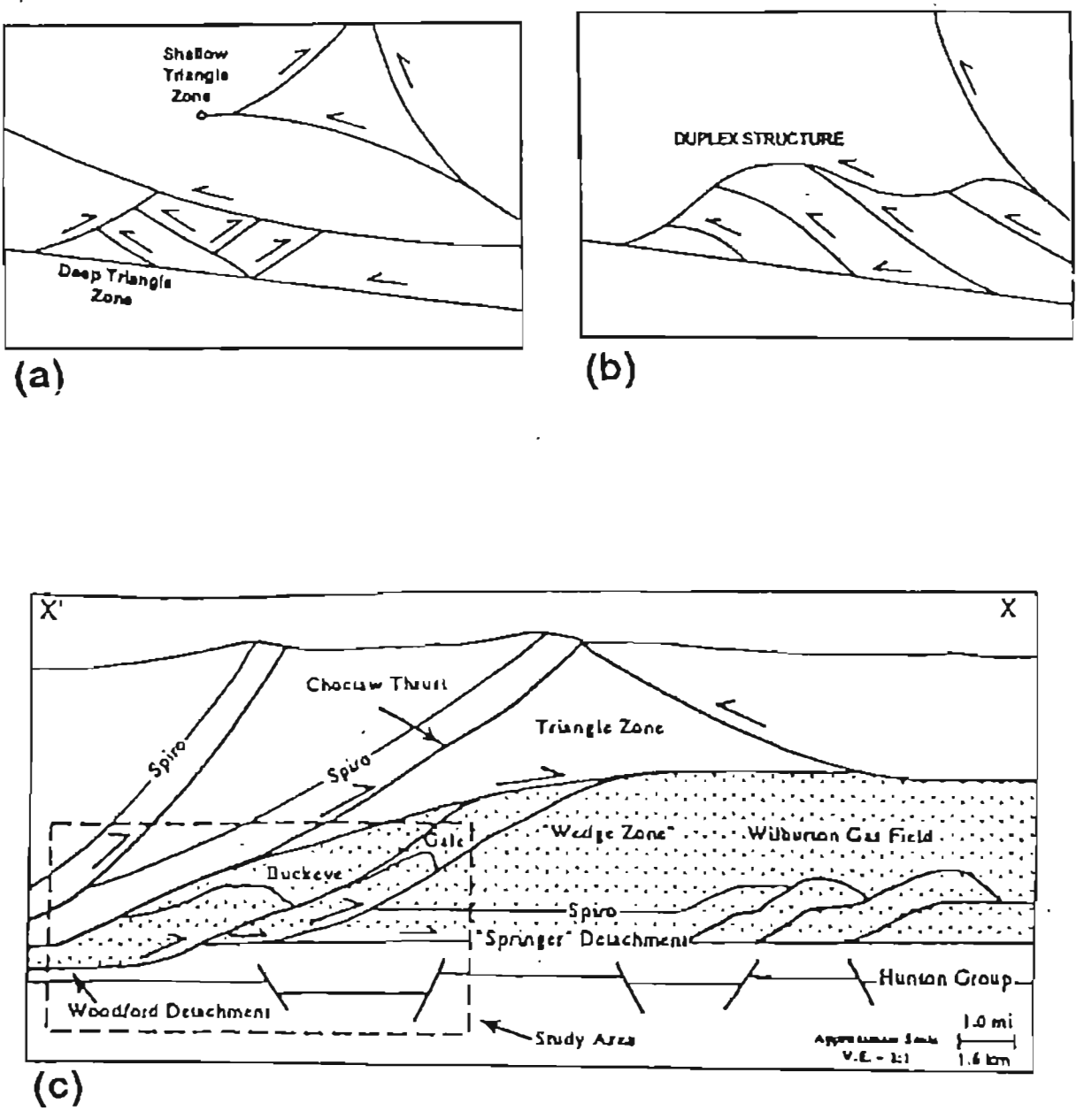

Figure 10. sketch cross-sections illustrating the transition zone geometry according to: (a) Perry and Suneson (1990); (b) Roberts (1992); and (c) Wilkerson and Wellman, (1993). (From Suneson, 1995).

Perry and Suneson (1990) proposed a shallow triangle zone along with a series of deep triangle zones. They were also the first to suggest that the triangle zone is bounded by both a roof and floor thrust (Figure 10a).

Roberts (1992) postulated on the basis of seismic data and sparse well control, that the folds exposed on the surface are the result of an underlying duplex structure. Further, he showed a basal decollement in the lower part of the Atoka Formation extending far into the basin (Figure 10b).Wilkerson and Wellman (1993) suggested that a thin triangle zone is present, the floor thrust of the triangle zone is the roof thrust of a duplex structure (also referred as
the "Gale-Buckeye" thrust sequence), and blind imbricates are present near the base of the duplex structure (Figure 10c).

Cemen and others (1994, 1995 and 1997), Al-Shaieb and others (1995), Akhtar (1995) and Sagnak (1996), in a research project funded by Oklahoma Center of Advancement in Science and Technology (OCAST), proposed a structural model for the Wilburton gas field and surrounding areas (Figure 11). In their study, they established that a triangle zone underlain by a duplex structure does exist within the footwall of the Choctaw fault (Figure 12). This triangle zone is bounded to the north by the Carbon fault, to the south by the Choctaw fault, and is floored by the Lower Atokan Detachment (LAD) surface. An even deeper detachment, which also serves as the floor to the duplex, called "Woodford detachment", is within the Woodford Shale to the south, and ramps into the Springer shale to the north. Thrusting in the duplex structure probably occurred in a break-forward sequence. It was also concluded that in the Wilburton and surrounding areas, the amount of shortening was around 60 %. Evans (1997) and Ronck (1997)

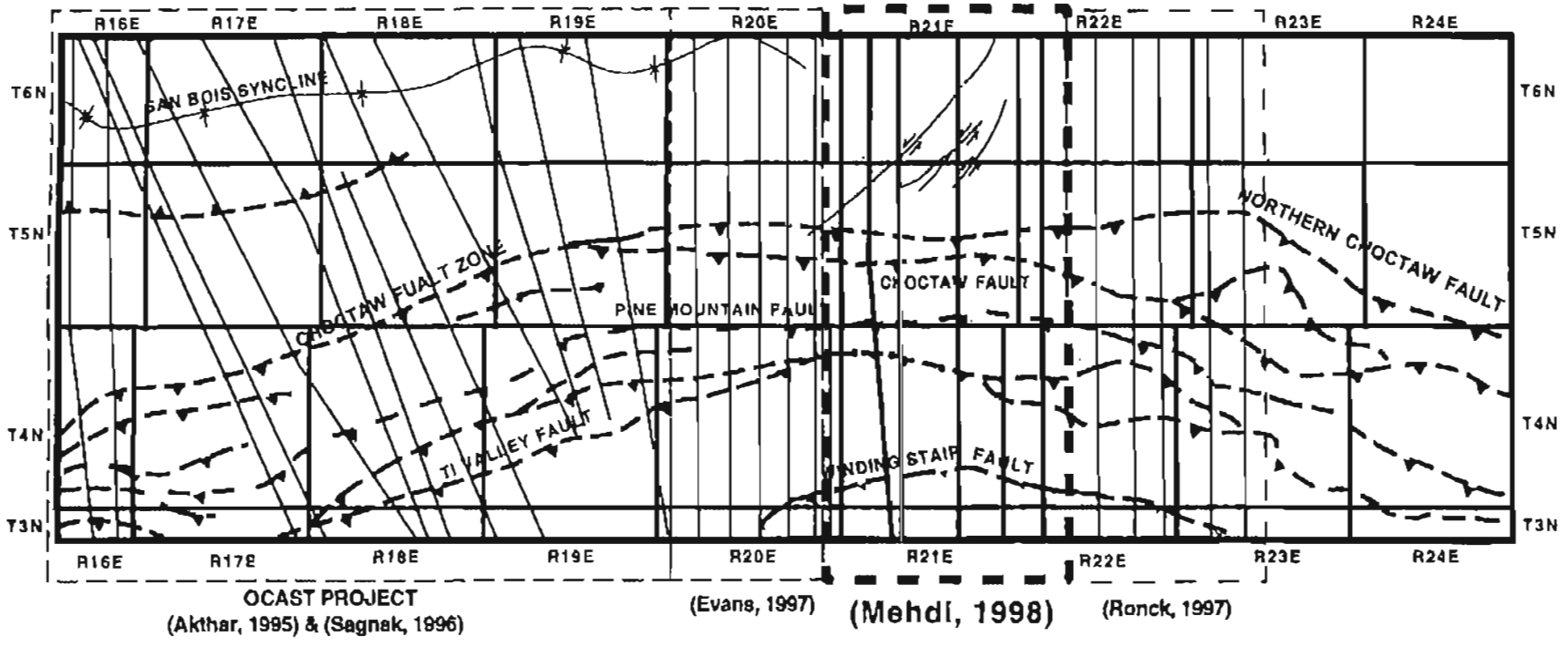

Figure 11. Regional base map for the OCAST project area and eastward into LeFlore County. Thesis authors are listed below their study areas.

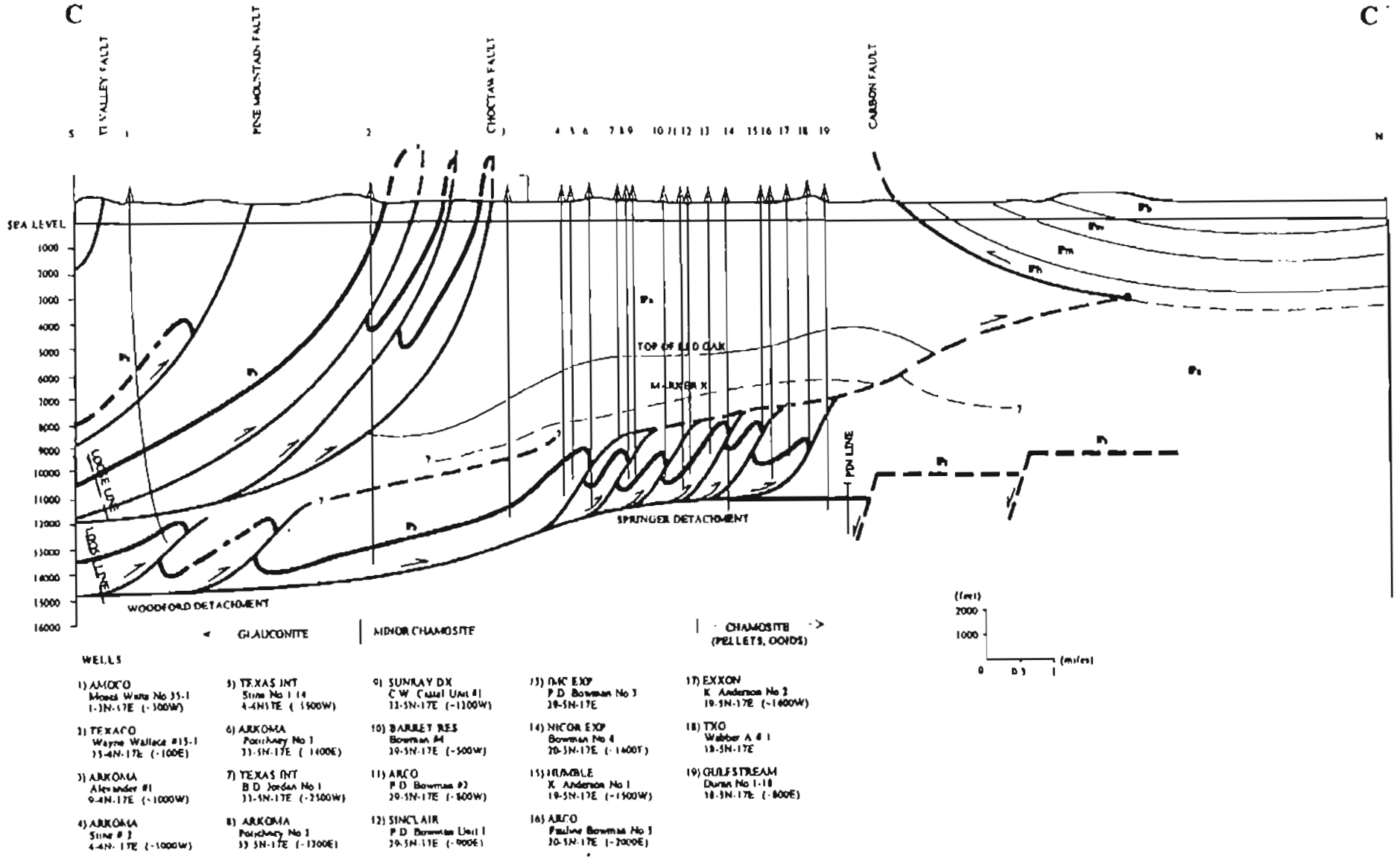

Figure 12. A cross-section constructed in the OCAST project showing triangle zone, duplex structure, detachment surfaces, imbricate thrusts etc.

analyzed the 'Panola and Baker Mountain quadrangles' and 'LeFlore and Blackjack Ridge quadrangles' respectively for subsurface structure styles.

Red Oak Field

The northeastern part of the study area includes the largest gas field in the prolific Arkoma basin of Oklahoma and Arkansas, i.e. the Red Oak Field. (Figure 13). Although, the earliest well in this field goes to 1912, when Gladys Belle Oil Company drilled a well near the crest of the Brazil anticline, north of the town of Red Oak, and produced gas from the Hartshorne sandstone, the real potential of the field was discovered about half a century later. In May 1959, Midwest Oil Corporation spudded a well located on the known axis of the Brazil anticline at the Hartshorne horizon, and its objective was to test the Atoka section down to the Spiro sandstone. The well encountered a sandstone unit (about 145 ft thick) at around 7000 ft in depth. This unit turned out to be a major gas-bearing unit and was named Red Oak sandstone. At about 11,500 ft, gas bearing Spiro sandstone was encountered. Thus, within two years, 25 development wells were completed and ultimate gas recovery was estimated at more than 1.1 tcf. (Houseknecht and McGilvery, 1990).

Development drilling revealed structural discordance between the Red Oak and Spiro horizons. At the Red Oak horizon, the structure is a large asymmetrical, doubly plunging anticline that is thrust faulted along its crest. In contrast, the Spiro horizon is broken into a series of normal fault blocks (Figure 14).

Not only did development drilling establish significant reserves in the Red Oak and Spiro sandstones, but other locally distributed reservoir sandstones were also

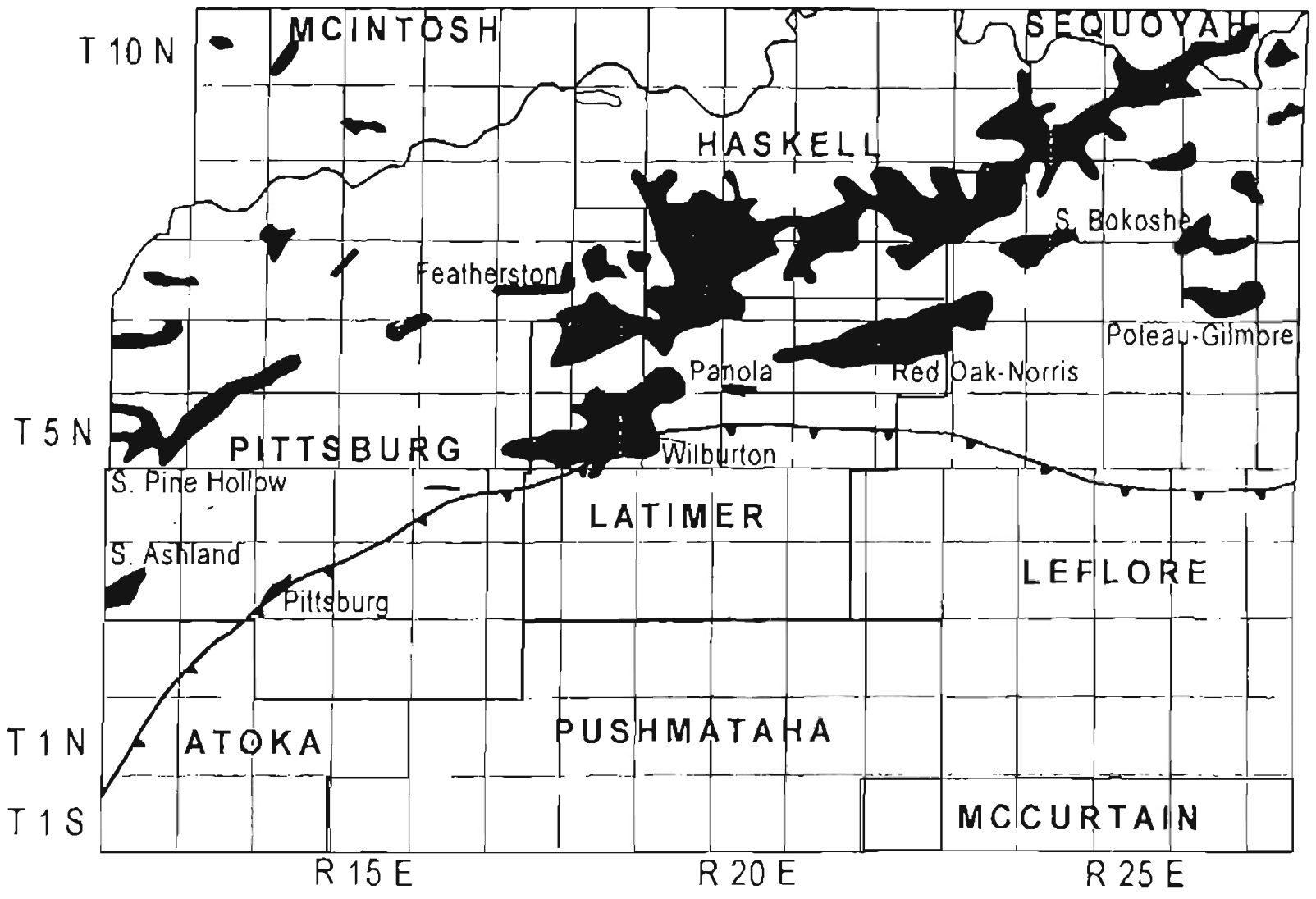

Figure 13. Major gas fields in and around the study area.

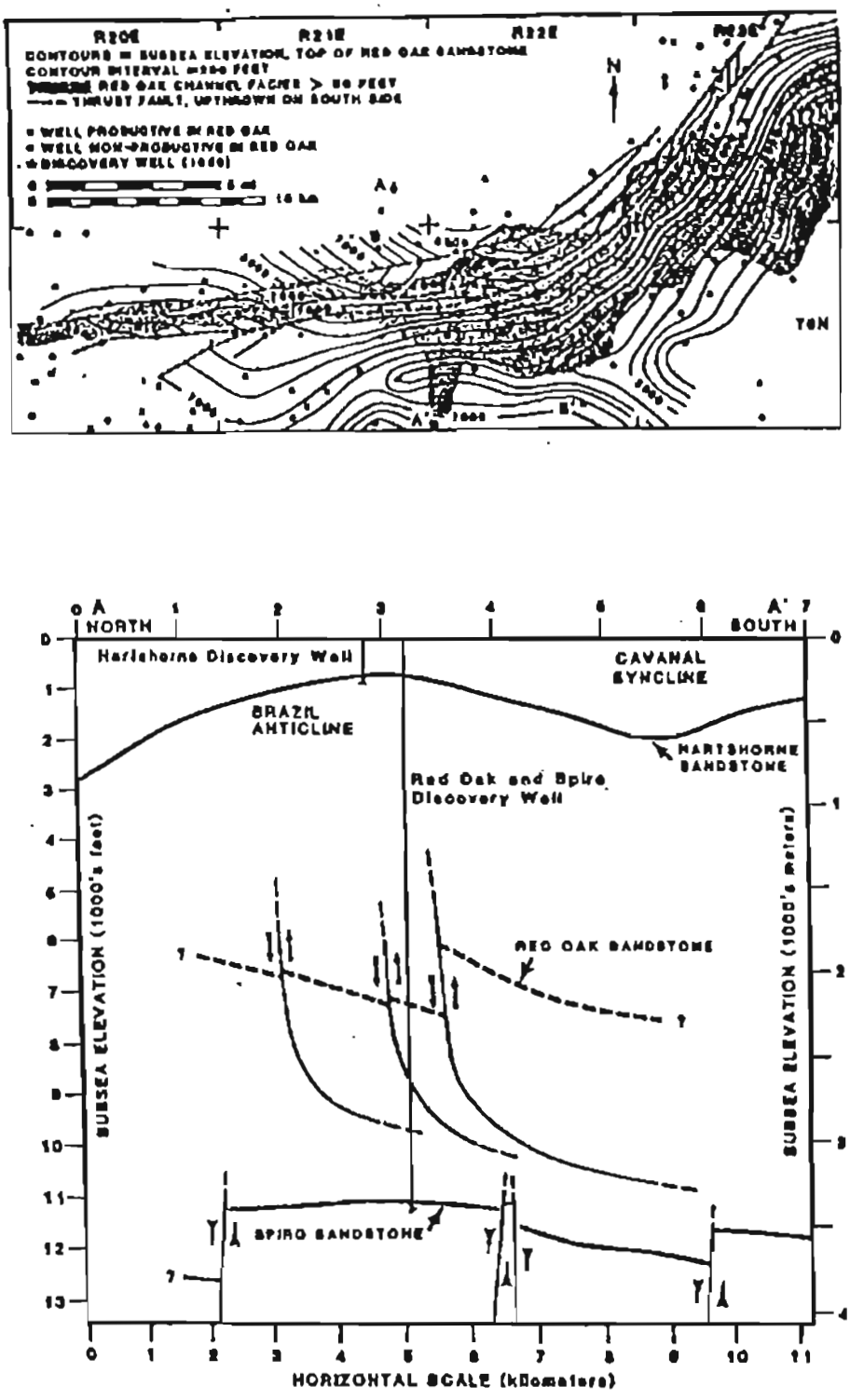

Figure 14. Structure map along the Brazil Anticline. A cross-section is included to display the common style of thrusting observed in the Red Oak field. (From Houseknecht and McGilvery, 1986)

discovered with the Atoka Formation. Among these, the Fanshawe, Panola, and Brazil sandstones have been most productive; the Fanshawe has been the most prolific of these.

CHAPTER III

STRATIGRAPHIC FRAMEWORK OF THE ARKOMA BASIN AND OUACHITA MOUNTAINS

Arkoma Basin stratigraphy has been well documented over the last few decades. Both the Arkoma Basin and Ouachita Mountains are represented by thick accumulations of sedimentary rocks spanning Cambrian to Pennsylvanian time (Figure 15). These strata record the collapse of the deep ocean basin and the development of a foreland basin through continental collision (Sutherland, 1988). In the study area, the surface rocks consist solely of Early to Middle Pennsylvanian strata, with the exception of Mississippian Stanley group.

Although a detailed account of stratigraphy is outside the scope of this study, a generalized framework is pertinent in order to establish the relationships between individual intervals of strata. Much of the following discussion is taken from Ham (1978) and Sutherland (1988).

PRE-PENNSYLVANIAN STRATIGRAPHY

Proterozoic Granite, rhyolite, and metamorphic rocks comprise the crystalline basement of eastern Oklahoma (Figure 15). The Upper Cambrian Reagan Sandstone of the Timbered Hills Group represents a time-transgressive unit which was deposited in all

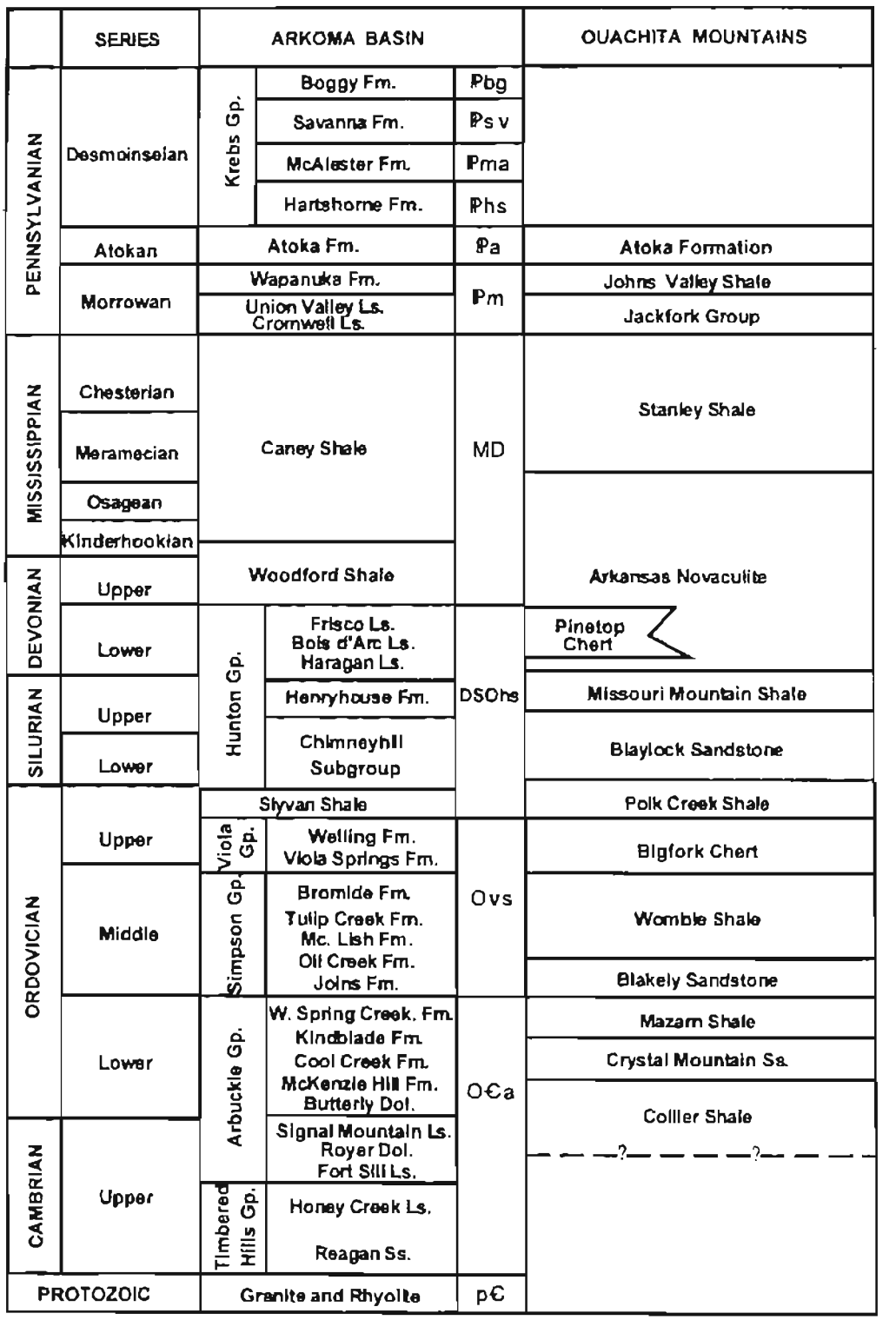

Figure 15. Stratigrpahic chart for the Arkoma Basin - Ouachita Mountain provinces. (From Johnson, 1988)

areas except topographical highs across a rugged basement floor (Johnson, 1988). Overlying the Reagan Sandstone is the shallow, trilobite-rich, pelmatozoan Honey Creek Limestone (Ham, 1978).

The Cambro-Ordovician Arbuckle Group conformably overlies the Timbered Hills Group. The Lower Arbuckle Group, representing the Upper Cambrian, is composed of the Fort Sill Limestone, Royer Dolomite, and Signal Mountain Limestone. The Upper Arbuckle Group, consisting of the Butterfly Dolomite, McKenzie Hill, Cool Creek, Kindblade, and West Spring Formations, represent the Lower Ordovician. These units represent shallow water facies and outcrop in the Arbuckle Mountains. Deep-water facies of the Ouachita trough are listed beside their shallow water stratigraphic equivalent (Figure 15).

Middle and Upper Ordovician strata are represented by shallow water carbonates of the Simpson and Viola Groups on the shelf, and deep-water shales and cherts toward the basin. Limestones of the Simpson Group, in ascending order, are the Joins, Oil Creek, McLish, Tulip Creek, and Bromide Formations. These represent a change toward shallower environments and are characterized by skeletal calcarenites, skeletal carbonates, mudstones, sandstones, and shales (Ham, 1978). Prominent sandstones are generally found at the base of each successive limestone. Basinal equivalents are the Blakely Sandstone and Womble Shale (Morris, 1974).

The Upper Ordovician Viola Group conformably overlies the Simpson Group. Consisting of the Viola Springs and Welling Formations, these shallow carbonates display nodular chert-rich mudstones, packstones, porous grainstones, and wackestones, some of which are dolomitized (Sykes, 1995). The Upper Ordovician Sylvan Shale, a

green to gray shale with well-developed laminations, unconformably overlies the Viola Group.

The Ordovician to Lower Devonian Hunton Group overlies the Sylvan Shale (Ham, 1978). The Kinderhookian Woodford Shale (Upper Devonian to Lower Mississippian) lies unconformably upon the Hunton Group (Figure 15). This extensive source rock is predominantly dark, fissile shale, with interbedded vitreous and siliceous chert (Ham. 1978). Along the frontal Ouachitas, this stratigraphic unit represents a major basal detachment surface (Woodford Detachment) for the ensuing thrust system.

The Mississippian Caney Shale was conformably deposited atop the Woodford Shale. Near the top of the Caney is a shale sequence commonly known as the Springer Shale. The upper stratigraphic boundary for the Caney is based on the first appearance of siderite or clay-bearing ironstone beds, which represent shallower deposition. Ham (1978) placed the Springer Shale in the Late Mississippian (Chesterian), based on the appearance of spores and pollens. Basinal equivalents of the Mississippian are the Devonian to Mississippian Arkansas Novaculite and the Mississippian Stanley Group. The Stanley Group reflects a period of marked increase in subsidence rates for the trough. The Stanley sequence of shales and sandstones is much thicker than its shallow water were counterparts to the north (Houseknecht and Kacena, 1983).

PENNSYLVANIAN STRATIGRAPHY

Pennsylvanian deposition records the onset of orogeny within the Arkoma Basin and only rocks of the Morrowan, Atokan, and Desmoinesian series are represented. Sedimentation patterns on the shelf experienced little change during Morrowan time,

although large amounts of sand are present within individual facies (Johnson, 1988). Morrowan facies are approximately 1,000 feet thick towards the north, but thicken extensively to the south (up to 6,000 feet) in the deeper parts of the basin. On the shelf, Morrowan rocks consist of the Cromwell Sandstone, Union Valley Limestone, and the Wapanucka Limestone. These units were deposited during a series of small-scale transgressions and regressions, in which a number of discontinuous limestones and sandstones were deposited between shale packages (Sutherland, 1988). In particular, the Wapanucka Limestone was deposited during a regressional episode of sea level, interrupted by minor shoreward movements of the coastline. It consists of thick platform carbonates to the west, but becomes thin and shaly to the east (Gross and others, 1995).

While sedimentation on the shelf shows only minor lithological and sedimentological variations, the deep basin underwent vast changes. Extensive growth faulting in the southern margin of the basin was occurring by the Late Mississippian (Figure 16) (Houseknecht and Kacena, 1983). Morrowan shelf facies thicken southward where deep-water marine sediments that are characterized by flysch deposition are found. Large accumulations of sediment that were primarily derived from the east were shed into the downthrown blocks along submarine canyons. The Jackfork and overlying Johns Valley Formations reflect Morrowan deposition in this trough.

During an ensuing lowstand episode, the Atoka Formation was unconformably deposited atop the Wapanucka Formation. Atokan deposition represents the thickest formation in the basin, approximately 15,000 feet thick in the deepest portions (Berry and Trumbley, 1968). It is informally divided into the lower, middle, and upper Atoka (Figure 17). The distinctions for each are based on the occurrences of syndepositional

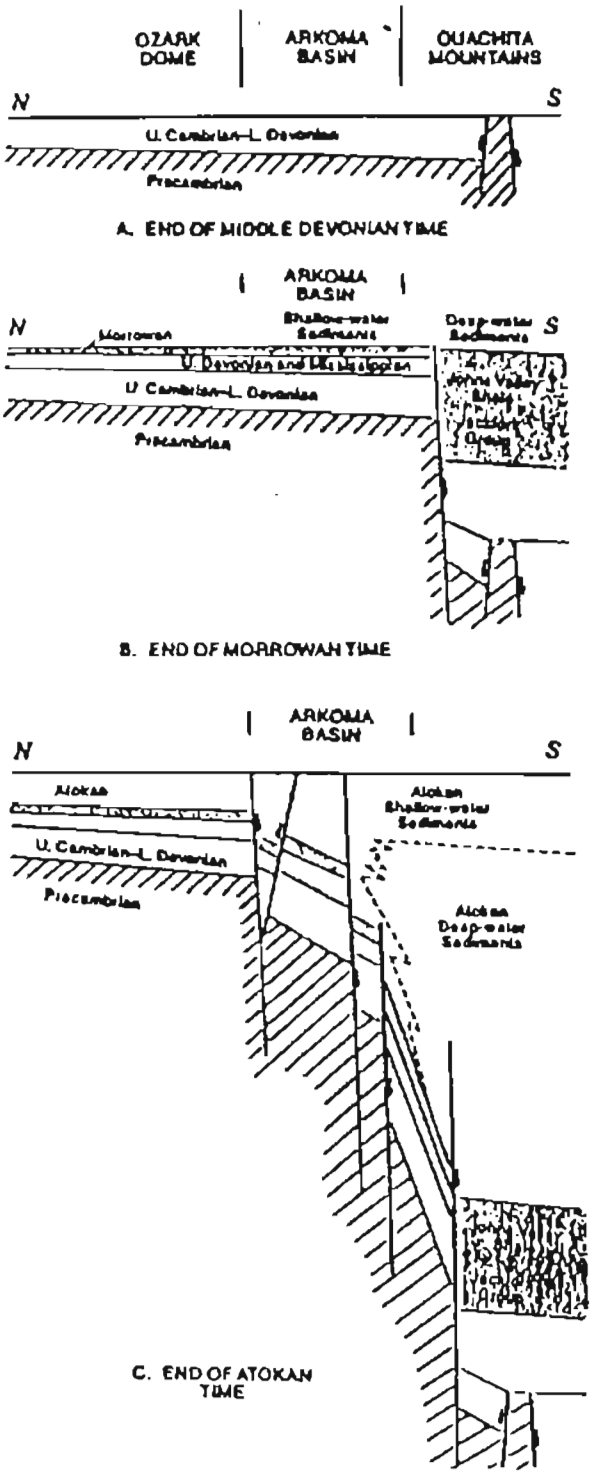

Figure 16. Generalized cross-section characterizing growth faulting and subsequent sedimentation patterns from Cambrian through Atokan time. (From Johnson, 1988).

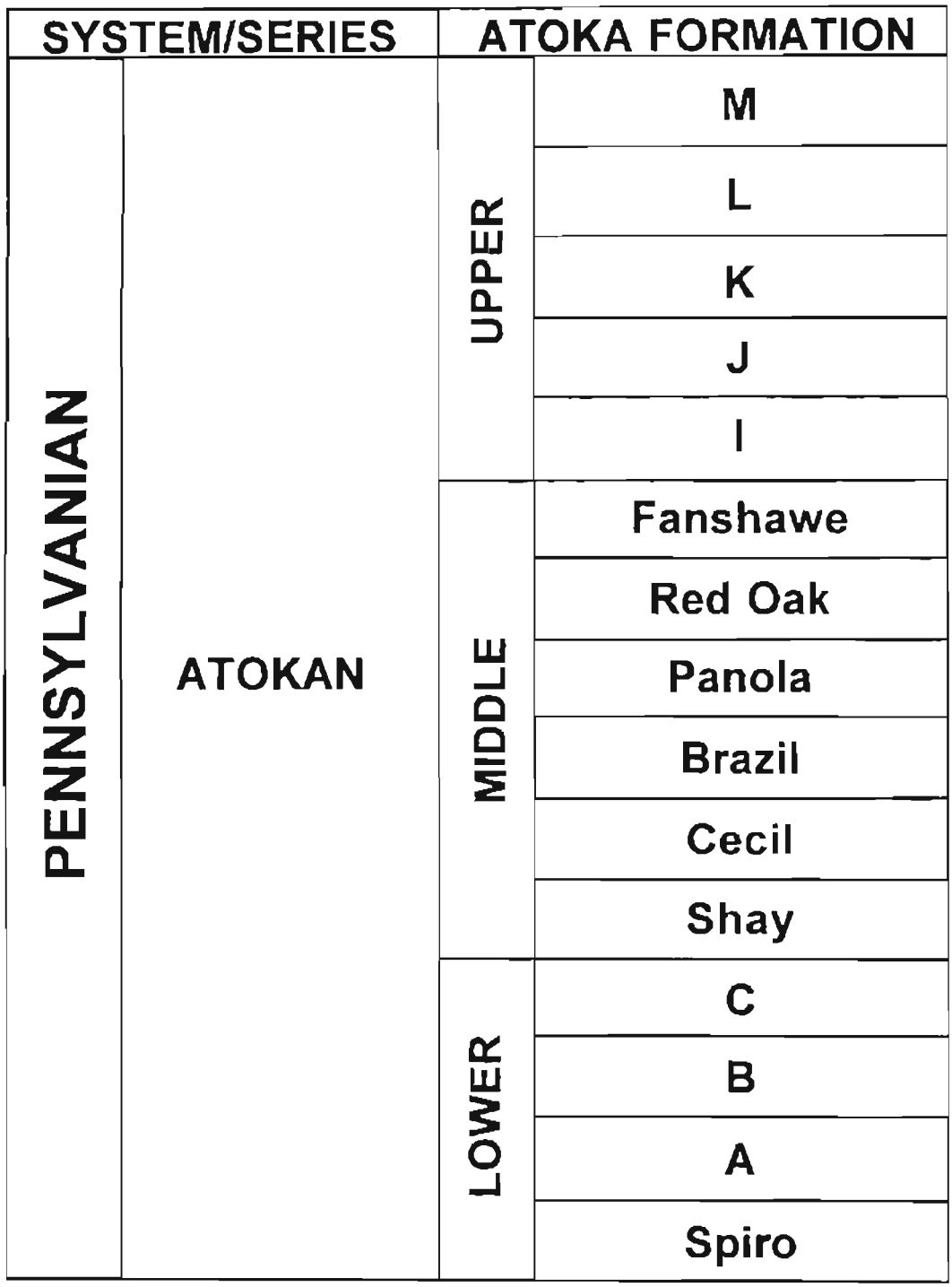

Figure 17. Stratigraphic chart, Atokan strata, informal rock-stratigraphic units, Arkoma Basin.

normal faults which characterize sedimentation within the basin (Johnson, 1988). Shales comprise most of the Atokan strata (nearly 70%), which are broken by intermittent sandstones deposited by fluvio-deltaic processes (Sutherland, 1988). Sediment transport on the shelf is believed to be predominantly from the north and northeast and carried west via longshore currents (Sutherland, 1988).

The basal Atokan is unconformable with the Morrowan Series. It consists of the Spiro Sandstone underlain by the thin, sub-Spiro shale. In general, the Spiro Sandstone was deposited on a broad shelf from northern fluvial systems southward toward shallow marine environments (Figure 18). It consists of a basal progradational/aggradational sandstone overlain by a retrogradational parasequence set (Gross and others, 1995). Depositional environments include tidal flats, deltaic, barrier islands, tidal channels, and shallow marine sand bars and carbonates (Houseknecht, 1983). A representative well log signature for the Spiro in the study area is given in Figure 19.

Middle Atoka sandstones include, in ascending order, the Shay, Cecil, Casey, Panola, Red Oak, and Fanshawe. Wire-line log signatures for the Cecil, Casey, and Red Oak Sandstones are displayed in Figures 20-22. These sandstone intervals are wrapped in extensive shale packages throughout the basin and frontal Ouachitas. Deltaic complexes interrupted by small-scale sea level changes are the dominant depositional setting, with off-shore sands characterized by gravity flow sedimentation at the base of submarine fans (Figure 23) (Vedros and Fisher, 1978).

The upper Atokan consists almost entirely of mudstones deposited within shallow shelf to deltaic environments (Sutherland, 1988). Growth faulting that dominated middle Atokan stratigraphy does not penetrate these shales, suggesting that the normal faulting

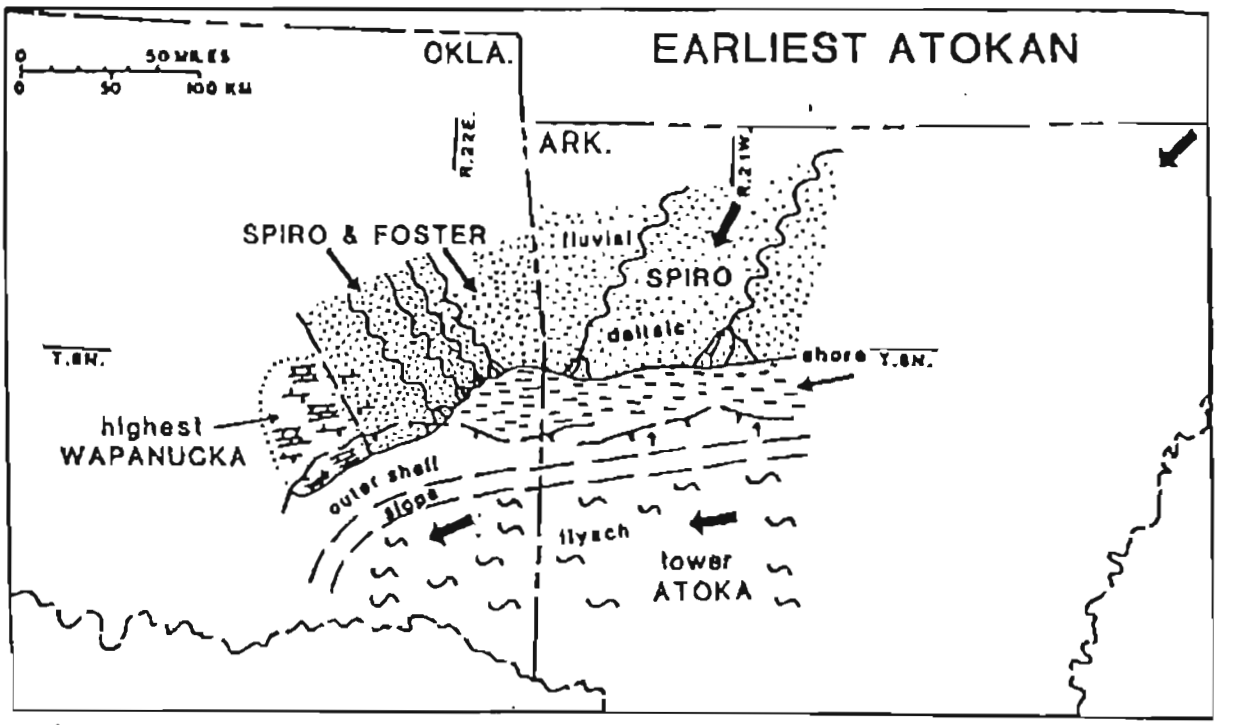

Figure 18. General depositional environment for the lower Atokan Spiro sandstone (From Sutherland, 1988)

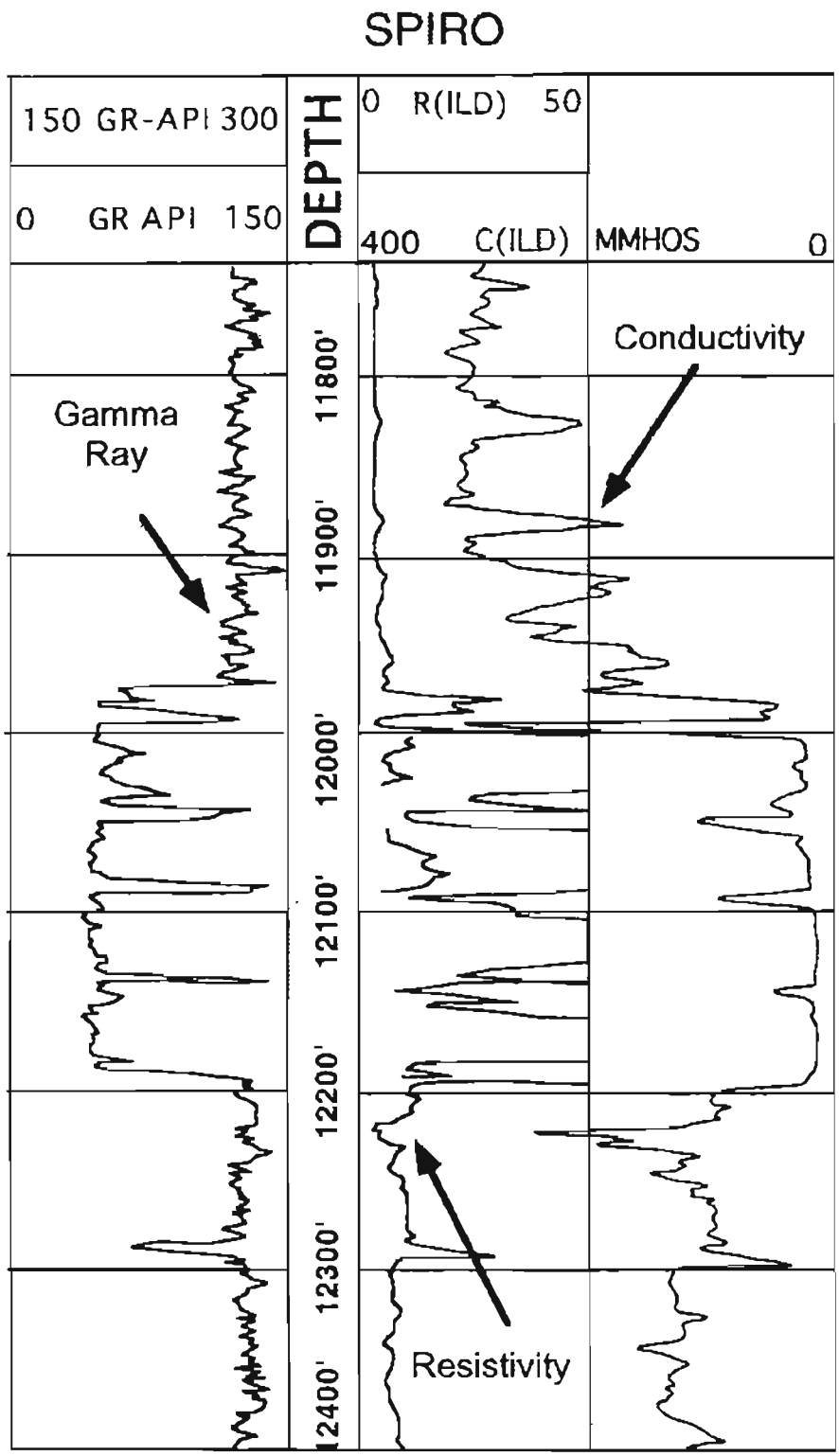

Figure 19: Log signature of Spiro sandstone:Sun Exploration & Production Co.: William Gallagher Unit no. 2,Red Oak - Norris Field, Latimer County, Oklahoma, Section - 14; Township - 6 N; Range - 21 E

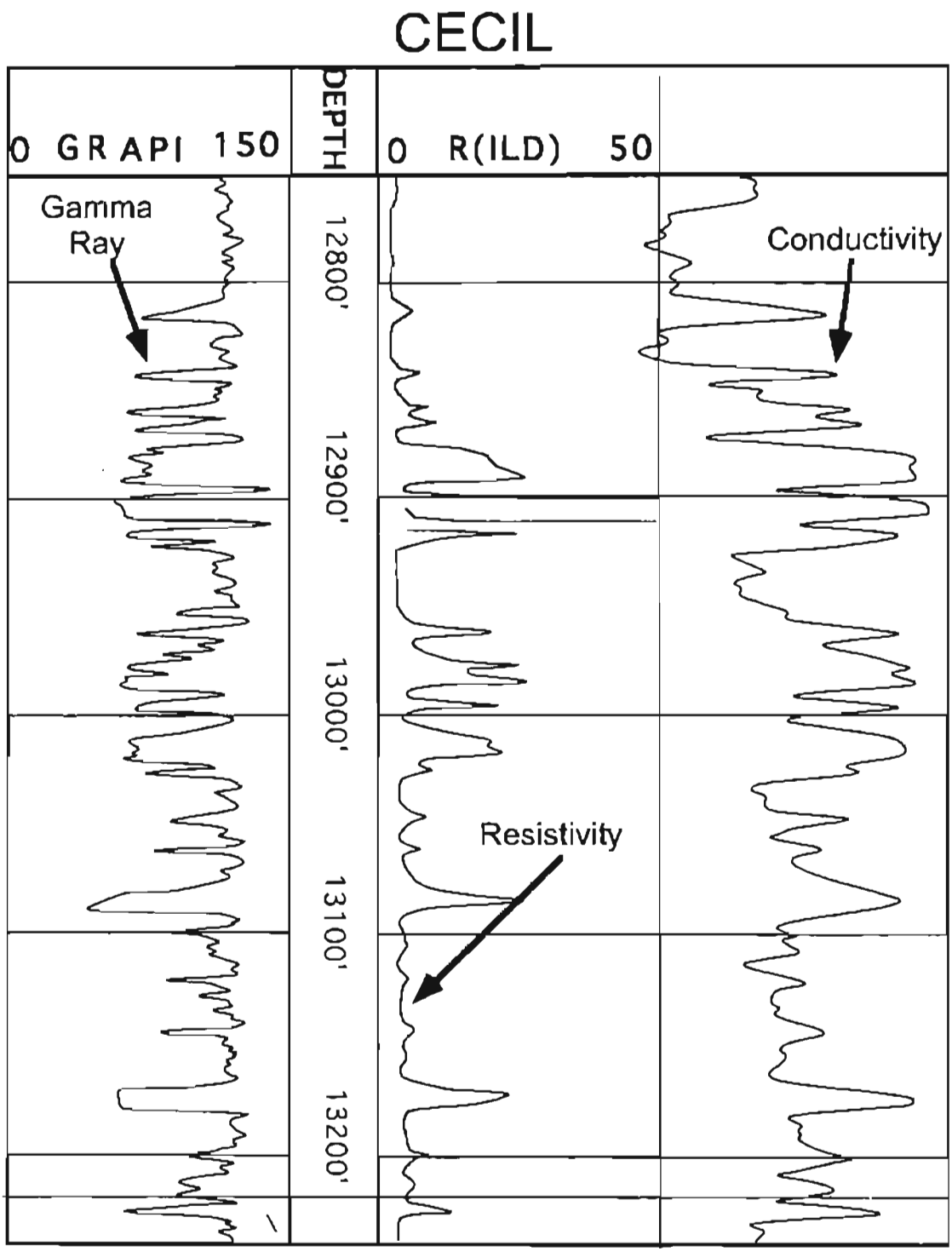

Figure 20: Log signature of Cecil sandstone: Exxon Company: Ellis # 1, Wildcat, Latimer, Oklahoma : Sec: 4; T 4 N ; R - 21 E

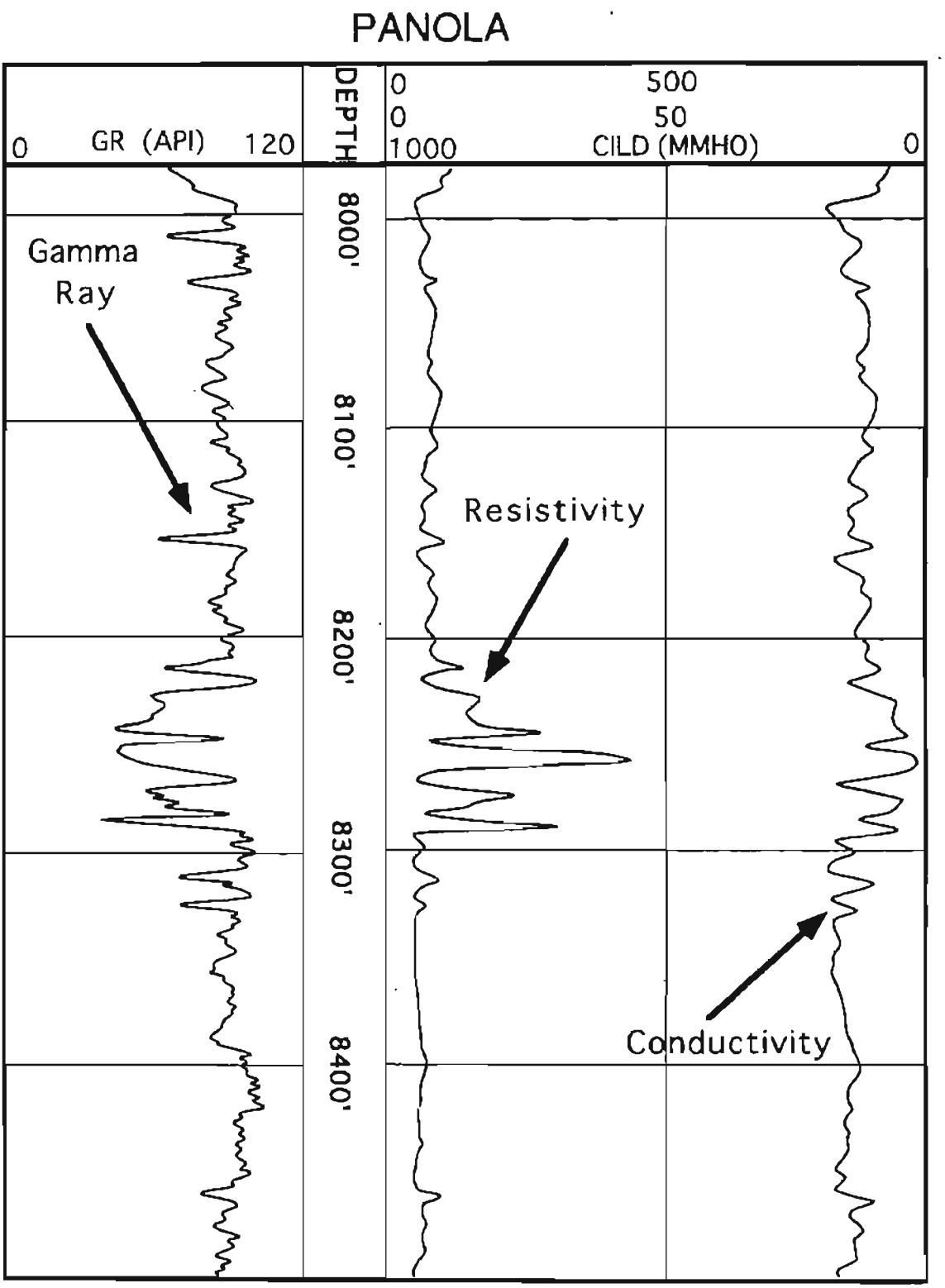

Figure 21: Log signature of Panola sandstone: Amoco Production Co. Kent unit no. 2, Red Oak Field, Latimer County, Oklahoma Section - 19 Township 6 N, Range - 22 E

RED OAK

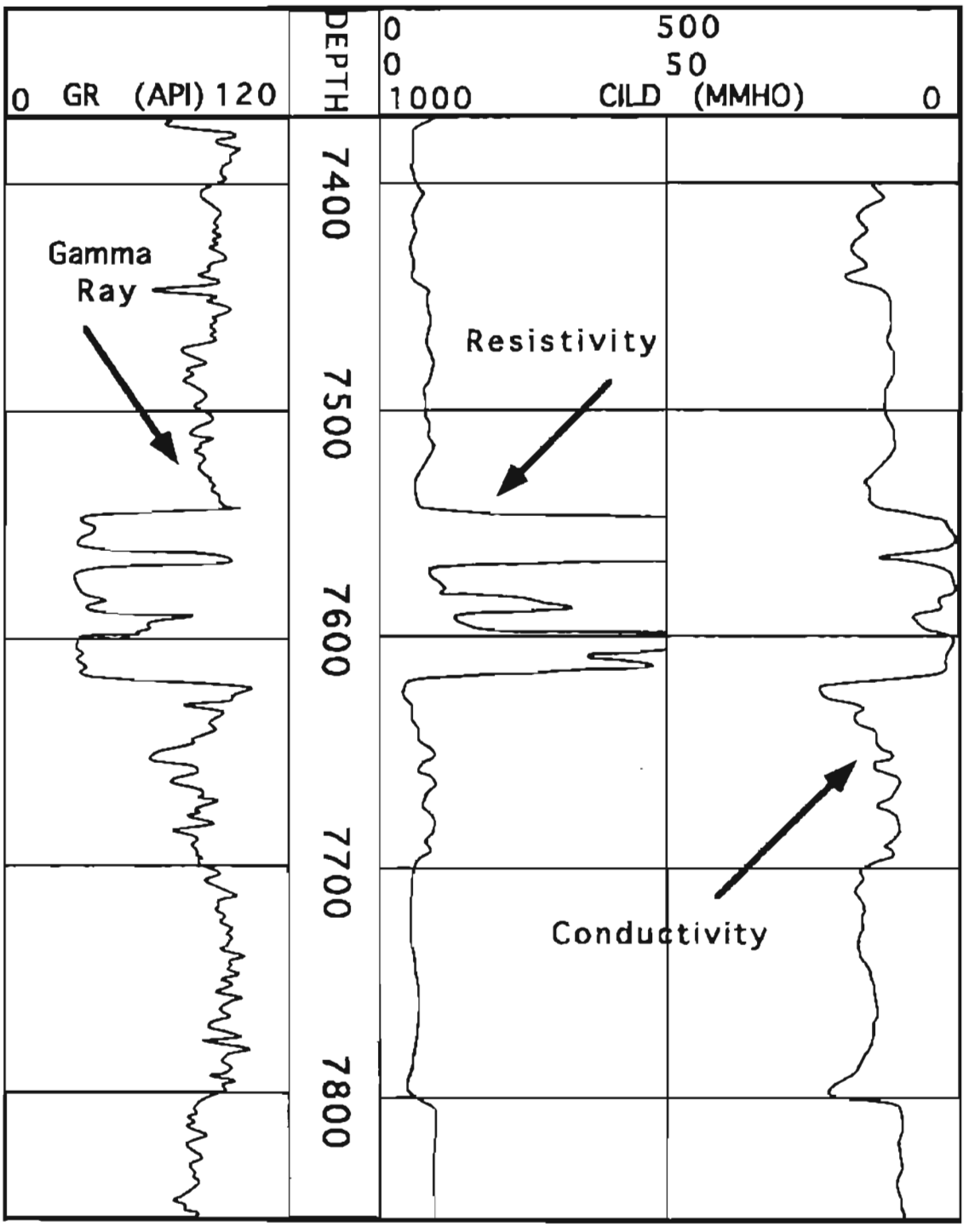

Figure 22: Amoco Production co., Kent unit # 2; Red Oak field
Latimer County, Oklahoma; Sec - 19, Township - 6 N, Range - 22 E

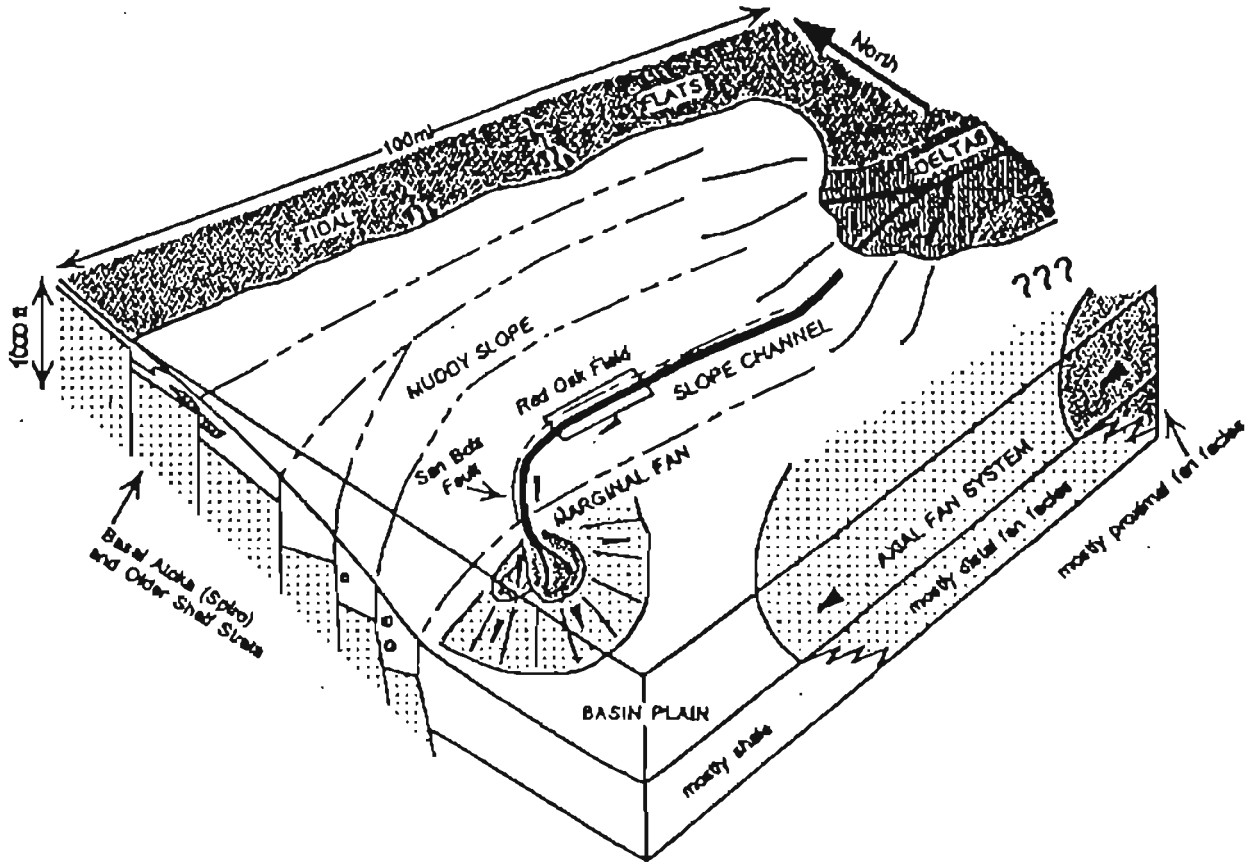

Figure 23 Depositional setting for middle Atokan sandstones, particularly the Red Oak. (From Houseknecht and McGilvery, 1990)

induced by flexural down warping had ceased by middle Atokan time. However, compaction and dewatering of the underlying shales could have absorbed any continued displacement along individual faults (Sutherland, 1988).

The basin is overlain in the axial part by Desmoinesian rocks. This series consists of the Krebs, Cabaniss, and Marmaton Groups (Figure 24). Desmoinesian strata are not found in the frontal Ouachitas and it is unknown whether younger strata were ever deposited in the region. Northward on the shelf, the depositional environment continued to be influenced by fluvio-deltaic processes, with intermittent sandstones separated by thick, shallow marine shales (Sutherland, 1988). The Krebs Group is composed of the Hartshorne, McAlester, Savanna, and Boggy Formations. No strata younger than the Boggy Formation are found within the study area.

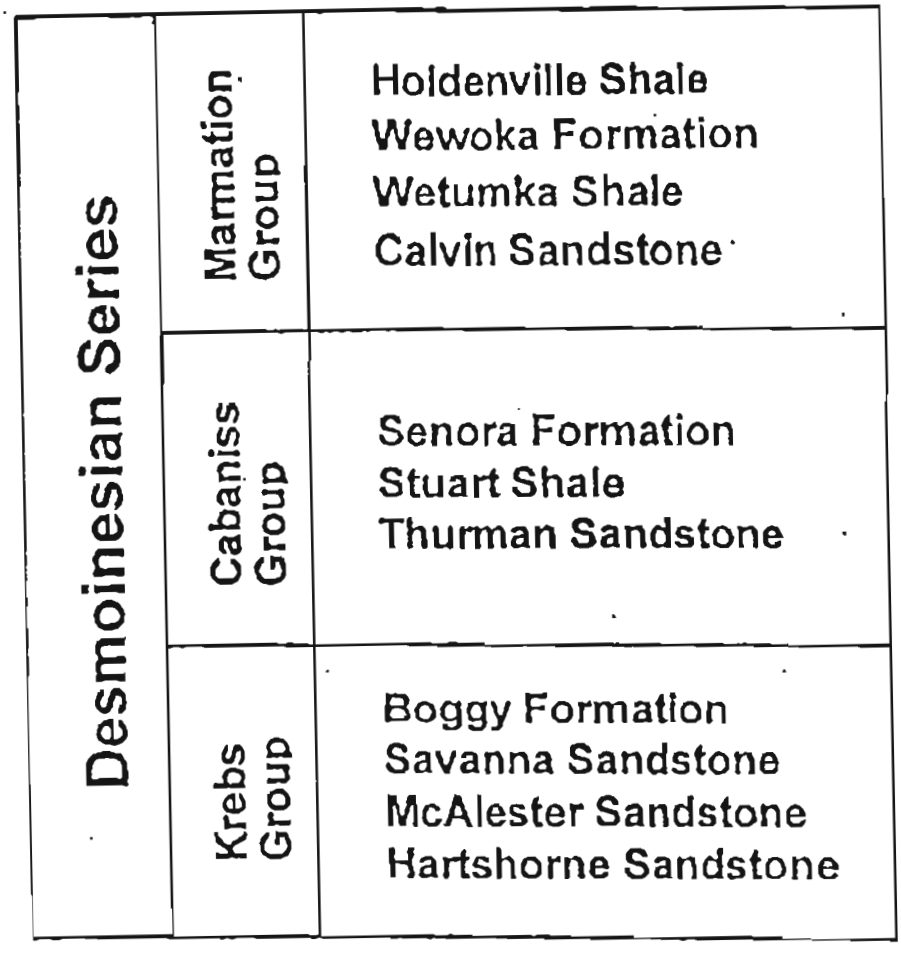

Figure 24. Stratigraphic chart for the Desmoinesian Series in the Arkoma Basin of Oklahoma. (From Sutherland, 1988)

CHAPTER IV

PETROGRAPHY OF SPIRO SANDSTONE

The Lower Atokan Spiro Sandstone is one of the major gas reservoirs in the Arkoma Basin. Extensive research on the petrographic and diagenetic characteristics of the Spiro Sandstone, along with its depositional environment has been performed by Al-Shaieb (1988), Al-Shaieb and others (1995), Akhtar (1995), Sagnak (1996), Evans (1997), and Ronck (1997). These studies serve as the foundation for this study, during which 29 thin sections from the outcrop of the Spiro sandstone and subsurface core obtained from Sarkey- Thrift well # 1-17.

Also examined during this study was the effect of deformation bands on the porosity of the Spiro sandstone on the surface outcrop of the sandstone on the hanging wall of the Choctaw fault zone.

Petrology

Detrital Constituents

The dominant detrital grain in the Spiro sandstone is quartz which composes about 90 to 95 percent of the rock (Figure 25 and 26). The grains are mostly single crystals with uniform extinction (Al-Shaieb, 1988). Quartz grains are medium to fine grained and exhibit straight to slightly undulose extinction. Compaction of grains is indicated by interlocking of grains. Most of the quartz grains are monocrystalline, although minor

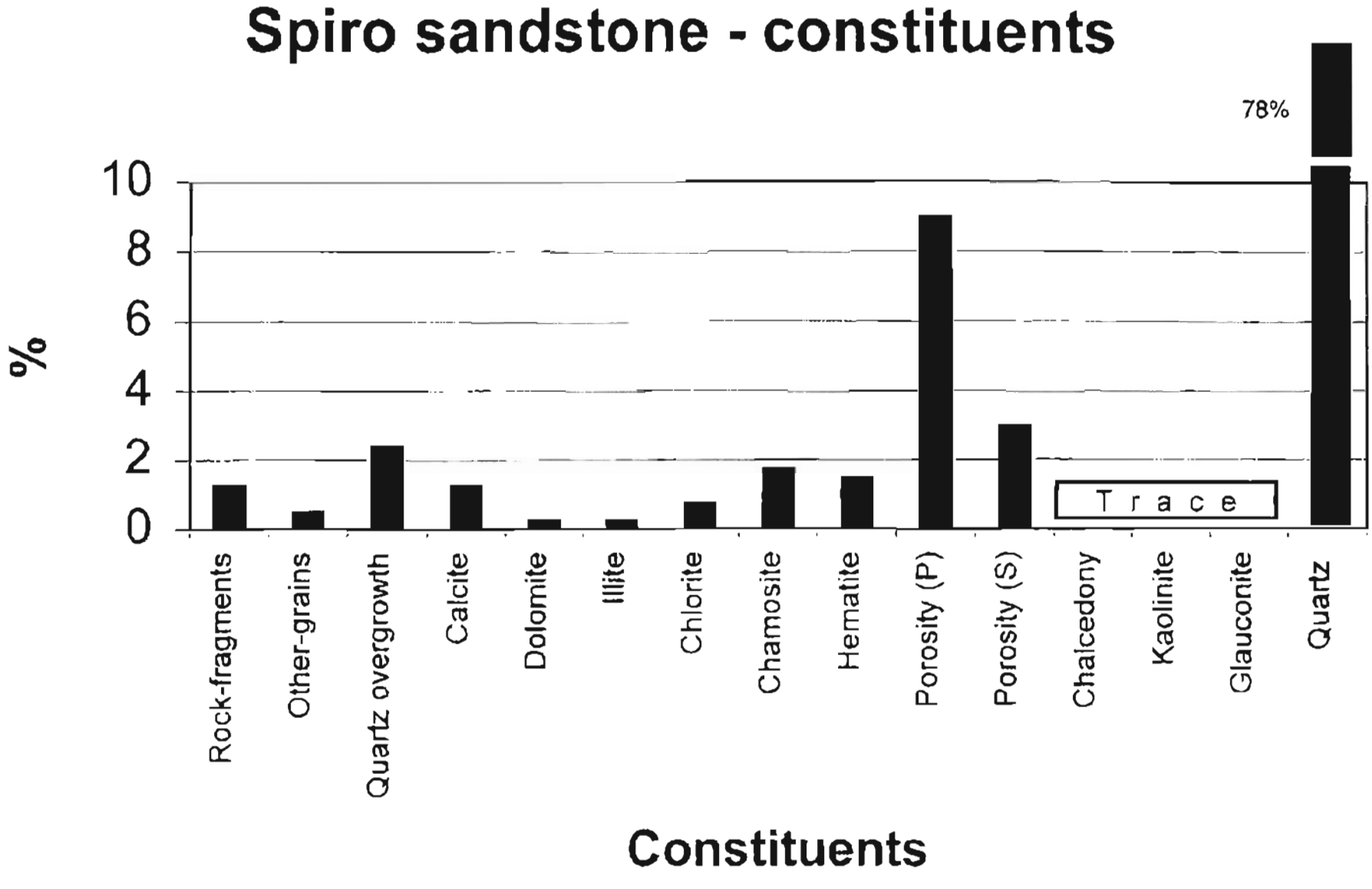

Figure . 25. Mineralogical constituents of Spiro sandstone (histogram)

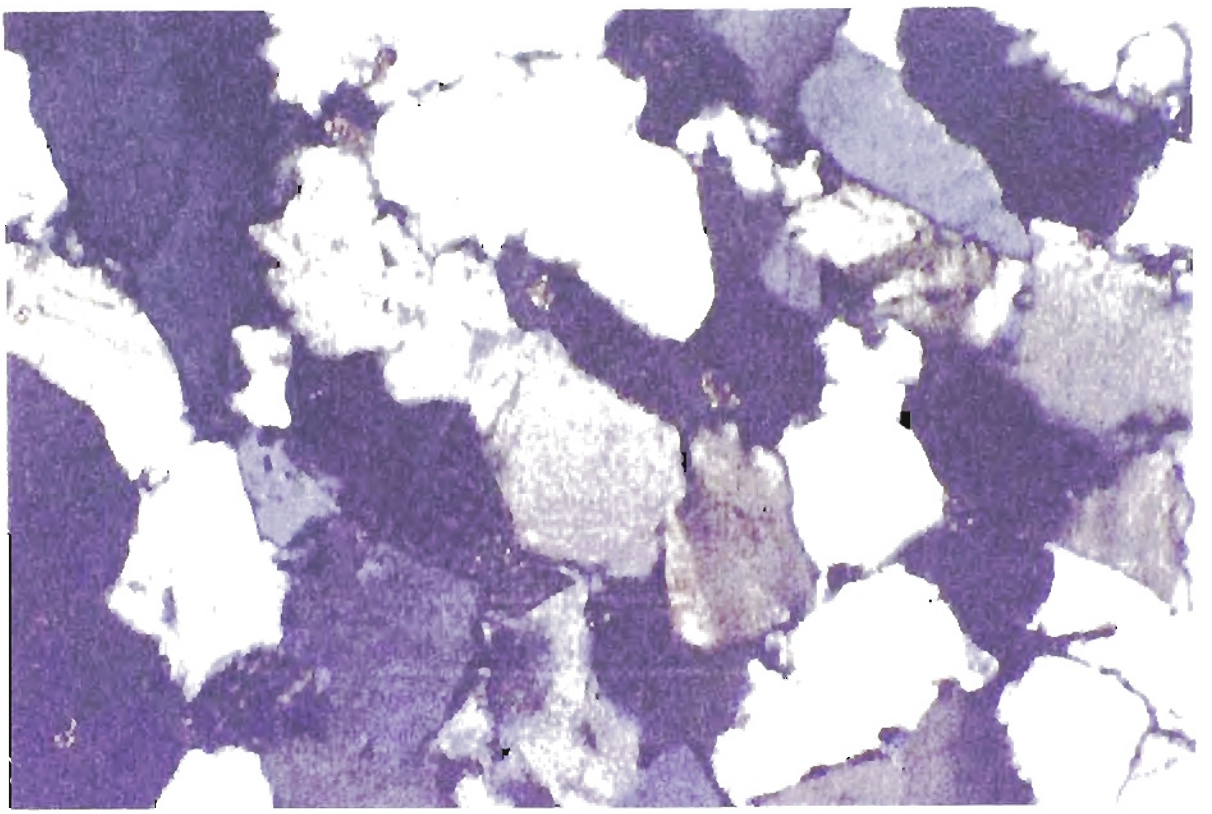

Figure 26 : Photomicrograph showing quartz as the dominant framework grain. The Spiro is generally medium to very fine grained. (x100; XN)

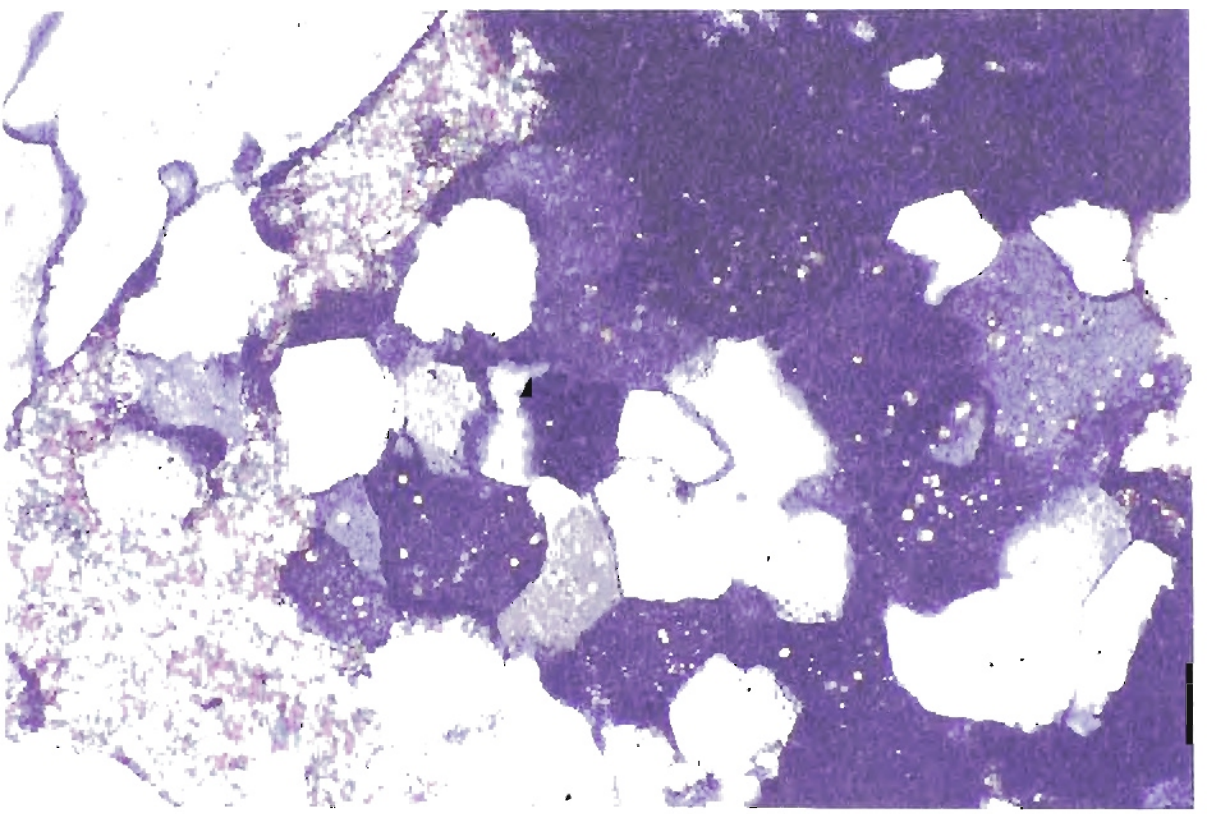

Figure 27 : Photomicrograph showing polycrystalline quartz with calcite cement (x200; XN)

amount of polycrystalline quartz is also identified (Figure 27). Vacuoles and inclusions are present in many quartz grains. In addition to quartz, rock fragments, skeletal grains, and glauconite were present. They constitutes the remaining 5 – 10 percent of the detrital constituent. Minor constituents also include zircon, phosphate, muscovite and biotite (Figure 28) (Al-Shaieb, 1988).

Rock fragments though not common in the Spiro, include both metamorphic and sedimentary rocks. Sedimentary rock fragments are shale clasts and siltstones.

According to Al-Shaieb (1988), Al-Shaieb and others (1995), and Sagnak (1996), the major skeletal debris within the Spiro Sandstone includes echinoderm plates and stems, brachiopod shells and spines, and bryozoan fragments, with minor traces or trilobites, ostracods, gastropods, fusilinids, and coral fragments. These fragments range in size from medium pebble to medium sand. Spiro thin sections of the outcrop within the study area and the thin sections of Sarke - Thrifty well # 1-17 core contain only minor traces of bioclastic debris.

Diagenetic Constituents:

Cements: Silica and carbonate are the major cementing agents identified in the Spiro Sandstone. Minor amount of dolomite cement is also present. Silica occur in the form of syntaxial quartz overgrowths on individual quartz grains (Figure 29). These overgrowths are marked by dust rims that separate the grain and overgrowth. Al-Shaieb (1988), Al-Shaieb and others (1995), Akhtar (1995) and Sagnak (1996) identified these dust rims as chlorite or iron rich chlorite (chamosite) (Figure 30). In the footwall of the Choctaw fault, chamosite acts to prevent the formation of quartz overgrowths and preserves the primary porosity. However in the hanging wall of the Choctaw fault,

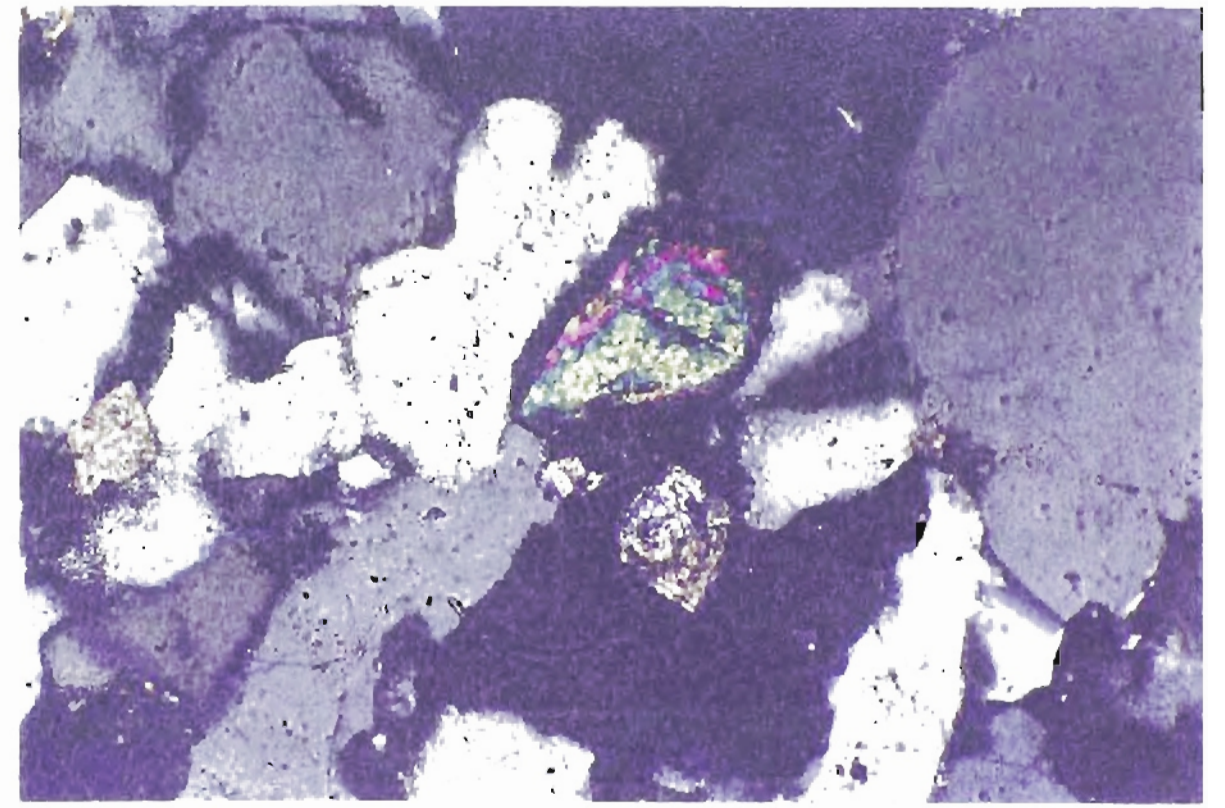

Figure 28 : Photomicrograph showing a detrital zircon crystal. It is identified on the basis of strong to extreme birefreingence and very high relief (x200; XN)

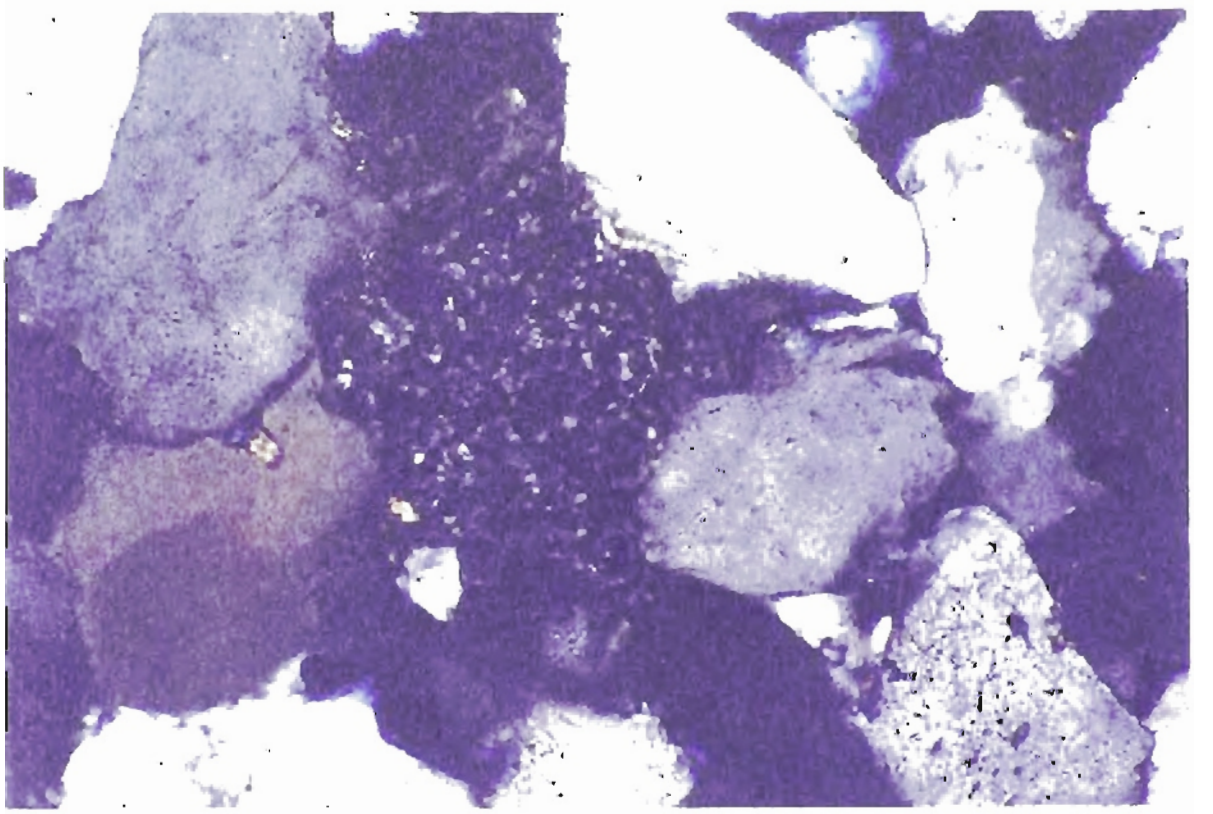

Figure 29 : Photomicrograph showing authegenic kaolinite filling primary pore spaces, and is surrounded by quartz grains (x200, XN).

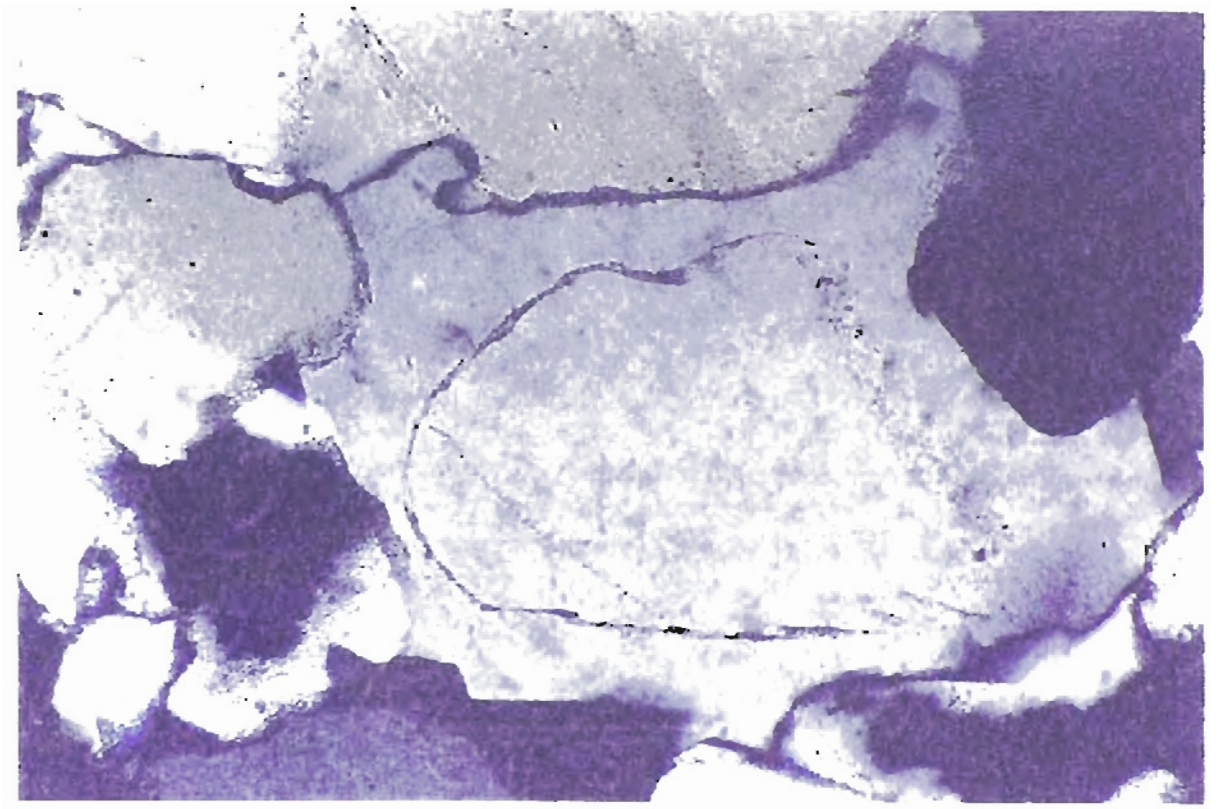

Figure 30 : Photomicrograph of a quartz overgrowth. The original grain is seperated from the overgroth by a dust rim. (x200; XN)

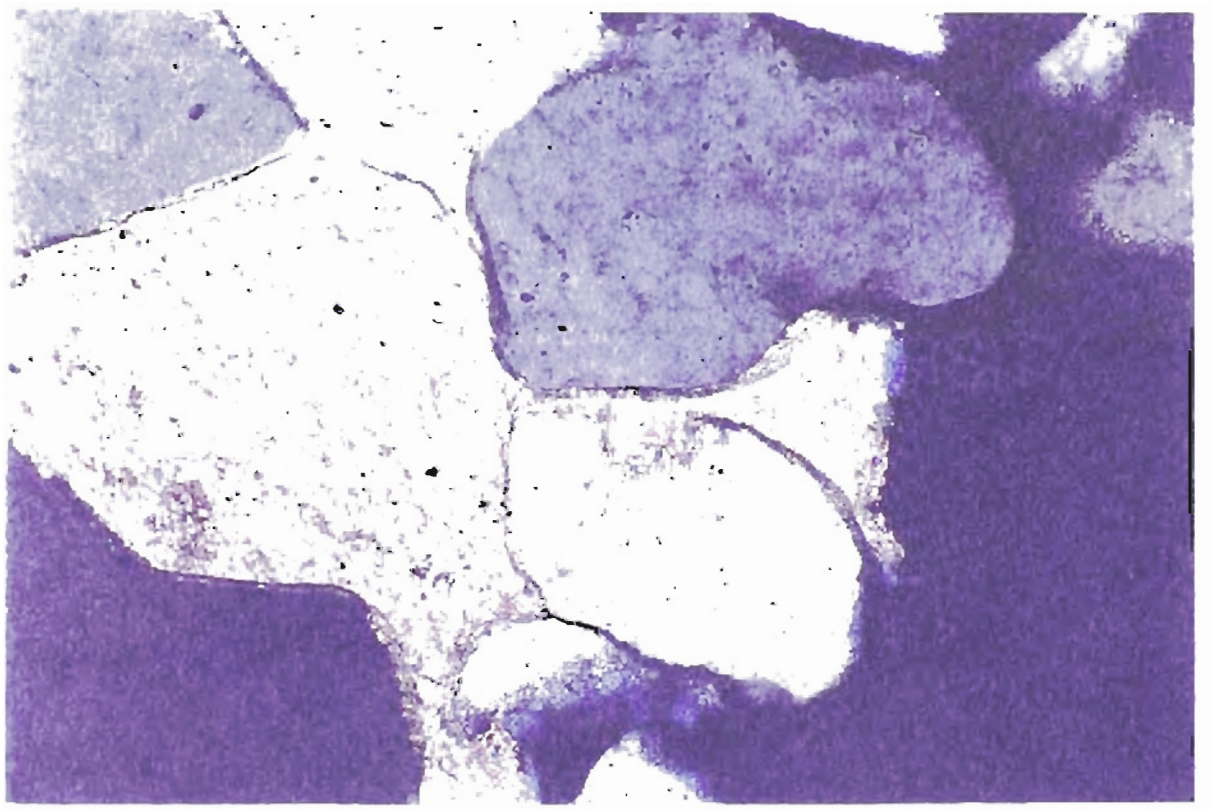

Figure 31 : Photomicrograph showing calcite cement filling voids and partially replacing metastable constituents such as quartz (x200; XN).

absence of chamosite resulted in the cementation and destruction of primary porosity (Figure 31). Thin sections examined in this study were from both the hanging wall and the footwall of the Choctaw fault.

Calcite cement fills void spaces and replaced bioclastic debris, quartz grains and other metastable constituents (Figure 32). Calcite cement is present in several forms. It varies from being patchy to being widespread. The latter is exhibited by quartz grains gloating in calcite to form poikilotopic texture. In some instances, the migration of fluids has allowed adequate dissolution of calcite, resulting in moldic and vuggy porosity.

Diagenetic Clays: Chlorite and chamosite were the major diagenetic clays identified in the thin sections, along with minor amounts of siderite. Chlorite, which is typically brownish-green in both plane-polarized light and under crossed-nichols, coats grains, and fills voids. Chamosite, on the other hand was predominantly grain coating. This resulted in preservation of primary porosity and thus represents the reservoir facies of the Spiro Sandstone. The amount of chamosite in the Spiro Sandstone ranges from traces to around 4 percent in the footwall of the Choctaw fault, and only negligible traces in the hanging wall of the Choctaw fault (Figure 33).

Porosity: Both primary and secondary (intergranular and intragranular) porosities were observed in the thin sections of the study area, but primary porosity was more abundant (Figure 34 & 35). Cementation, compaction and dissolution greatly modified the intergranular primary porosity. Complete preservation of the primary porosity is only observed in those areas where quartz grains were lined with coats of almost syndepositional chamosite.

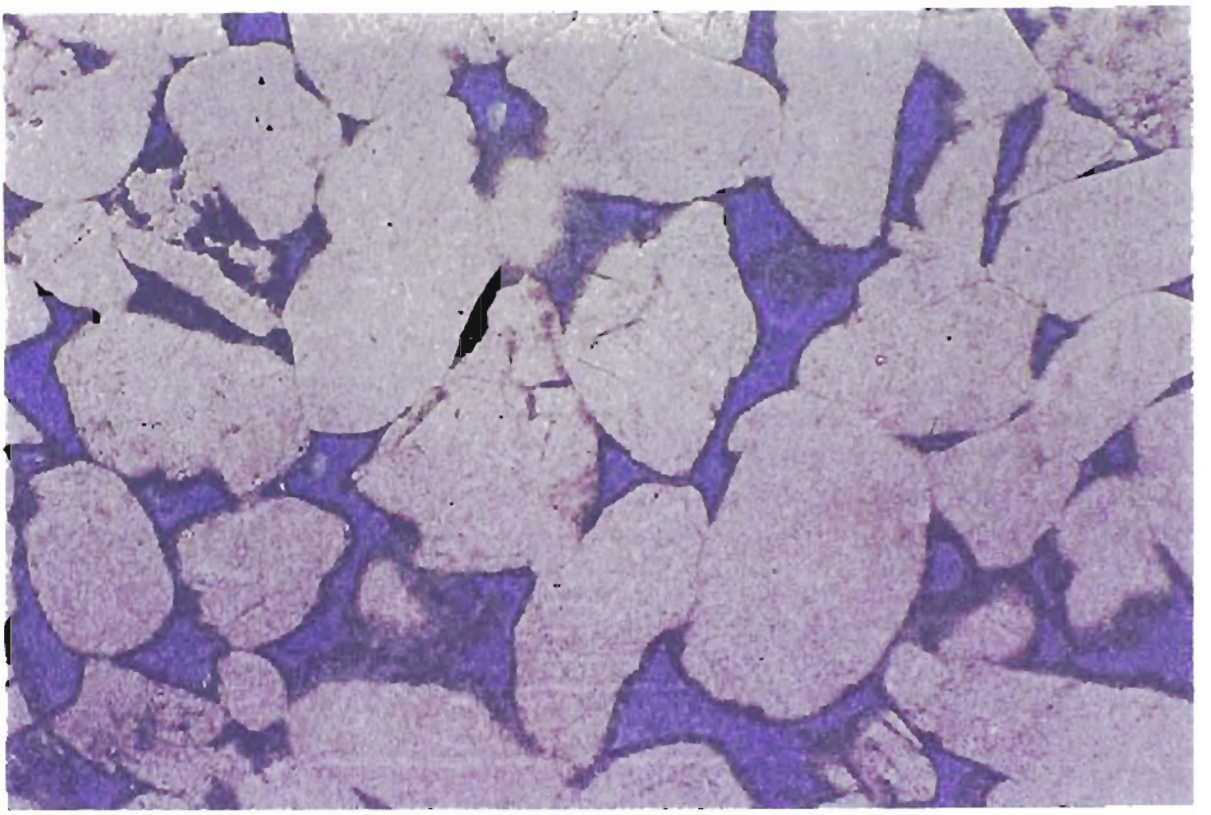

Figure 32 : Chamosite clay is coating the quartz grain and preserving the primary porosity (blue) (x100; PP).

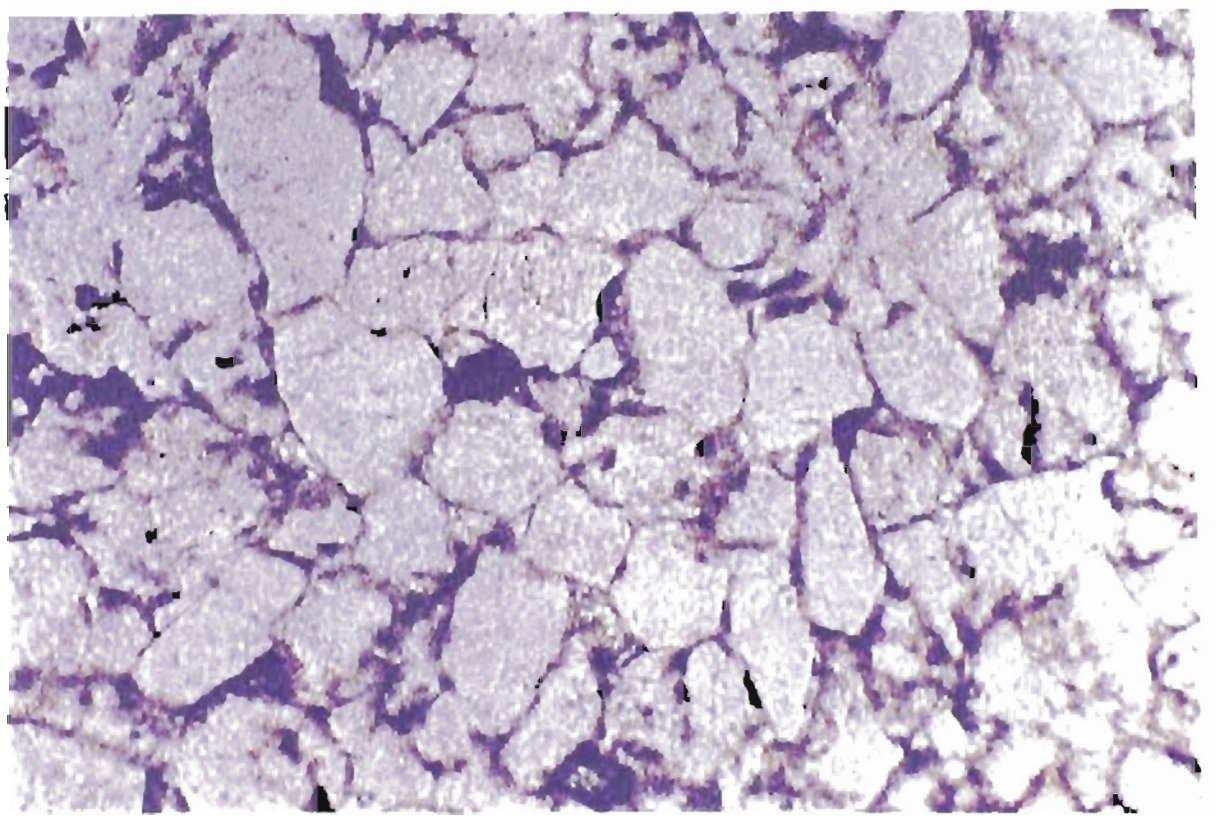

Figure 33 : Photomicrograph showing effects of cementation and destruction of primary porosity in the absence of chamosite coating around the quartz grains (x100; PP).

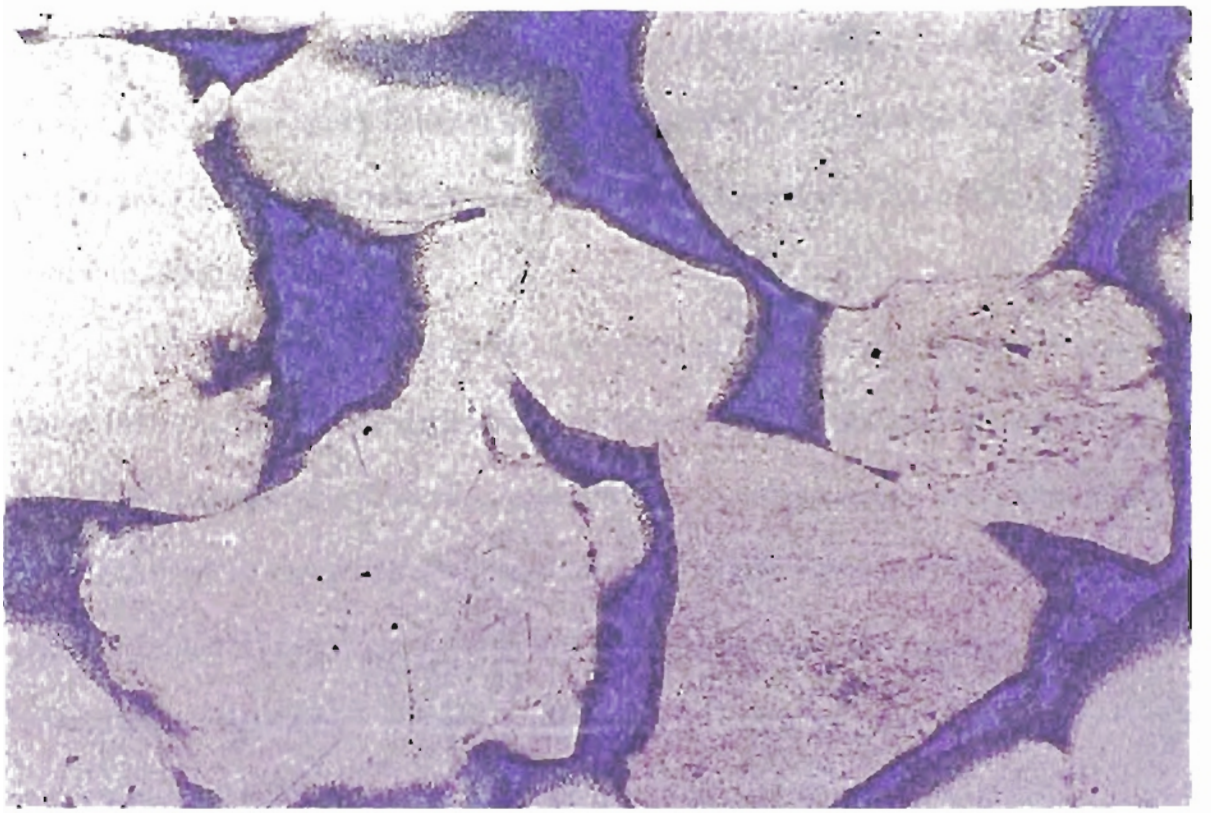

Figure 34 : Primary porosity preserved due to coating of chamosite around the quartz grains (x200, PP)

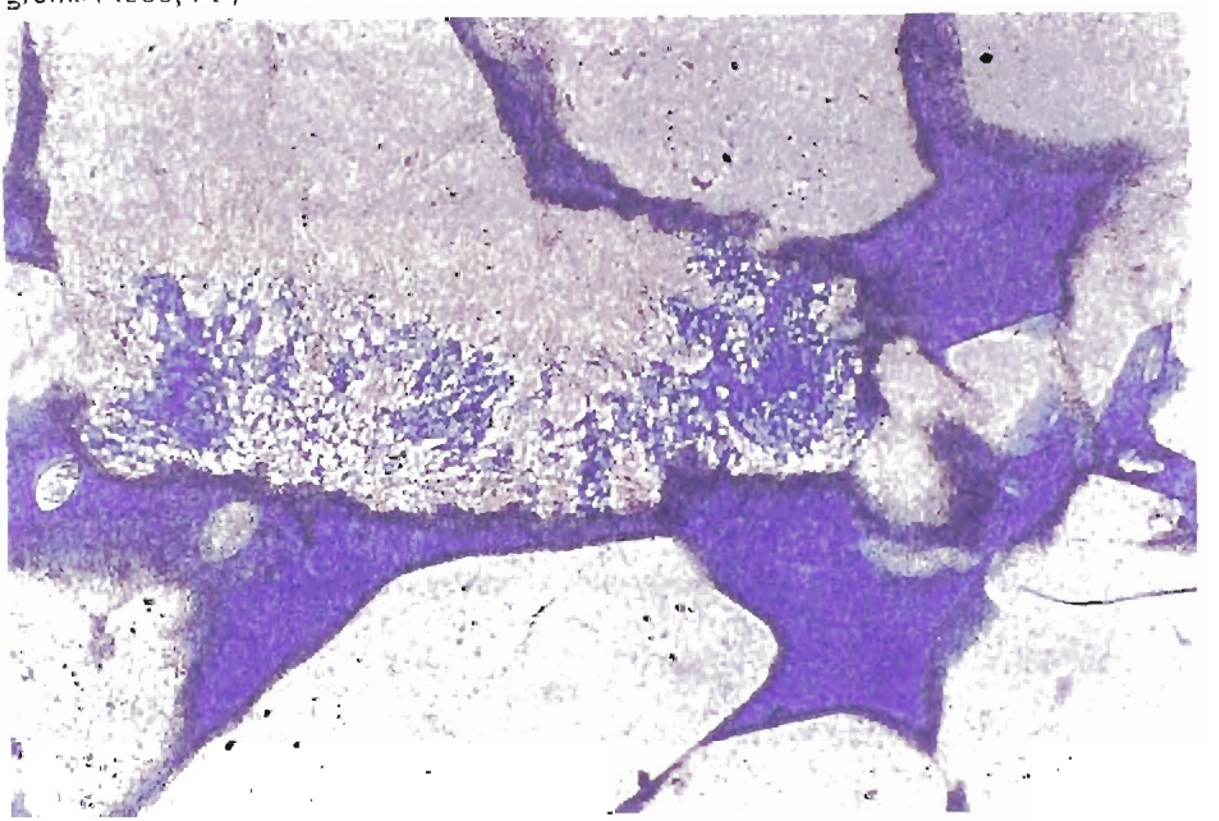

Figure 35 : Intragranular secondary porosity resulting from dissolution of quartz grains. Some preserved primary porosity also identified in this photomicrograph. (x200; PP).

Diagenetic History: Lumsden and others (1971), Al-Shaieb (1988); Al-Shaieb and others (1995); Hess (1995); Feller (1995); Akhtar (1995); Al-Shaieb and others (1995) and Sagnak (1996) have made extensive contributed to interpretation of the diagenetic history of the Spiro Sandstone.

Al-Shaieb (1988) concluded that diagenesis of the Spiro sandstone occurred almost immediately after the deposition with selective areas within the Spiro experienced coating by chamosite due to settling. Quartz grains in chamosite rich zones were coated with thick coats of chamosite, whereas in relatively chamosite poor environment, quartz grains remained relatively clean. With increasing depth of burial, compaction processes reduced part of the primary porosity.

Quartz overgrowth has a significant role in reducing the primary porosity. These overgrowths are precipitated around those quartz grains where very little or no chamosite. Advanced stages of overgrowths usually occluded pore space completely (Figure 29). On the other hand, quartz grains with thick coats of chamosite that retarded pressure solution, retained primary pore space which allowed fluid circulation (Al-Shaieb, 1988). Calcite cementation followed silica precipitation/cementation stage. In calcite cemented areas, both primary and secondary porosities are negligible. Calcite cement decreased the permeability of the rock and inhibited fluid migration. By the end of the calcite cementation stage, porosity was completely obliterated in clean sandstone facies by either quartz overgrowths or carbonate cements. However, significant amount of primary porosity was still preserved in the relatively chamosite rich sandstone. The porosity provided migration pathways for constructive fluids to create secondary porosity, increased permeability, and helped the migration and accumulation of hydrocarbons.

Figure 36 shows the relationship between the various diagenetic stages and the porosity preservation and development in the Spiro sandstone.

Depositional Environment: Al-Shaieb (1988), Al-Shaieb and others (1995), Akhtar (1995) and Sagnak (1996) suggested through their studies of outcrop and cores, that the Spiro sandstone was deposited in shallow marine environment. Chamosite, glauconite and skeletal debris observed in the thin sections confirm the interpretation. The Spiro is marked by medium scale trough cross-bedding with flow structures. Houseknecht (1987), Lumsden (1971) and others suggested that sedimentary structures within the Spiro indicate a fluvial depositional environment. The blocky log character commonly observed along the base of the Spiro suggests a prograding or aggrading sand unit (Gross and others, 1995). Sutherland (1988) concluded from his own findings that the Spiro sandstone was deposited in a tidal-flat environment.

DEFORMATION BANDS IN THE SPIRO SANDSTONE

Within the study area, deformation bands occur in the Spiro Sandstone outcrops near major thrust. They are small 'fault-like' structures that develop in porous granular Materials.

Samples were collected from several outcrops of Spiro Sandstone in the Ouachita Mountains (Figure 37). Figure 38 shows a Spiro sandstone sample within deformation bands and another sample without deformation bands. 28 thin sections impregnated with blue epoxy (to enable porosity determination) were studied in order to understand the types of deformation bands and to estimate the amount of porosity. Point counting of thin sections was conducted to determine the two-dimensional porosity within the

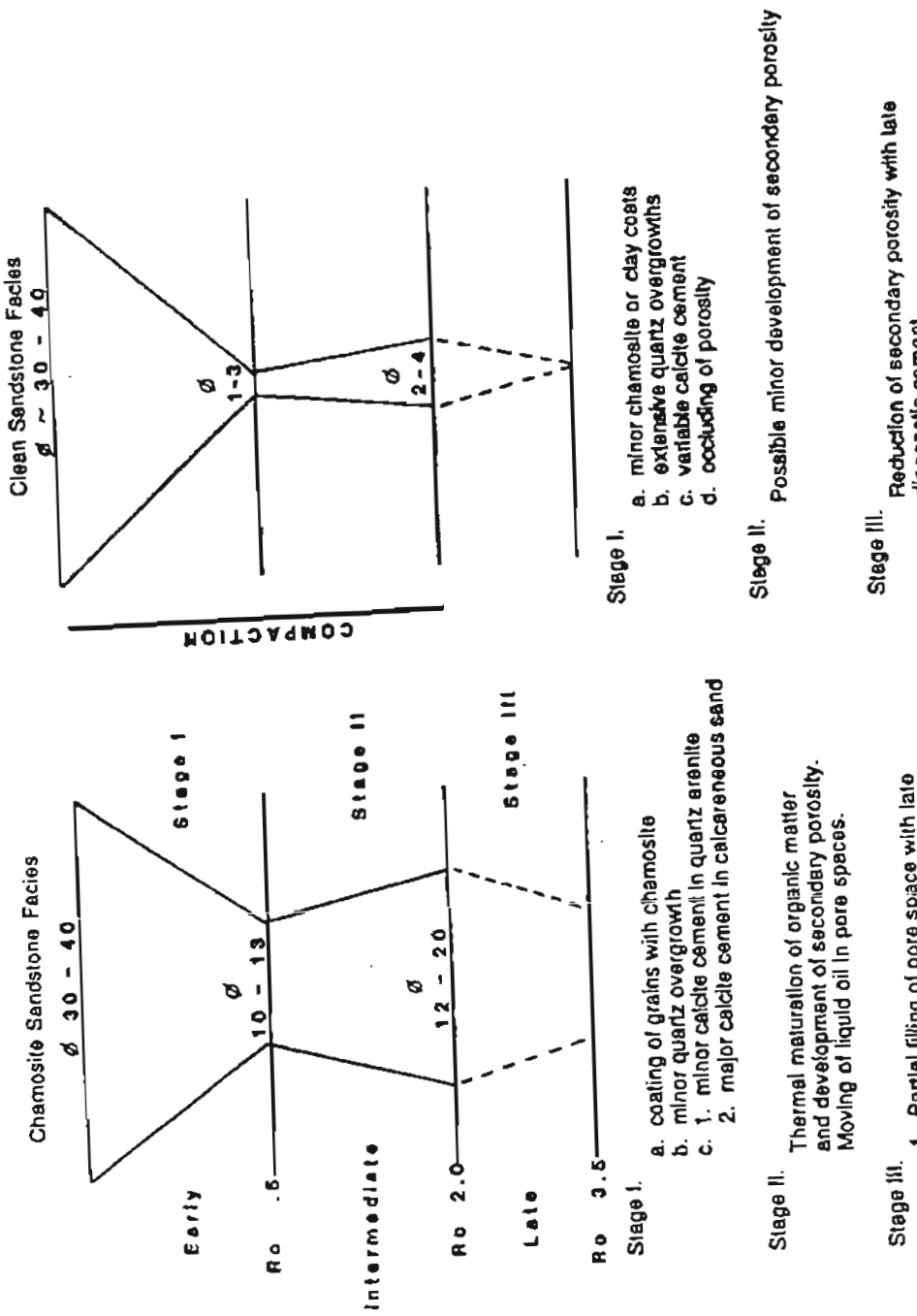

Figure 36. Preservation and /or development of porosity as related to diagenesis (From Al-Shaieb, 1988)

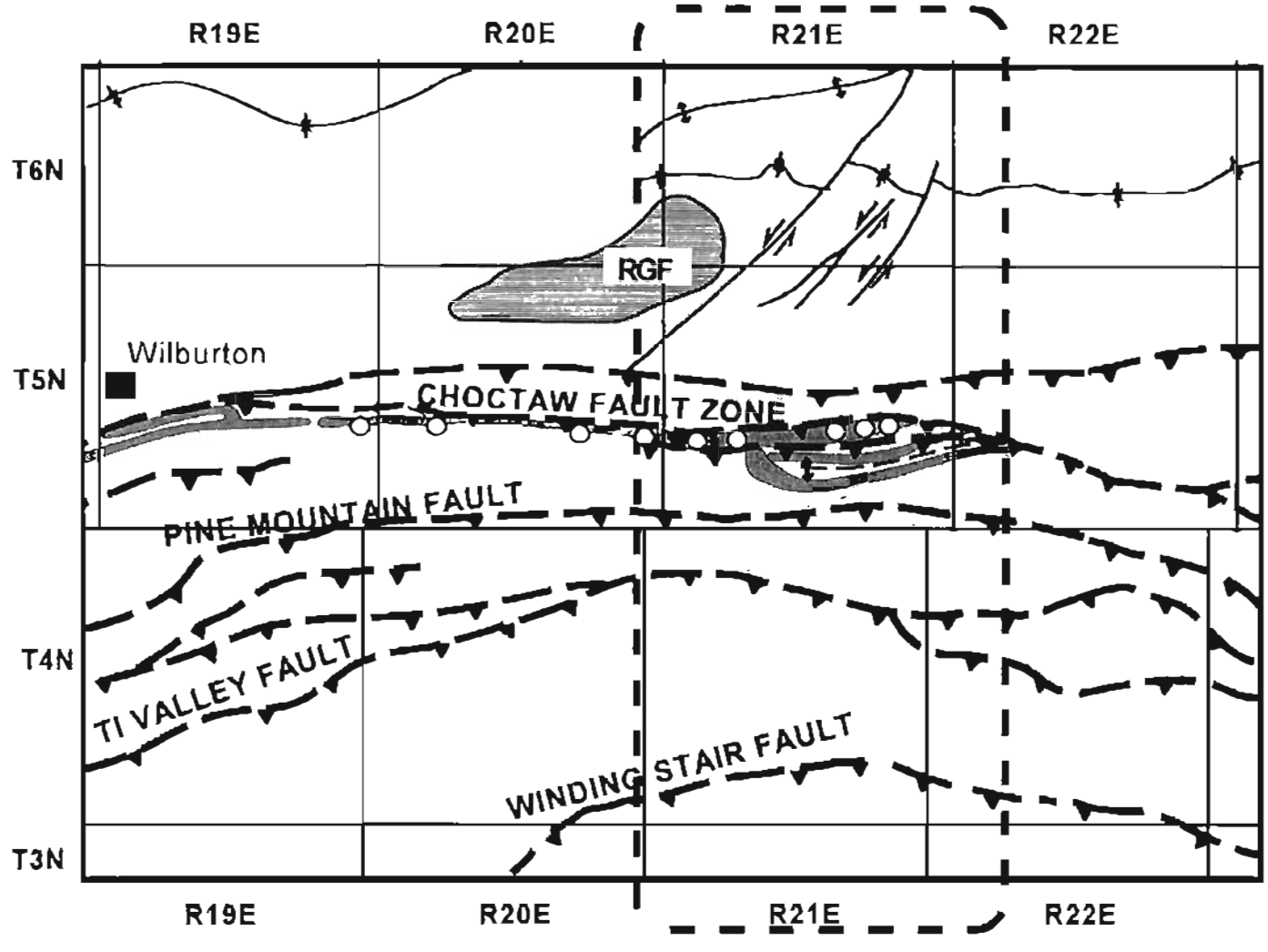

Figure 37: location of the samples that were collected for the study of the deformation bands in the Spiro sandstone. The study area is shaded.

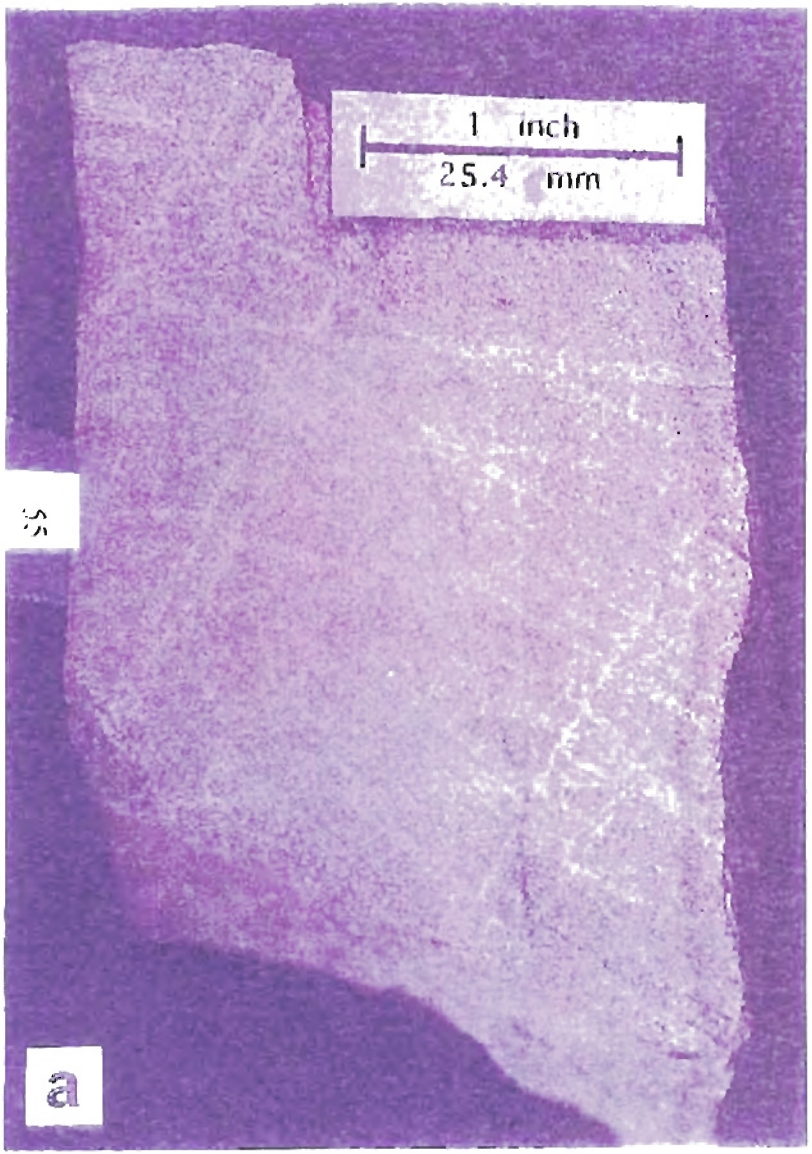

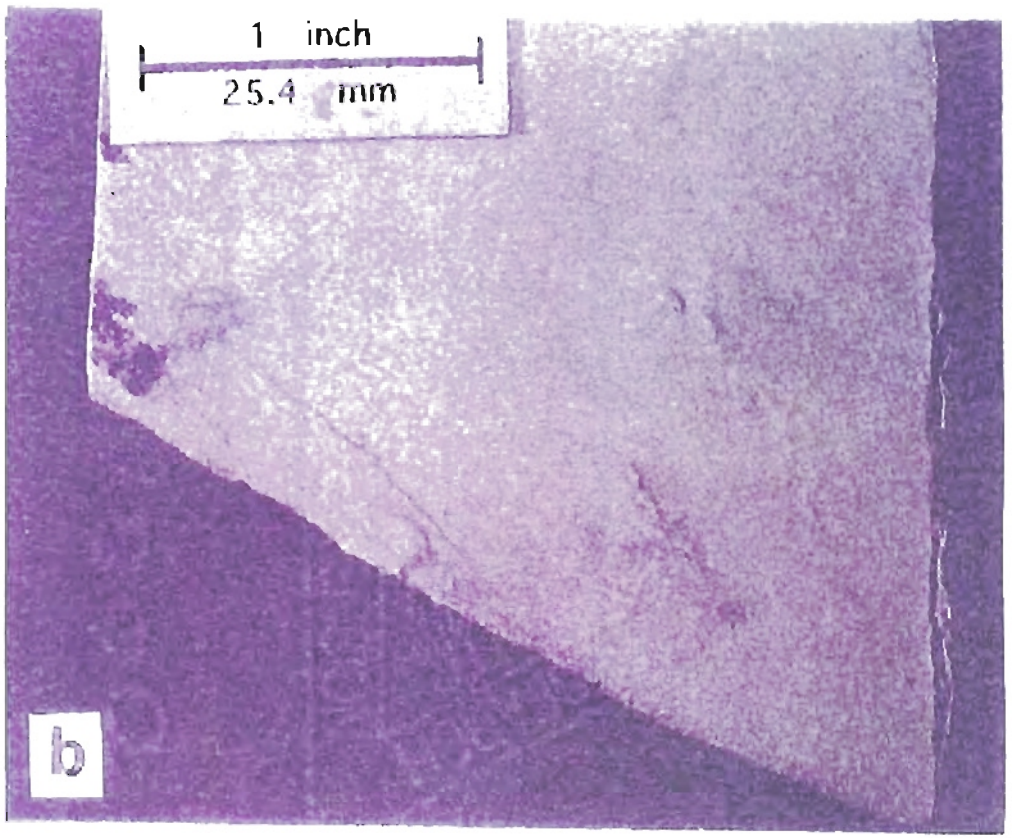

Figure 38 . Photographs showing spiro sandstone samples (a) with deformation bands and (b) without deformation bands

deformation bands, outside the deformation bands, and in the rocks away from the faulted zone within the Spiro Sandstone.

The deformation bands observed in the thin sections are associated with cataclasis deformation within the fault zone (Figure 39 a and b). A characteristics of these deformation bands is the presence of grain crushing and porosity reduction, similar to the ones observed in the porous sandstones at Arches National park, Utah by Antonellini and others (1994). The amount of cataclasis is variable from a few patches of crushed grains in pods and pockets aligned along a line to a fully developed cataclastic zone about 1 – 2 mm thick. Deformation bands with cataclasis have a thickness that is not dependent on grain size. The amount of cataclasis is more in bands closer to fault planes, or in zones near fault planes where the host rock has been compacted (Figure 39 a-b).

From thin-section studies, it was identified that porosity within the deformation bands is almost negligible (< 1 %), whereas the porosity in the immediate vicinity of the deformation bands is around 4 % (Figure 40). Porosity in rocks away from the faulted zones ranged between 4 – 20 % (Figure 41). Therefore, porosity determinations in the thin sections of the Spiro sandstone suggest that deformation bands have substantially lowered porosity with respect to their surrounding.

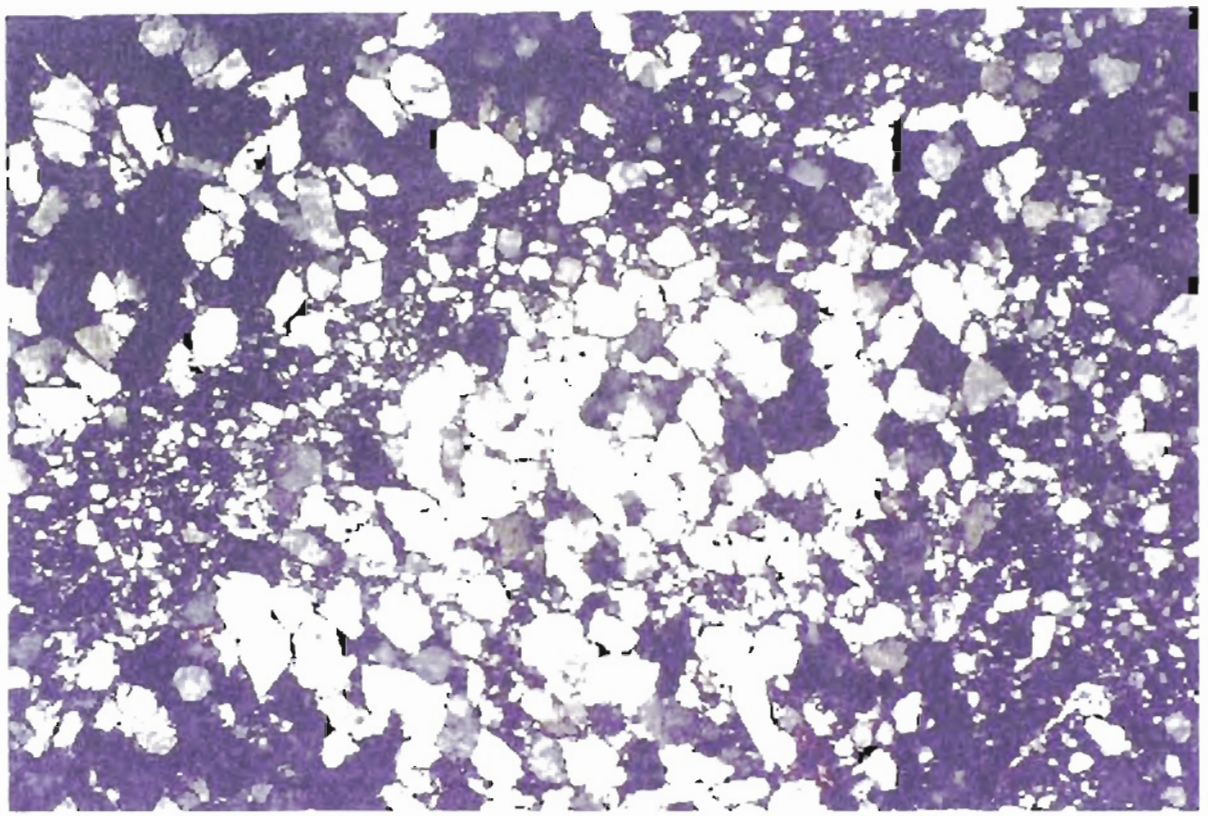

Figure 39a : Photomicrograph of Spiro sandstone showing sparse cataclastic zone to thick fully developed cataclastic flow (x40, XN)

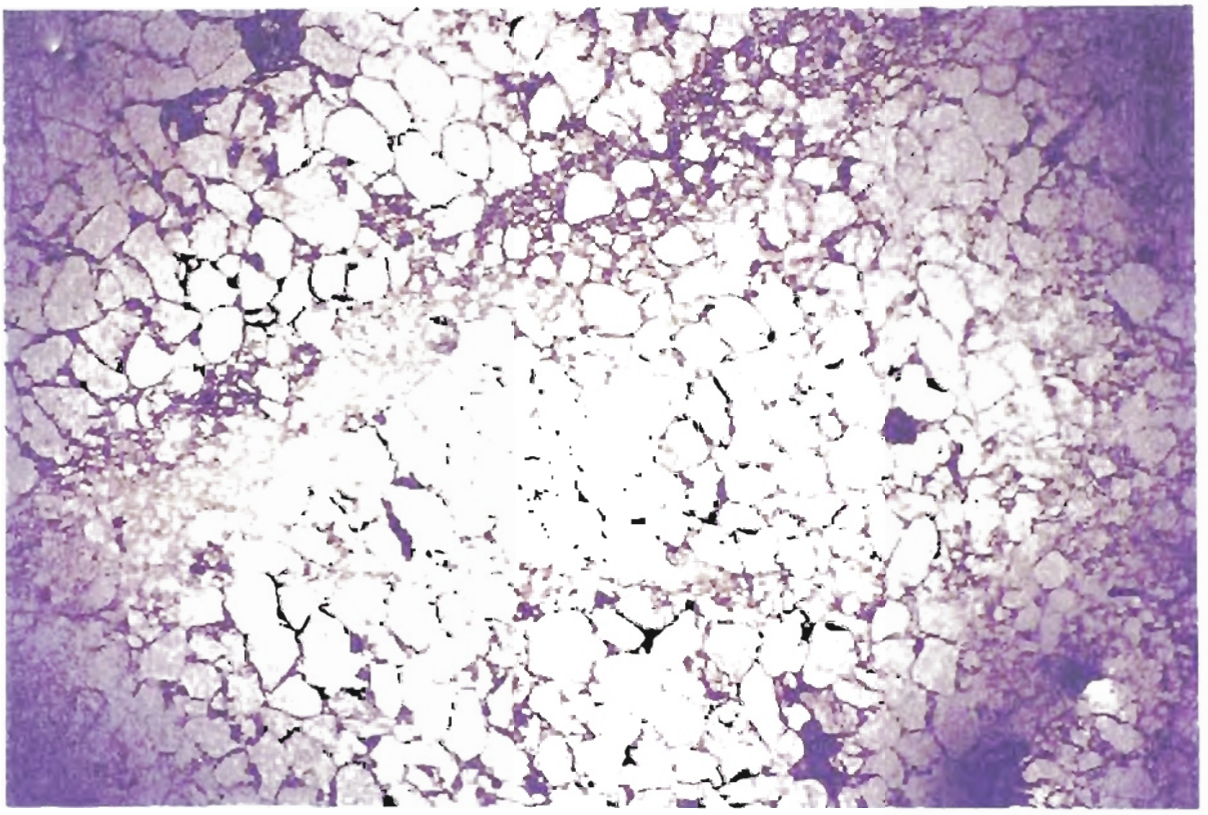

Figure 39b : Photomicrograph of Spiro sandstone showing thick fully developed cataclastic flow to sparse cataclastic zone (x 40; PPL)

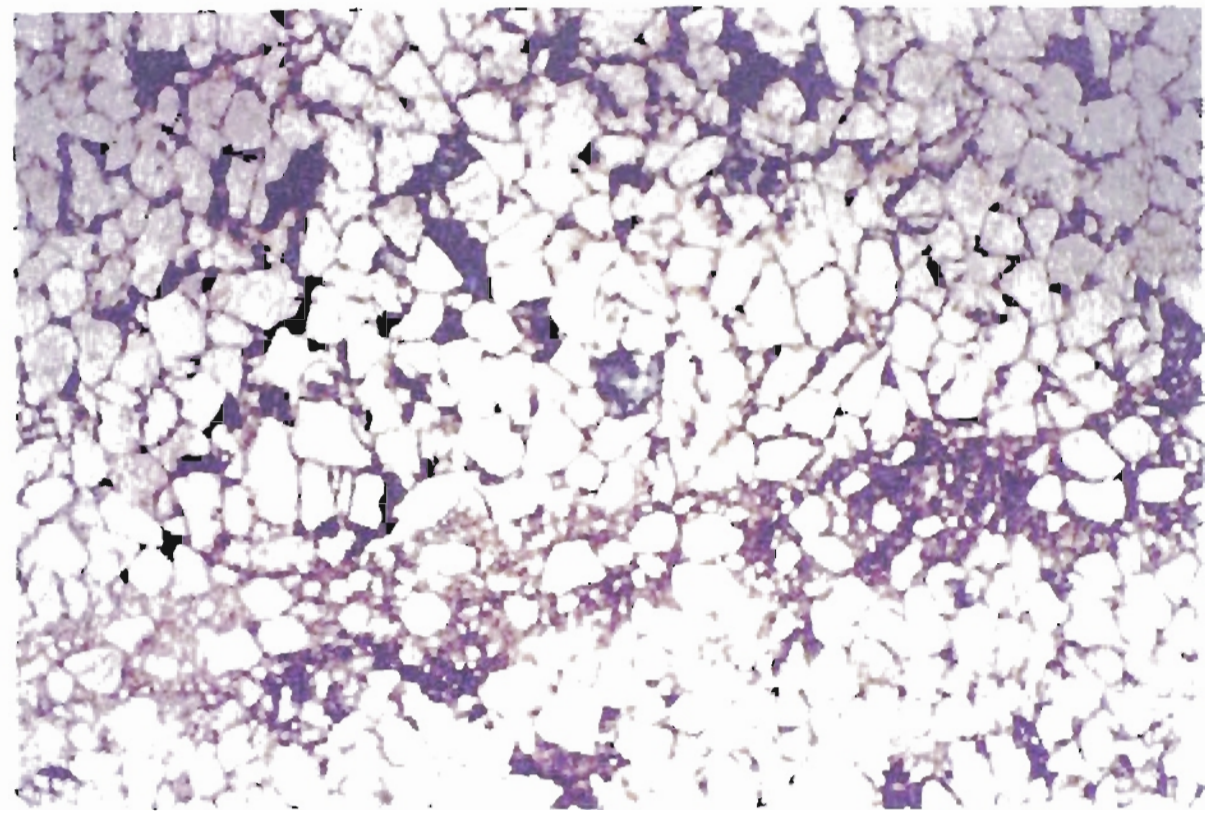

Figure 40 : Photomicrograph of Spiro sandstone showing deformation bands in rocks within the fault zone. Figure is clearly indicating lower porosity (x 40, PPL).

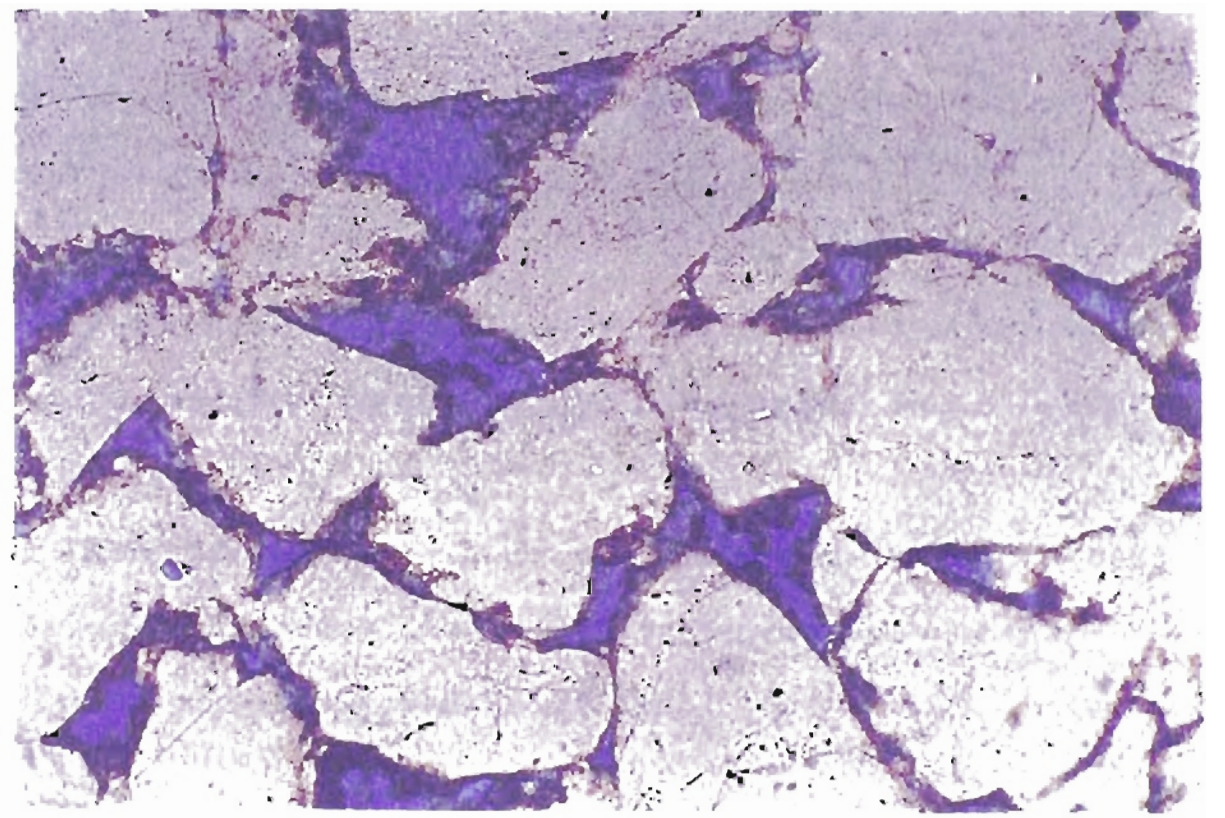

Figure 41 : Photomicrograph of Spiro sandstone showing no deformation bands outside of the fault zone. Figure is clearly indicating higher porosity (x 200; PPL).

CHAPTER V

STRUCTURAL GEOMETRY OF THRUST SYSTEMS

Introduction

Thrust systems are an integral part of structural geology in general and of 'folds and thrust belts' in particular. A thrust system basically comprises several nearby faults joined in a closely related branching array. Marshak and Woodword (1986, p.307) described thrust system as "an exclusive collection of kinematically related faults that developed in sequence during a single regional deformation and are associated with deformation above a basal detachment." Imbricate fans and duplexes are the basic parts of a thrust system.

IMBRICATE FANS

An imbricate fan is a type of thrust system in which faults cut up section from a basal detachment but do not rejoin at a higher stratigraphic level. There are three types of imbricate fans:

a. *Leading Imbricate Fan:* It is an imbricate fan that has most of its displacement on the 'leading' or 'lowermost' thrust (Figure 42). Leading imbricate fan has minor displacement on hanging wall of a major thrust.

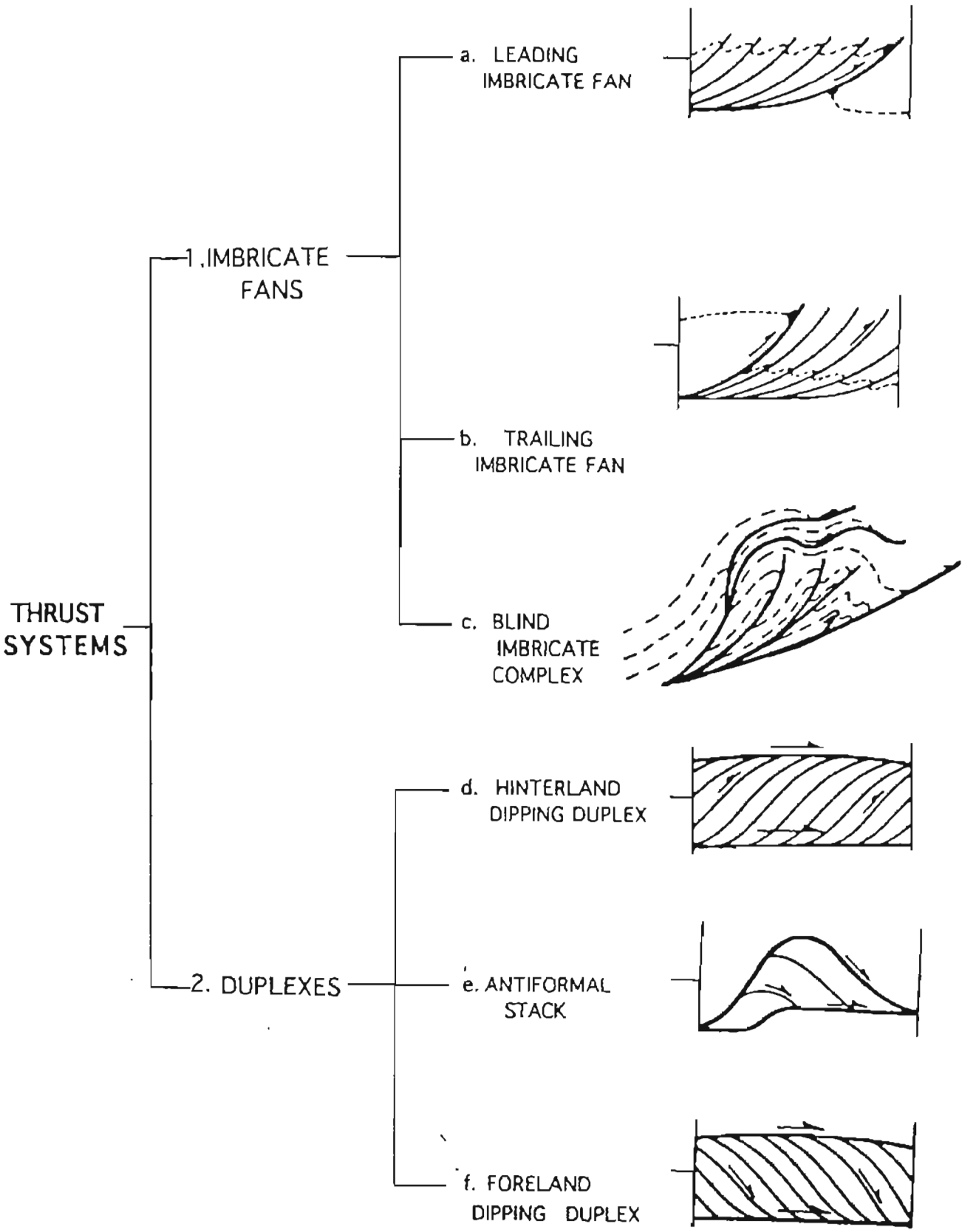

Figure 42. Classification of different systems of thrusts (After Boyer and Elliot, 1982)

b. Trailing Imbricate Fan: It is an imbricate fan that has most of its displacement on the 'trailing' or 'highest' thrust (Figure 42). Trailing imbricate fan has minor displacement on footwall.

c. Blind Imbricate Complex: It is an imbricate fan that remains buried such that the displacement on the imbricate fault below is compensated at a higher structural level by folding, cleavage development, or another set of structures having a different style.

DUPLEX

A duplex is a thrust system in which the faults propagate upward from the basal detachment and rejoin to another detachment surface at a structurally higher level (Figure 42). A simplest duplex consists of a system of ramp-related anticlines with a floor thrust (i.e. the lower thrust surface that bounds a duplex), a roof thrust (the upper thrust that bounds a duplex), and a series of imbricate thrusts connecting the roof and the floor thrusts. The faults cut up from the floor to the roof thrust surrounding by the bodies of rocks - horses. Boyer and Elliot (1982) identified the following types of duplexes:

a. Hinterland Dipping Duplex: When the displacement of the horses are relatively small, they dip predominantly toward the hinterland and form a zone of roughly constant thickness between the roof and floor thrusts, the resulting duplex is called as hinterland dipping duplex. (Figure 42). In this kind of duplex, if the slip on the subsidiary faults is roughly equal to the length of the horse, the adjacent branch lines will bunch up and the horses will lie on the top of one another. This occurs from time to time in a normal duplex. On the other hand if the bunching of the branch lines is widespread, the shingle-

like imbricate pattern is destroyed (Boyer and Elliott, 1982). These duplexes are usually composed of upward-facing horses and always have a forward facing structure.

b. Antiformal Stack: It is formed either when a duplex has a displacement equal to the spacing on the individual imbricates (Figure 42), or each higher horse is folded above the lower ones. This folding dies out downward and provides unambiguous evidence of sequence in which the horses are accumulated into the stack (Boyer and Elliott, 1982).

c. Foreland-Dipping Duplex: It is formed when displacement is twice the spacing and structurally dips towards the foreland (Figure 42). The dipping duplexes were first proposed by Woodward (1981). They usually consist of downward-facing horses, even when the beds are upside down and originated at a footwall syncline with a rolling hinge. They always have a forward structural facing like hinterland dipping duplexes.

FAULT BEND FOLDS:

Fault bend folds are one of the two commonly recurring fold styles within the low temperature portion of thrust belts; the other being fault propagation fold. Fault bend folds were first described by Rich (1934) in the Pine Mountain thrust region of the Appalachians (Tearpock & Bischke, 1991), where he recognized that this fold style consisted of symmetric anticlines. Rich (1934) also recognized that these folds were associated with thrust faults and postulated that the folds were the result of the thin-skinned deformation.

FAULT PROPAGATION FOLDS:

Fault propagation folds are the most common fold types to be observed in outcrops and in seismic (Tearpock & Bischke, 1991). They possess the particular characteristic that as the fold grows the deformation advances at the tip of a propagating

thrust fault. As long as the structure has not been faulted through, the slip is consumed by bedding plane displacements located along the frontal limb of the fold (Figure 43c). Fault propagation folds typically have higher cutoff angles than fault bend folds, in the range of about 20 deg. to 40 deg, which causes these folds types to possess steeply dipping to overturned frontal limbs.

THRUST SEQUENCES

FORWARD BREAKING SEQUENCES

The simplest case of thrust propagation to consider is where displacement are transferred onto a new fault surface generated in the foot wall of the previously active zone. In most cases, this will occur by a flat propagation into the footwall at a ramp so that the higher portions of the fault zone are abandoned. The new fault segment will eventually climb a new ramp and if this process continues in a multiple fashion, an array of thrusts will be generated, all appearing to splay from a single detachment level - the floor thrust. Earlier faults are abandoned and passively carried by later, deeper levels displacements hence this propagation sequence is called "piggyback" or forward breaking.

Development of a Duplex: There are several geometric arguments for the successive development toward the foreland, or a forward progression of a subsidiary faults in duplexes. The oldest argument is best illustrated by Dahlstrom (1970), where a higher horse is folded over a lower one proving a forward development. The method of development based on a series of simple graphic experiments developed by Boyer (1978) (Figure 44). This method can be taken in account after constructing an idealized model based on typical dimensions and angles of observed duplexes assuming plane strains,

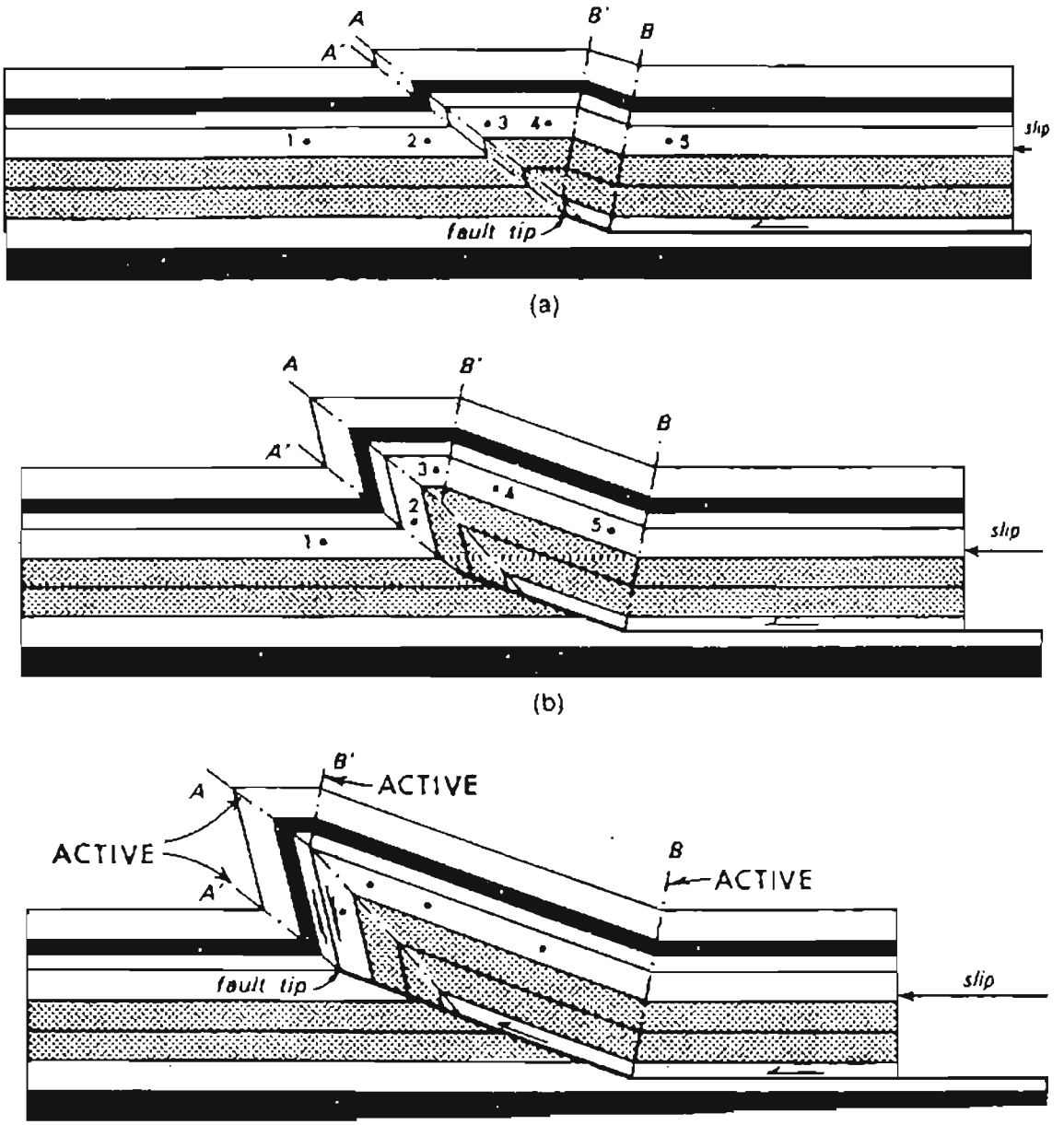

Figure 43. Fault propagation fold kinematics, illustrating the progressive development of beds deforming at the tip of a propagating thrust fault. (Modified after Suppe 1985).

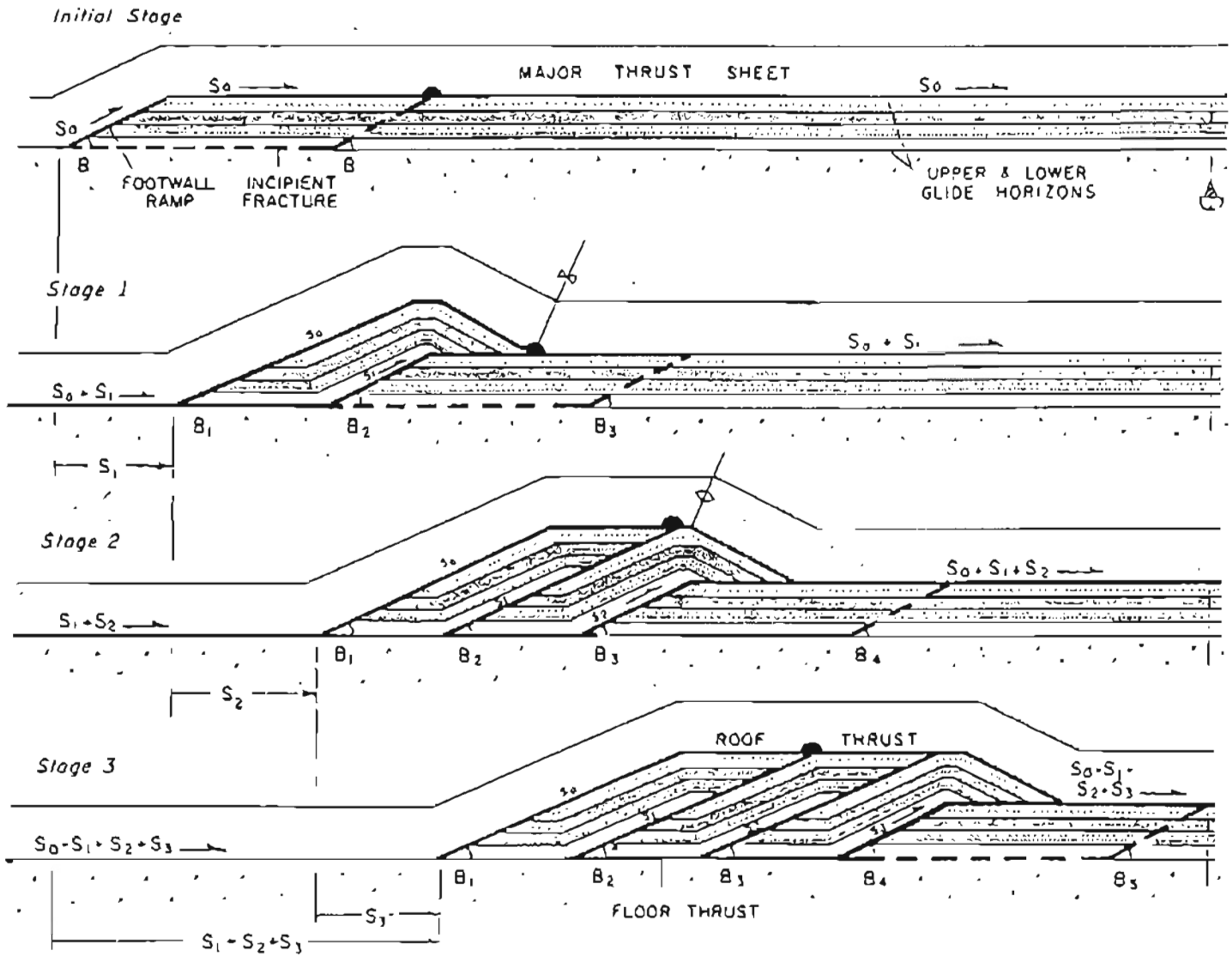

Figure 44 Progressive collapse of footwall ramp builds up duplex. This is measured graphical experiment, assuming plane strain and kink folding, with angles and ratios of dimensions typical of natural examples (Table 1). Roof thrust sheet undergoes complex sequence of folding and unfolding, seen by following black half dot. Modified from Boyer (1978).

constant bed lengths, and kink folding. In fact, the first major thrust with a slip (So) climbed upward in the section from a lower to an upper glide horizon making a steep footwall ramp in a more competent sequence. A second fracture with a slip (S1) progrades from the base of the ramp for some distance in the lower glide horizon where it rejoins the major thrust. This results in the formation of the first horse. Afterward, the slip is transferred to next fracture (S2) and the major thrust slips (So+S1) upward in front of the new horse which deactivate a portion of the major thrust that rides passively within the growing thrust sheet. Over the footwall ramp, the horse, which is an inactive portion of the major thrust and the rest of the overlying sheet are kink-like folded. This process is repeated thus resulting in elongate folds, imbricate horses, undisturbed bedding above the roof thrust and same stratigraphic unit in the hanging wall along the roof thrust (Figure 44).

Duplexes are mechanism for slip transfer from one glide horizon at depth to another at shallow levels. In the direction of movement, slip decreases along the floor and increases along the roof, and total slip at any point along floor or roof thrust is dependent on the number or horses that lie between that point and the head of the duplex. Slip transfer and the creation of new horses causes structural thickening, growth of duplex and an addition of mass to the moving thrust complex. Because the hanging wall rocks of the roof thrust are often flat-lying or only gently folded, one might suggest that the high-angle subsidiary faults formed first by branching upward from the floor thrust, then were truncated by the roof thrust (Boyer and Elliott, 1982).

BREAK BACKWARD THRUST SEQUENCE

In the forward breaking sequence, all thrust originated from footwall of the previously active fault so that thrusting propagated systematically from the hinterland to foreland. The reverse situation, where the trailing branch line of the next thrust lies within the thrust system, is termed as "break-back".

A geometrically trivial but rather common example of break-back thrusting occurs in thrust fold complexes when the propagation of an individual thrust is locally inhibited. In these situations, a zone of ductile deformation generally a fold, will develop to accommodate the continued movement on the uninhibited fault surface towards the hinterland. Studies show that commonly a new thrust segment will climb across the fold, forming a ramp, marginally behind the finite deformation front. With respect to this deformation and any detachment surface beneath, the climbing ramp will have developed *in a break-back sequence* (Figure 45). Boyer & Elliott (1982) suggested that break-back sequence were unlikely to form simple duplex structures, but would rather truncate any earlier imbricate fans. This truncating geometry was termed 'overstep' by Elliott and Co. (1980).

BACK THRUST SYSTEMS

In most orogenic belts, there are some faults, which move in a direction opposed to the regional movement direction. These are called back thrusts. A particularly important type of back-thrust can develop towards the end of the evolution of foreland thrust belts so that the deformation front is represented by a triangle zone. Figure 46 shows an example of back-thrust development. Back-thrust can also occur when there is

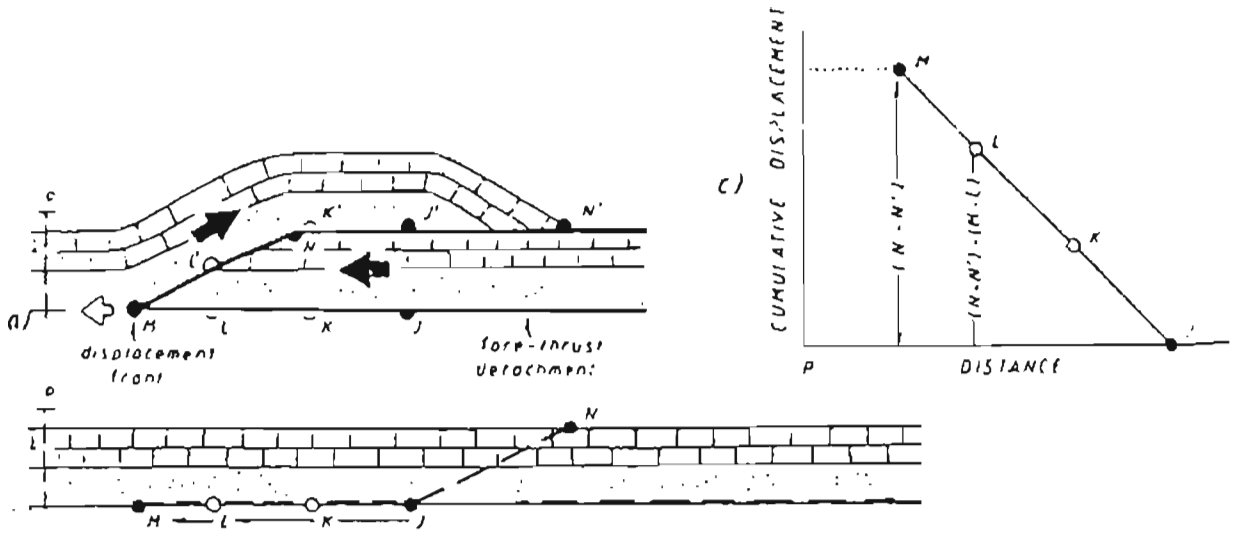

Figure 45. The displacement and propagation of a single back-thrust. (a) After displacement; (b) before displacement; (c0 resulting relationship between the position of the instantaneous displacement front with the amounts of displacement on the fore-thrust detachment.

no forward propagation of the deformation front despite continued convergence in the orogenic interior.

Back Thrust Sequence

Propagation of multiple back thrust is as possible from a fore-thrust detachment as is the individual back-thrust. In this case it is likely that with continued displacements new faults surfaces will develop. Neglecting the possible development of fore-thrust ramps, two options are open for the location of these new fault profiles. Figure 39 illustrates a new back-thrust can propagate into either the footwall or the hanging wall of the previously active fault surface. The first case to consider is where propagation into footwall occurs, thus the new back-thrust lies on the regional hinterland side of the old fault (Figure 46). For this to occur the frontal part of the fore-thrust detachment must be abandoned and a new back-thrust ramp develop windward of "w" (Figure 39c). With displacement the frontal part of the fore-thrust detachment is progressively reactivated until the two back-thrust ramps are juxtaposed. Thus antiformal back-thrusts stacks will develop and the faults will show an internally piggyback sequence. The instantaneous displacement front, however, will show a complex path as illustrated on the restored section (Figure 46-d).

TRIANGLE ZONES

The term 'triangle zone' was first used to describe the thrust belt termination in the southern Canadian Rocky Mountains. It is basically a combination of two thrusts with the same basal detachment and with opposing vergence such that they form a triangle zone (Figure 47). As deformation decreases toward the foreland, inherent stresses continue to propagate into the basin, manifested by thrusting, until it can no longer

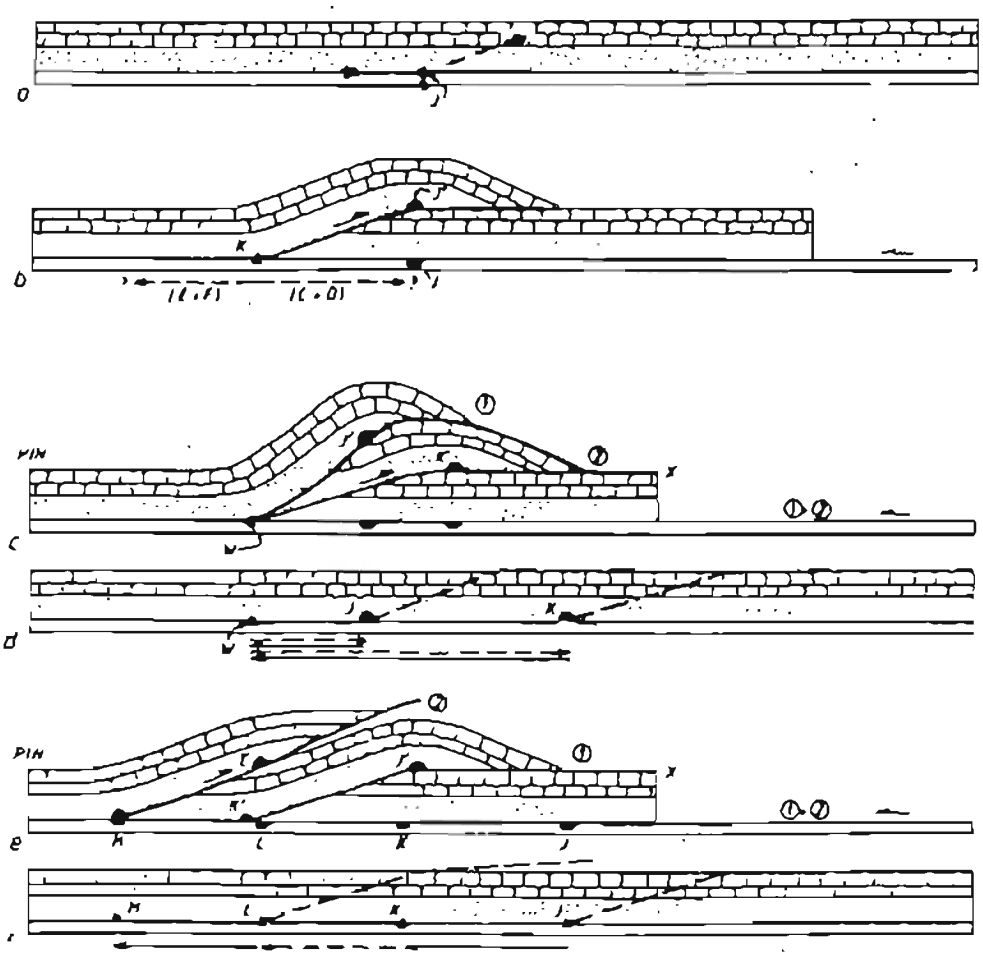

Figure 46. Generation of back-thrust sequences.

support the formation of a new fault surface. A hinderance in the foreland commonly leads to the creation of a backthrust.

Three basic types of triangle zones (Figure 47) were proposed by Couzens and Wiltschko (1994). The first case depicts "opposing thrusts with a symmetrical distribution above a single level detachment" 9Figure 47a). The second type indicates "opposing thrust with an asymmetrical distribution over a single detachment" (Figure 47b). The two triangle zones are believed to occur in areas with large amounts of component units that hinder the advancement of the thrust sheet. The third type consists of "opposed thrusts with an asymmetrical distribution and two detachment levels" (Figure 47c). Cemen and others (1994, 1995, 1997); Al-Shaieb and others (1995); Akhtar (1995); Sagnak (1996); Evans (1997); and Ronck (1997) identified a triangle zone along the transition between the frontal Ouachitas and the Arkoma Basin in the Wilburton gas field, Hartshore area, and Wister Lake area . This triangle zone is similar to the type three triangle zone reported by Couzens and Wiltschko (1994).

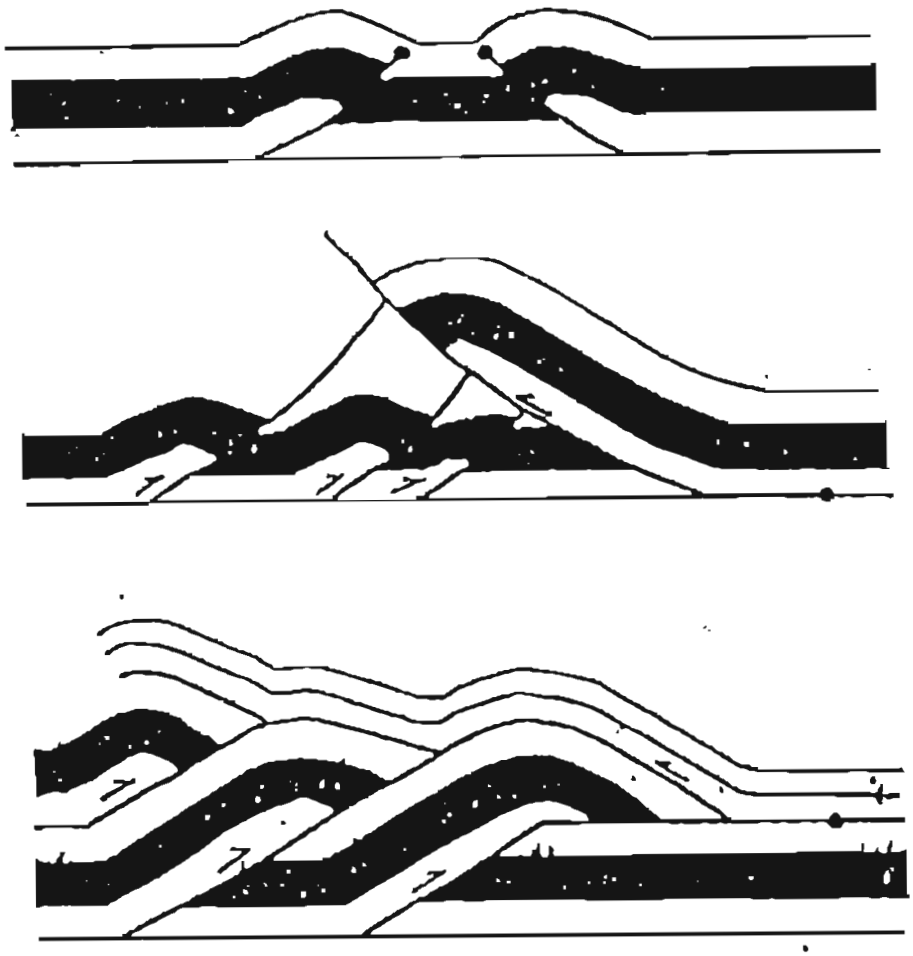

Figure 47. Three types of triangle zones proposed by Couzens and Wiltschko (1994)

CHAPTER VI

STRUCTURAL GEOLOGY OF THE STUDY AREA

Introduction

The surface geology of the Red Oak and Talihina quadrangles are very much similar to the structural characters seen in the transition zone of the Ouachitas and the thrust belt from the western limits of Arkoma basin (Hartshorne) to the study area (Figure 11). The surface trace of the Choctaw Fault serves as the dividing line between two extremely contrasting structural styles. To the north of the Choctaw fault, rocks are gently folded into symmetrical anticlines and syncline. In the study area, in addition to the NE trending strike slip faults, the Cavanal Syncline and Brazil Anticline are the two major structures to the north of the Choctaw fault.

To the south of the Choctaw Fault, the surface geology is dominated by numerous imbricate thrusts all dipping southward (Figure 48). The tools used in the interpretation of the structural features of the study area are well data (Figure 49 and Appendix I) and reflection seismic lines (Figure 50).

WINDING STAIR FAULT

The Winding Stair fault is the southernmost thrust fault in the study area

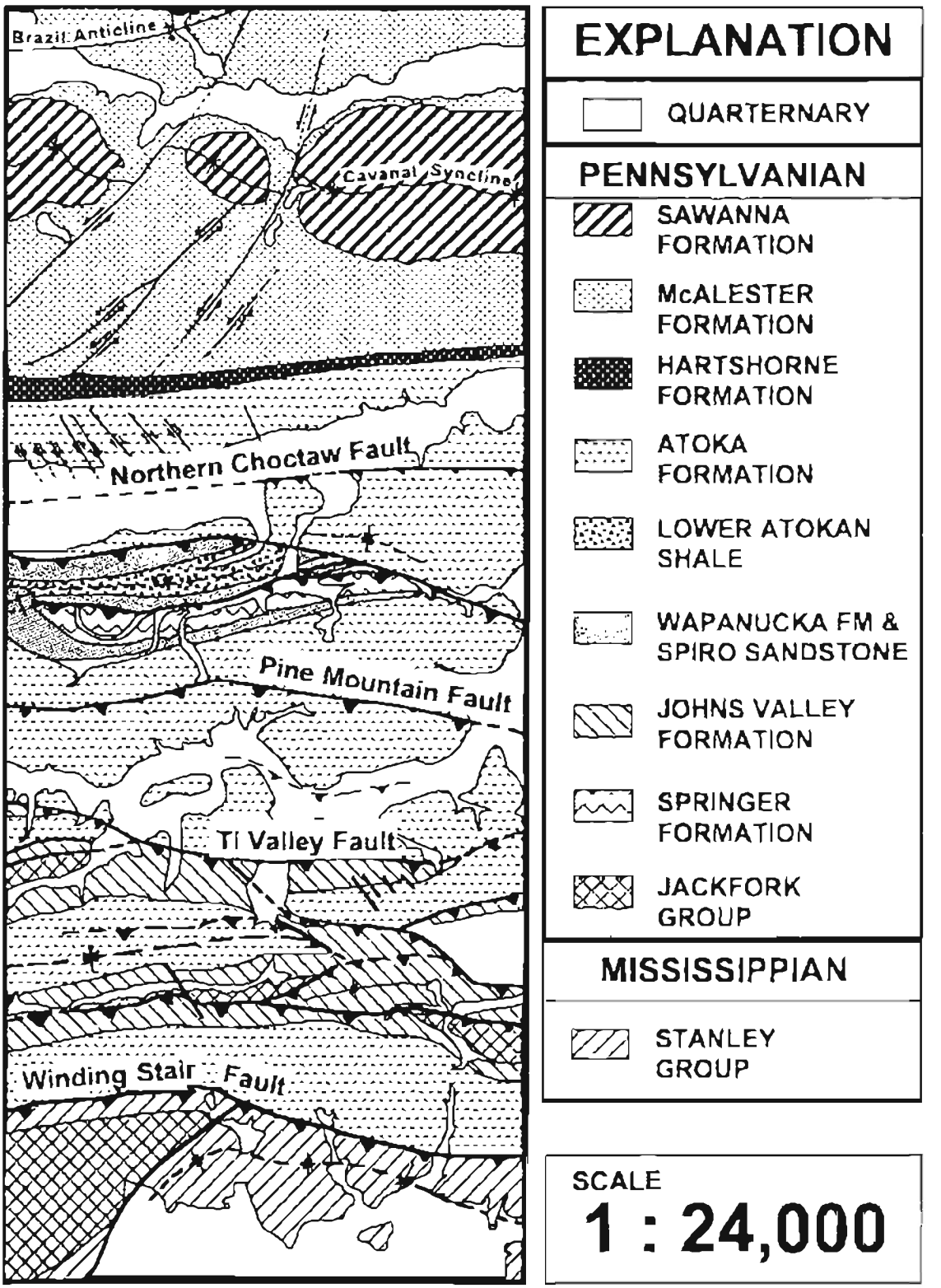

Figure 48. Simplified geologic map of Red Oak and Talihina quadrangles compiled from Fergosun and Suneson (1991)

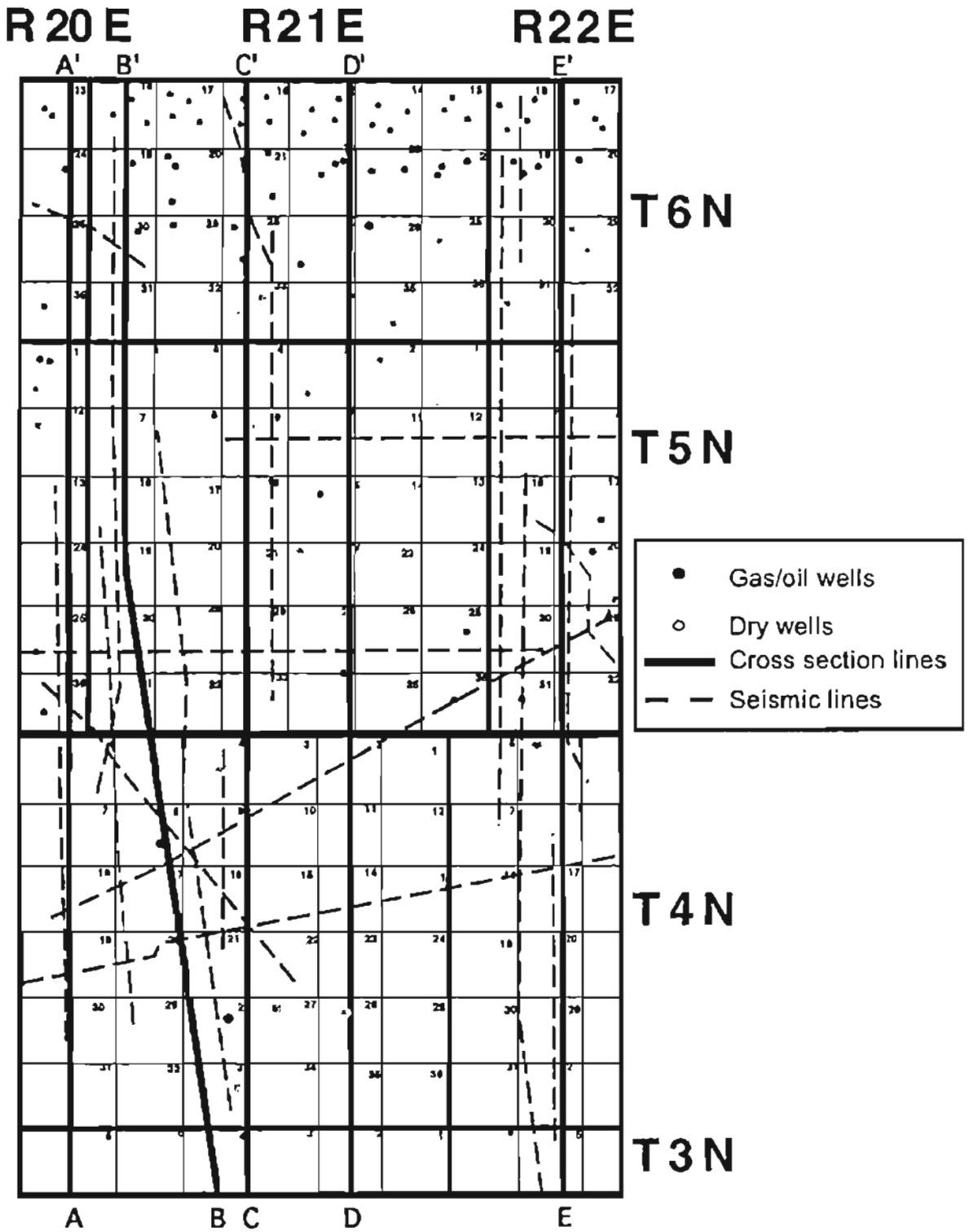

Figure 49. Map showing locations of cross-sections, seismic lines and well location in the study area.

Figure 50 : Interpreted reflection seismic line donated by AMOCO

(Figure 48). Surface geologic maps by Suneson, Fergosun, and Hemish (1990) indicate very high southward dip on the surface along this fault, which trends generally E-W, within the study area. The actual displacement along this thrust is unknown because of limited well control in the area leading to the lack of correlatable beds in both the hanging wall and footwall to serve as two piercing points.

The Winding Stair fault is located in the southernmost end of each of the cross sections (Figure 51 - 55 and Plates I –V). The Stanly group which is the oldest rock exposed in the area, is present in the hanging wall of the Winding Stair Fault. However, there is not enough evidence of its presence in the footwall of the Winding Stair Fault. Rocks of Jackfork group are also exposed in the southwestern part of the hanging wall block on the surface. The Pennsylvanian Atoka Formation is exposed in the footwall of the Winding Stair Fault throughout the study area, adjacent to the surface trace of the fault.

TI VALLEY FAULT

The Ti Valley fault is located north of the Winding Stair Fault and south of the Pine Mountain Fault (Figure 48). It strikes approximately east-west and extends for more than 240 miles across southeastern Oklahoma into Arkansas (Suneson, 1988). This thrust also dips at very high angle, around 70 degrees on the surface (Suneson, 1991) which is confirmed by the seismic and well-log data. Hendricks (1959) estimated the minimum displacement along the Ti Valley fault to have been around 20 miles, however within the study area the cross sections (Figure 51 - 55) suggests only about 9,000 ft. displacement. It is one of the thrust faults of the leading imbricate fan in the hanging wall of the Choctaw fault. Numerous minor thrusts splay from the Ti Valley fault. These

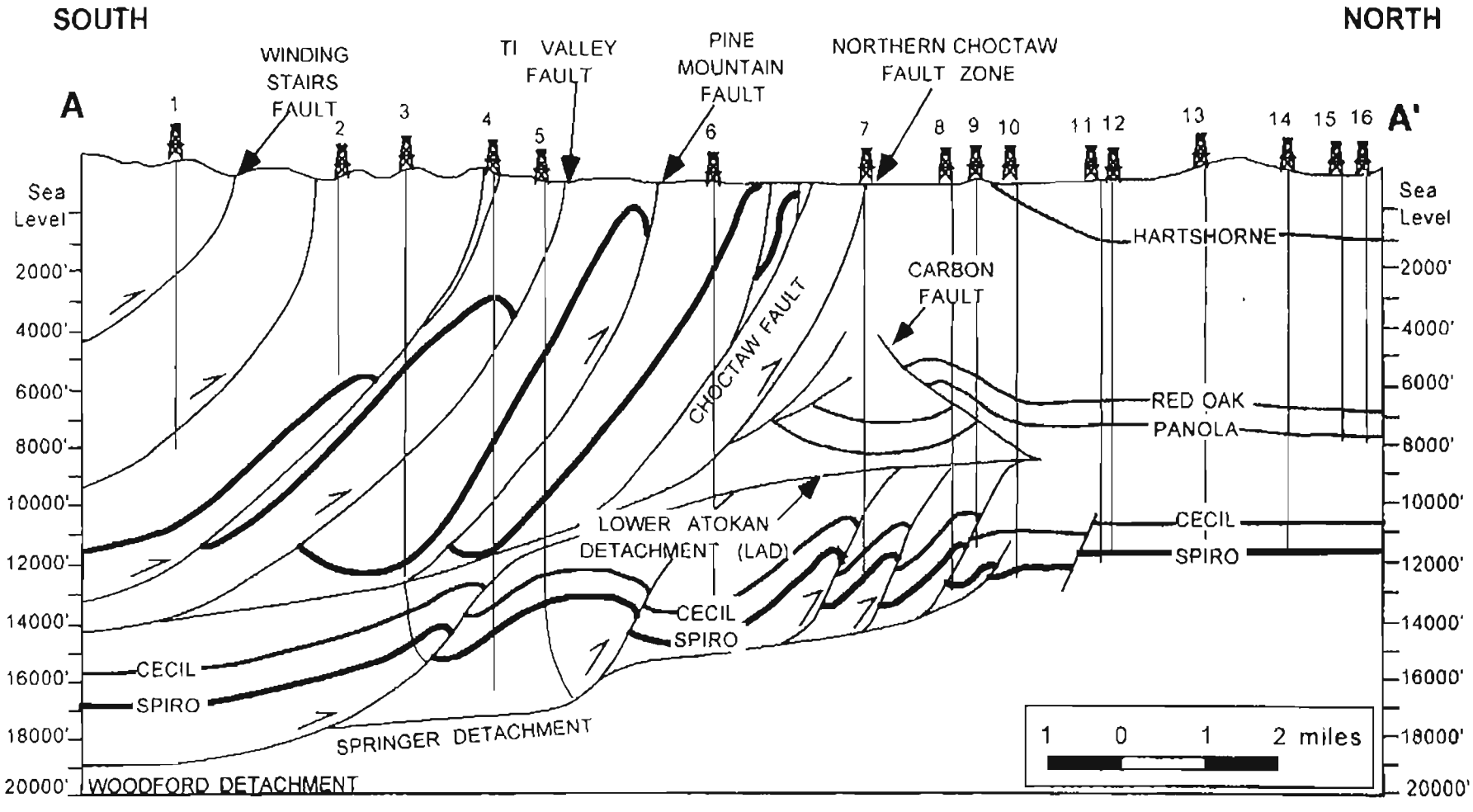

Figure 55 : Balanced structural cross section A - A'

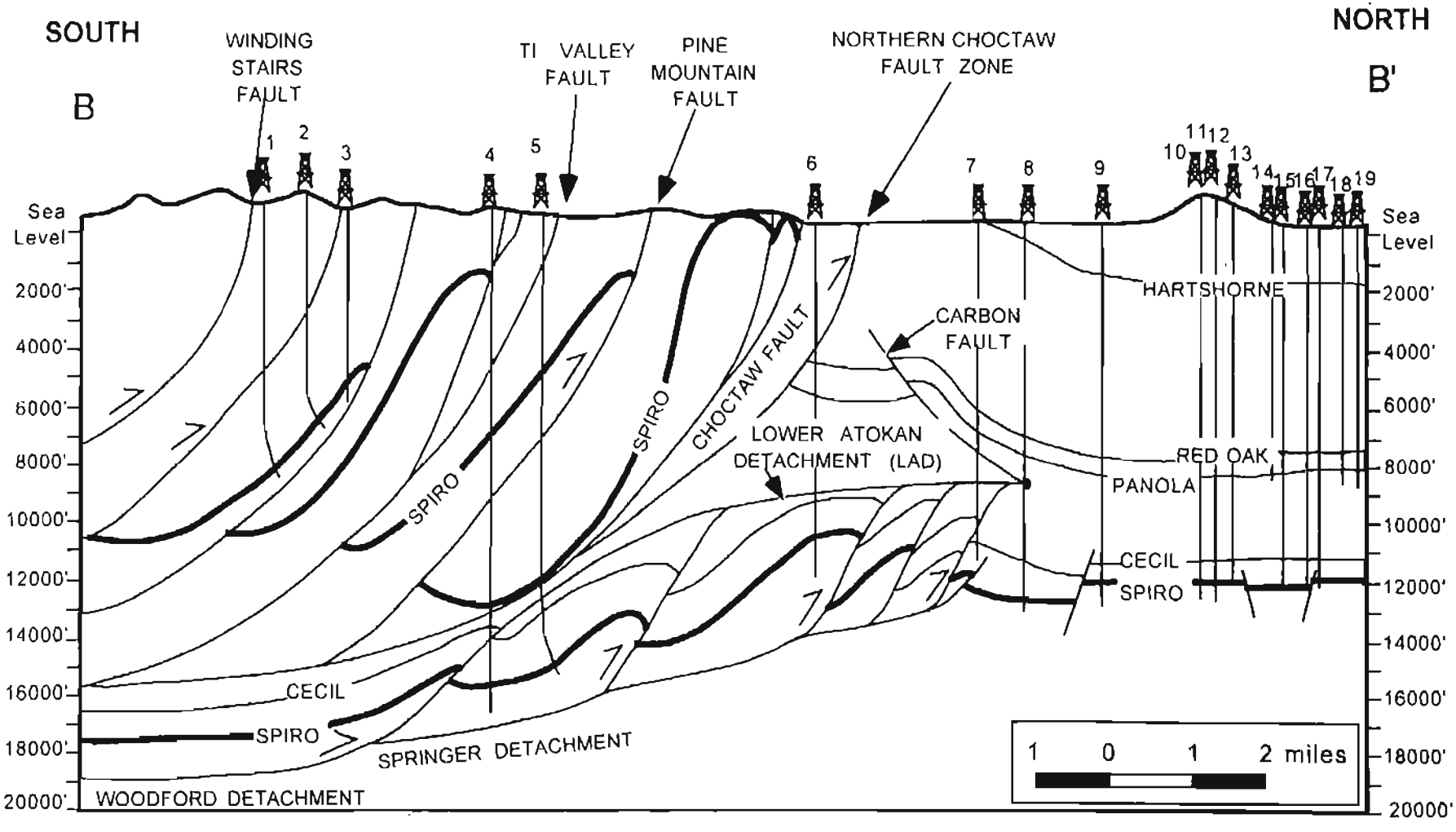

Figure 52 : Balanced structural cross section B - B'

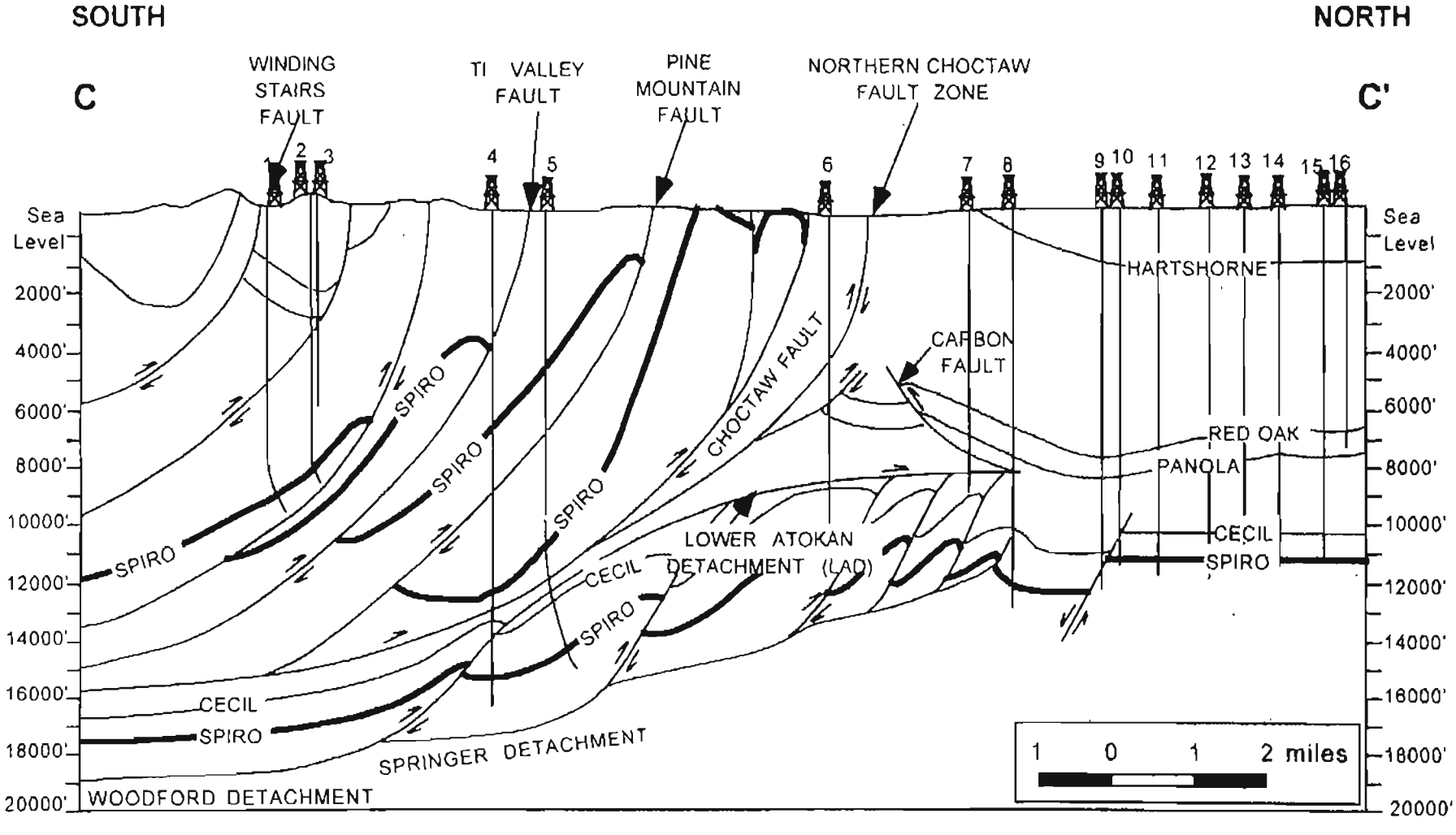

Figure 53 : Balanced structural cross section C - C'

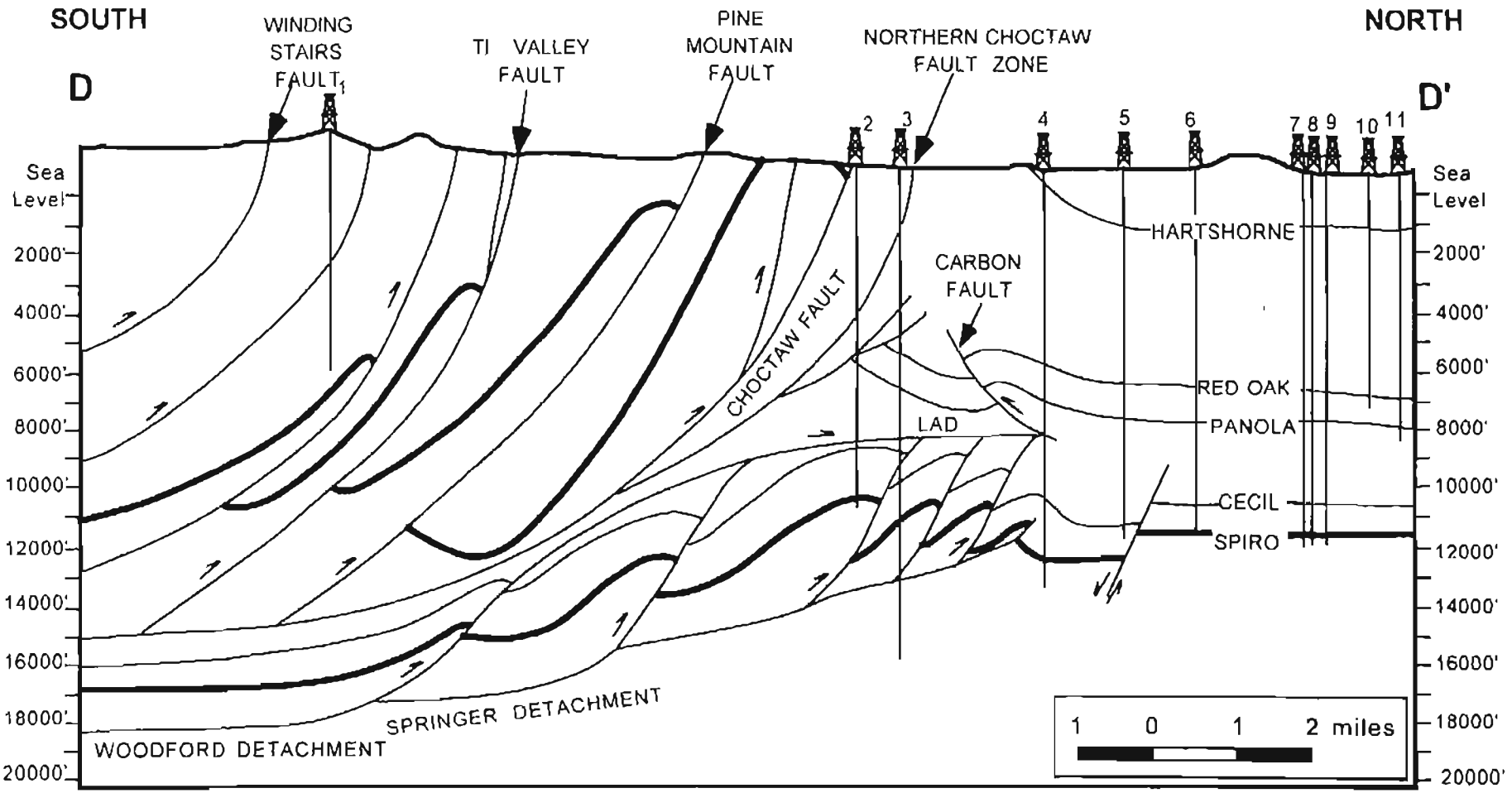

Figure 54 : Balanced structural cross section D - D'

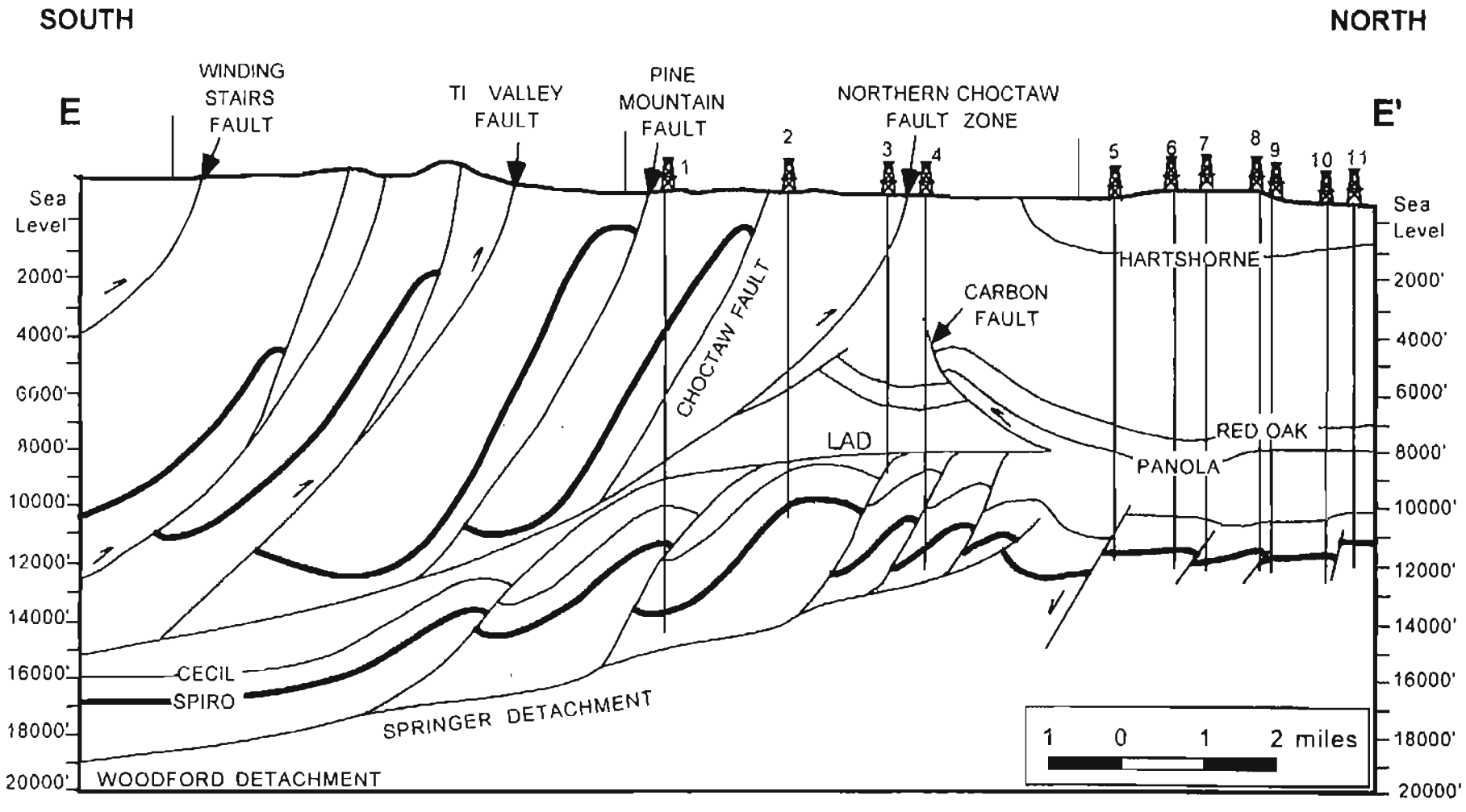

Figure 55 : balanced structural cross section E - E'

minor thrusts form as the main thrust fault loses displacement and the inherent stress is distributed among several anastomosing faults (Figure 51 - 55). The hanging wall of the Ti Valley Fault contains numerous anticlines and synclines within the Johns Valley Formation (Figure 48).

The Ti Valley fault is interpreted as being listric and joining to the Choctaw Detachment at depth of approximately 14,000 ft. Both footwall and hanging wall of the Ti Valley Fault contains the Spiro sandstone (Figures 51 - 55 and Plates I – V). The Spiro formed a hanging wall anticline in the subsurface as it was thrust over underlying strata. On the surface, this thrust is manifested by the folding of the Johns Valley Shale (Figures 48, 51 - 55 and Plates I – V). The hanging wall of the Ti Valley fault contains the northernmost extension of the deep-water Jackfork and Johns Valley juxtaposed over deep-water Atokan shales in a tectonic contact.

PINE MOUNTAIN FAULT

The Pine Mountains fault is located between the Ti Valley and Choctaw Faults (Figure 48, 51 - 55 and Plate I – V). It dips southward between 65 and 80 degrees, becoming less steep with depth. The Pine Mountain Fault is also interpreted as being listric and joining to the Choctaw Detachment surface at depth (Figures 51 - 55 and Plates I – V). The Pine Mountain fault shows a displacement of about 11,000 ft in the study area (Figures 51 – 55). Spiro sandstone is present in both the hanging wall and the footwall of the Pine Mountain fault. The footwall Spiro is exposed on the surface near the surface trace of Choctaw Fault (Figure 48).

CHOCTAW FAULT

The Choctaw fault is the leading-edge thrust of the Ouachita fold-thrust belt and serves as the boundary between the Arkoma basin and the Ouachita Mountains. The hanging wall and footwall blocks of the Choctaw Fault have different structural features. The hanging wall block incorporates several imbricate thrusts which merge into a single detachment (Figures 51- 55).

Evidence for the presence of this detachment surface was attained through detailed analysis of seismic and well log data westward of the study area in the Wilburton and surrounding areas by Cemen and others (1994, 1995, 1997), Al-Shaieb and others (1995), Akhtar (1995), and Sagnak (1996). In this study, the well data was tied with seismic data, and this detachment surface was placed at a subsea elevation of approximately - 6,000 feet (Figure 51 - 55).

In contrast to the geometry of Choctaw fault in the Wilburton and surrounding areas, where Akhtar (1995) and Sagnak (1996) showed the Spiro at the surface along the Choctaw fault, there is a thick fault block (called Northern Choctaw fault) basinward of the main Choctaw Fault that contains no Spiro sandstone (Figure 51 - 55). The absence of the Spiro sandstone in this block suggests that the leading-edge thrust in the study area is the Choctaw Fault. The Northern Choctaw Fault must be younger than the main Choctaw fault since it does not cut the Spiro sandstone.

The footwall geometry of Choctaw thrust is quite different from that of hanging wall block. The footwall consists of two detachment surfaces, one duplex structure, several horses, a triangle zone, and minor normal faults.

CARBON FAULT

The blind back-thrust (carbon fault) which is exposed on the surface in the western part of the study area is not exposed in this area. However, the presence of the Carbon Fault is evidenced in both seismic and well data (Figure 48, 51 - 55, Plates I – V).

As a whole, the study area is characterized by a foreland verging thrust movement. Duplexes and a roof thrust are the frontal part of this thrust belt. This kind of tectonic transport should be "accommodated by backthrusting with opposite vergence, in the section overlying the upper detachment" (Jones, 1994). The Carbon fault is believed to have formed in order to accommodate thrust movement in the study area.

Using evidence from the cross-sections and the seismic lines, the Carbon fault is interpreted as forming a backthrust, which ahs an upward and southward (Figures 51 - 55).

BASAL DETACHMENT

Below the Choctaw Detachment is a major decollement which floors the entire Late Paleozoic fold and thrust system. In the study area, this is the Woodford Detachment, named for the Upper Devonian Woodford Shale (Figure 51 - 55 and Plates I – V)(Hardie, 1988). There is around three thousand feet rise in this decollement surface from about 19,000 feet in the southern part of the study area to about 16,000 feet through the cross sections towards north. The Woodford detachment surface ramps about 1500 feet into the Springer Shale thus called as Springer Detachment. From here northward, it is in the Springer Shale, and is called as the Springer Detachment.

The Woodford and Springer detachment surfaces within the study area were sometimes difficult to locate. Their locations are based on the available subsurface

control. The Devonian Woodford Shale and the Mississippian Springer Shale are located at extreme depths, and few well penetrations were ever attempted throughout the area. Information about the detachments was extrapolated in the cross sections where no wells were drilled deep enough to penetrate these detachments.

The second detachment is relatively shallow in depth and it serves as roof thrust for the horses within the duplex structure and is informally referred as Lower Atokan Detachment (LAD) by Cemen and others, 1995, 1997; Al-Shaieb and others, (1995), Akhtar (1995) and Sagnak (1996). The LAD ramps from the Springer Detachment and forms a flat within the Atokan shale (Figure 51 - 55). The rock strata above the Lower Atokan Detachment are gently folded to horizontal and the rocks below thrusted and dip at relatively high angles. This contrast in geometry suggests the presence of a horizontal detachment surface between them. The northernmost end of the LAD exhibits backthrust, which will be discussed latter. The Spiro sandstone is contained within the duplex structure, which is enveloped between the two detachment surfaces.

DUPLEX STRUCTURE

A duplex structure floored by the Springer Detachment and roofed by the LAD is present in the footwall of the Choctaw Fault (Figure 51 - 55 & Plates I - V). Seismic data (Fig 43) suggests that at least four horses containing Spiro and Cecil exits within this duplex structure. However, due to little well control, and poor quality of seismic lines, the exact number of horses within the duplexes was difficult to determine. Therefore much of the information was extrapolated from the cross section A-A', B-B' and C-C' (Figure 51 - 53), which contained some deep wells and were very close to good quality seismic lines.

Correlation of the Spiro using the electric logs data suggests southward dips on the faults enveloping the horses. This thrust in turn suggests the presence of a hinterland dipping duplex structure. The imbricate splaying from the Springer Detachment join upward into the Lower Atokan Detachment which serves as the roof thrust of this Duplex structure.

TRIANGLE ZONE

As interpreted in the OCAST project, a triangle zone exists in the transition zone between the frontal Ouachita Mountains and the Arkoma Basin (Cemen and others, 1994, 1995, 1997; Al-Shaieb and others, 1995; Akhtar, 1995, Sagnak, 1996); (Evans, 1997); (Ronck, 1997) (Figure 51 - 55 & Plate I – IV). This triangle zone is flanked on the south by the Choctaw Fault and on the north by the Carbon fault. It is floored by the Lower Atokan Detachment. The detachment surface (LAD) reaches a "zero-displacement" point below the Canaval Syncline where there is no slip along the fault. A backthrust develops this point, dipping towards the foreland. This backthrust is the subsurface continuation of the Carbon fault which is exposed at the surface to the north of the town of Wilburton.

The Carbon Fault is very much evident in the seismic and well data (Figure 48, 51 - 55 & Plates I & V). Almost horizontal Spiro and Cecil are overlain by more steeply dipping Panola, Red Oak and Hartshorne sandstones. The Carbon Fault, along with the leading edge of the Choctaw Fault and the LAD, collectively form a triangle zone. This triangle zone is similar to the type three triangle zone of Couzen and Wiltschke (1994) (Figure 47).

Due to lack of well control, it is unknown that whether the Carbon fault intersects the Northern Choctaw Fault or not. Northward into the basin, the Carbon fault becomes listric with depth (Figure 51 - 55, Plates I – V), and with both the Carbon fault and the LAD dying within the Atokan shale, it is difficult to pinpoint the exact location of the zero displacement point. This point has been approximated from the reflection seismic lines (Figure 43).

STRIKE SLIP AND NORMAL FAULTS

Numerous strike slip faults are observed on the surface to the north of the Choctaw fault (Figure 48). There are two sets of strike-slip faults. The first set strikes northeast to southwest and is located in the northern part of the study area. The second set strikes northwest to southeast and is located immediately north of the Northern Choctaw fault. The second set is areally less extensive than the first set. These faults are believed to be tear faults and generally have shown as right lateral strike slip faults by Suneson, Fegosun (1991). No direct measurements of separation are reported, but probably is very minor based on their extent. The first set may have large displacement than the second set because they have longer lengths than the second set.

Few normal faults are identified in the subsurface north of the duplex structure below the triangle zone in the foot wall of the Choctaw fault in most of the cross sections (Figure 51 – 55, Plates I – V). These faults dip mostly southward and displace both the Spiro and Cecil sandstones. They were imaged by seismic lines (Fig 48) and were also evident with using the well data.

RESTORED CROSS SECTIONS AND SHORTENING

The balanced cross-sections were restored using the key-bed method of restoration using the basal Atokan Spiro sandstone as the key-bed. The restorations are used to determine the amount of shortening within the area (Figure 56 - 60). The Spiro was used as the key-bed because of its continuous nature and easy recognition in well log signatures.

The pin lines used for the restoration are located along the northern end of the cross-sections, just north of the tip of the duplex structure. To the north of the pin lines, the Spiro is believed to have been unaffected by the shortening of the Late Paleozoic thrust system. The loose line arbitrarily placed along the southern end of the cross-sections. Calculations in the study area suggested approximately 61 percent of shortening for the Atokan Spiro Sandstone along the length of cross-sections. This is very close to the 64 % shortening determined by Longden and Patterson (1997). These amounts were determined from the 1:24,000 geologic maps used in the construction of the cross sections. These restorations were reduced substantially in order to fit on the appropriate plates (I – VI).

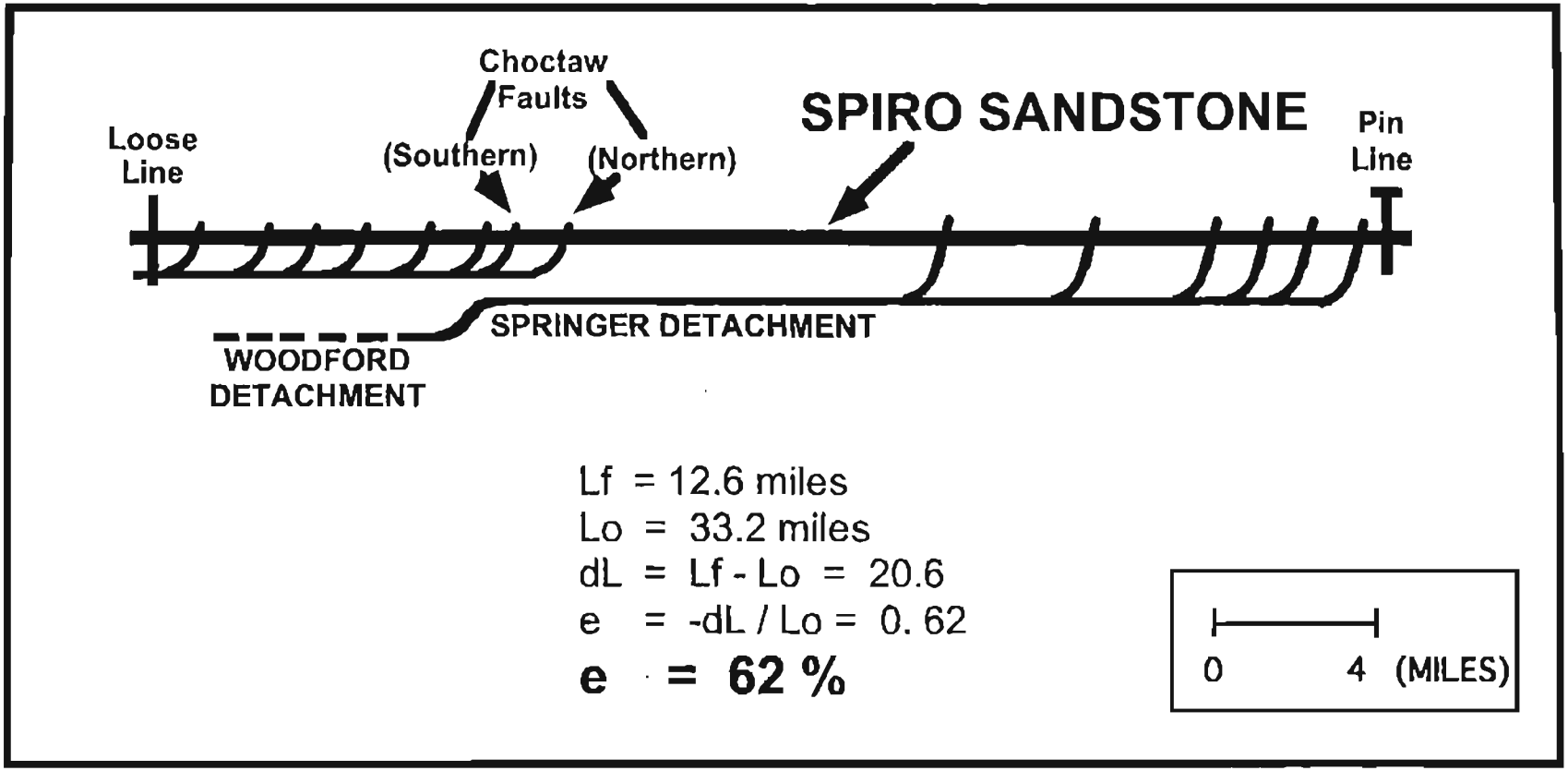

Figure 56 : Restored cross-section A – A'

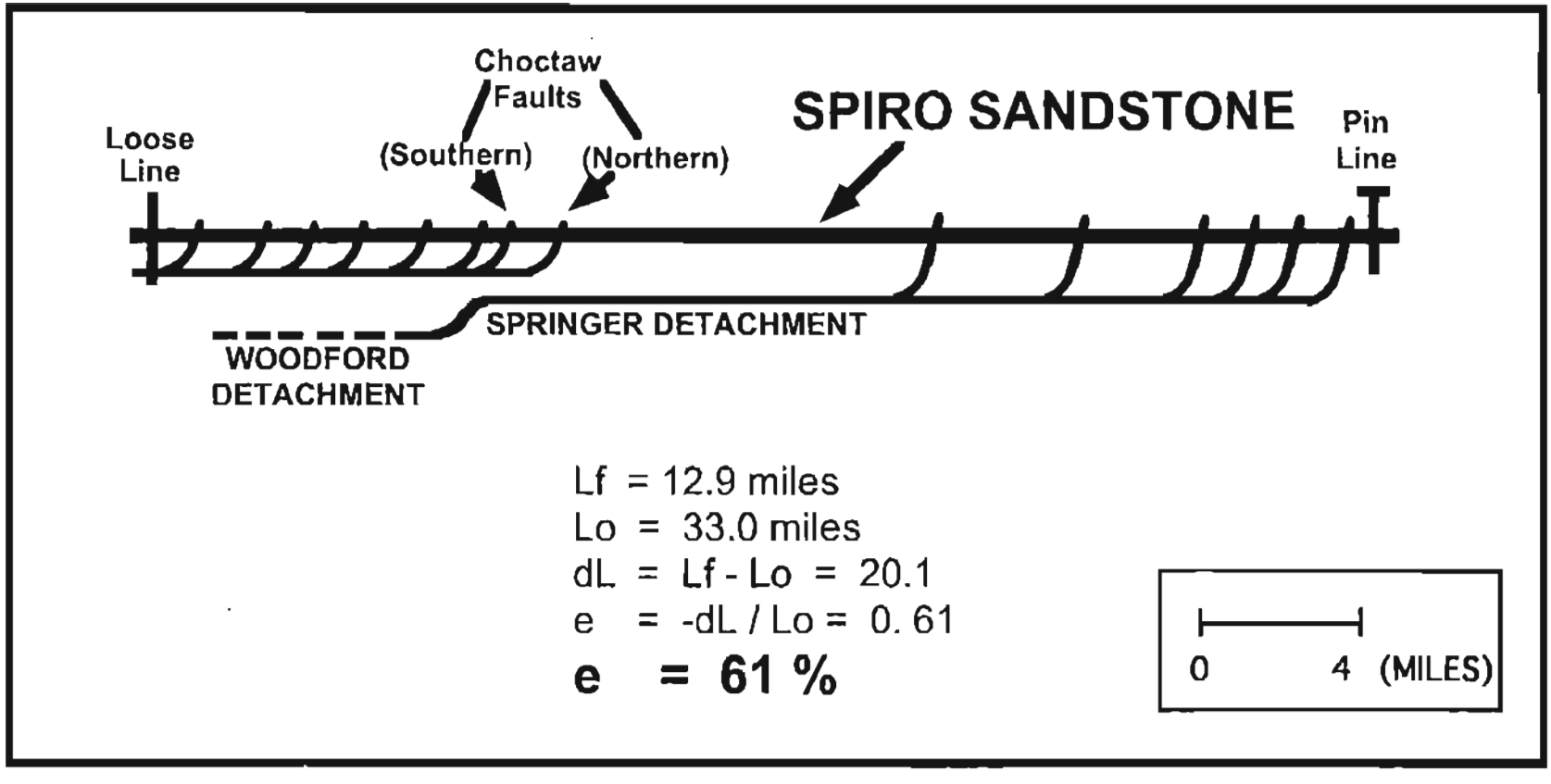

Figure 57 : Rrestored cross-section B – B'

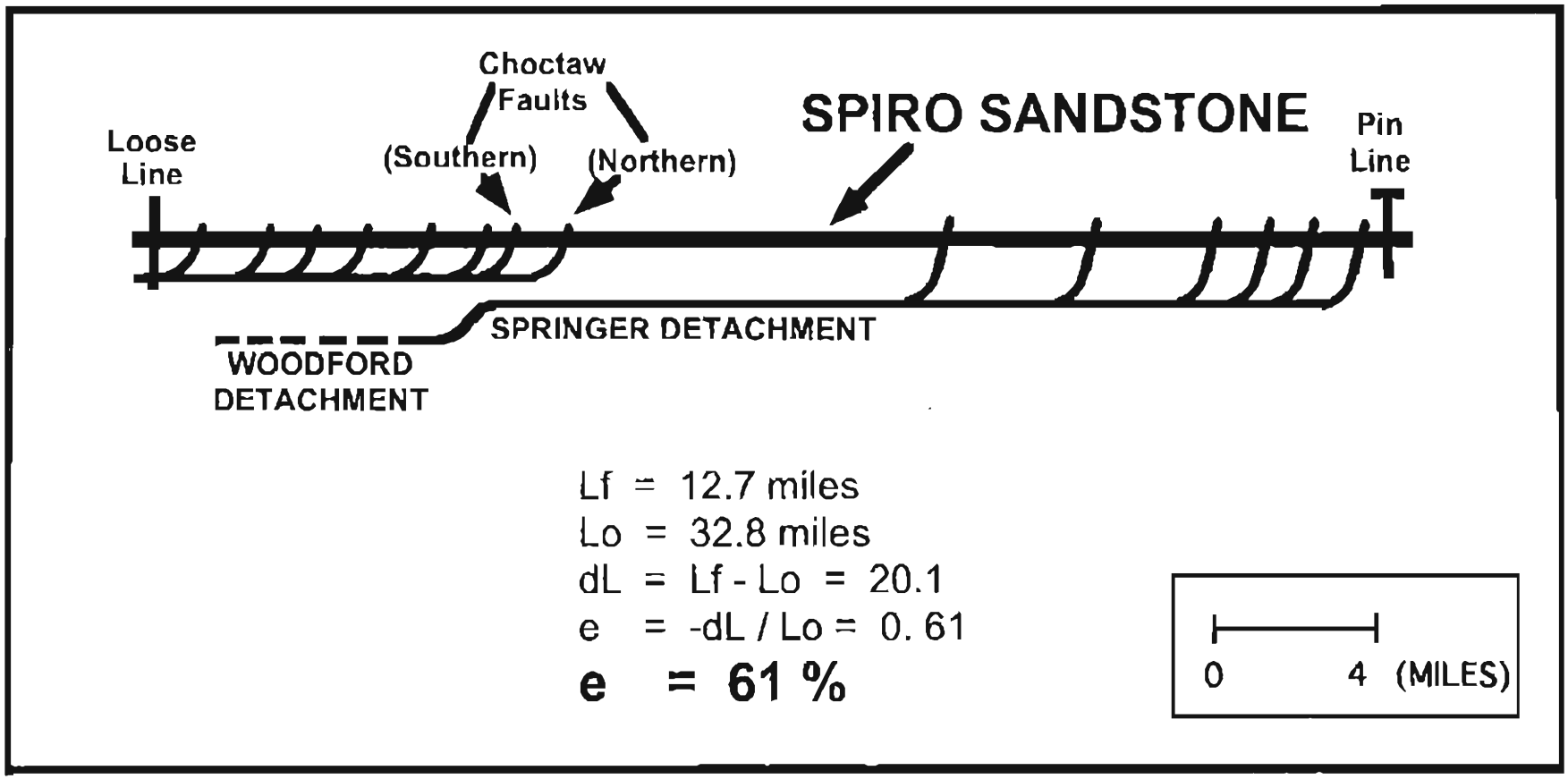

Figure 58 : Restored cross-section C – C'

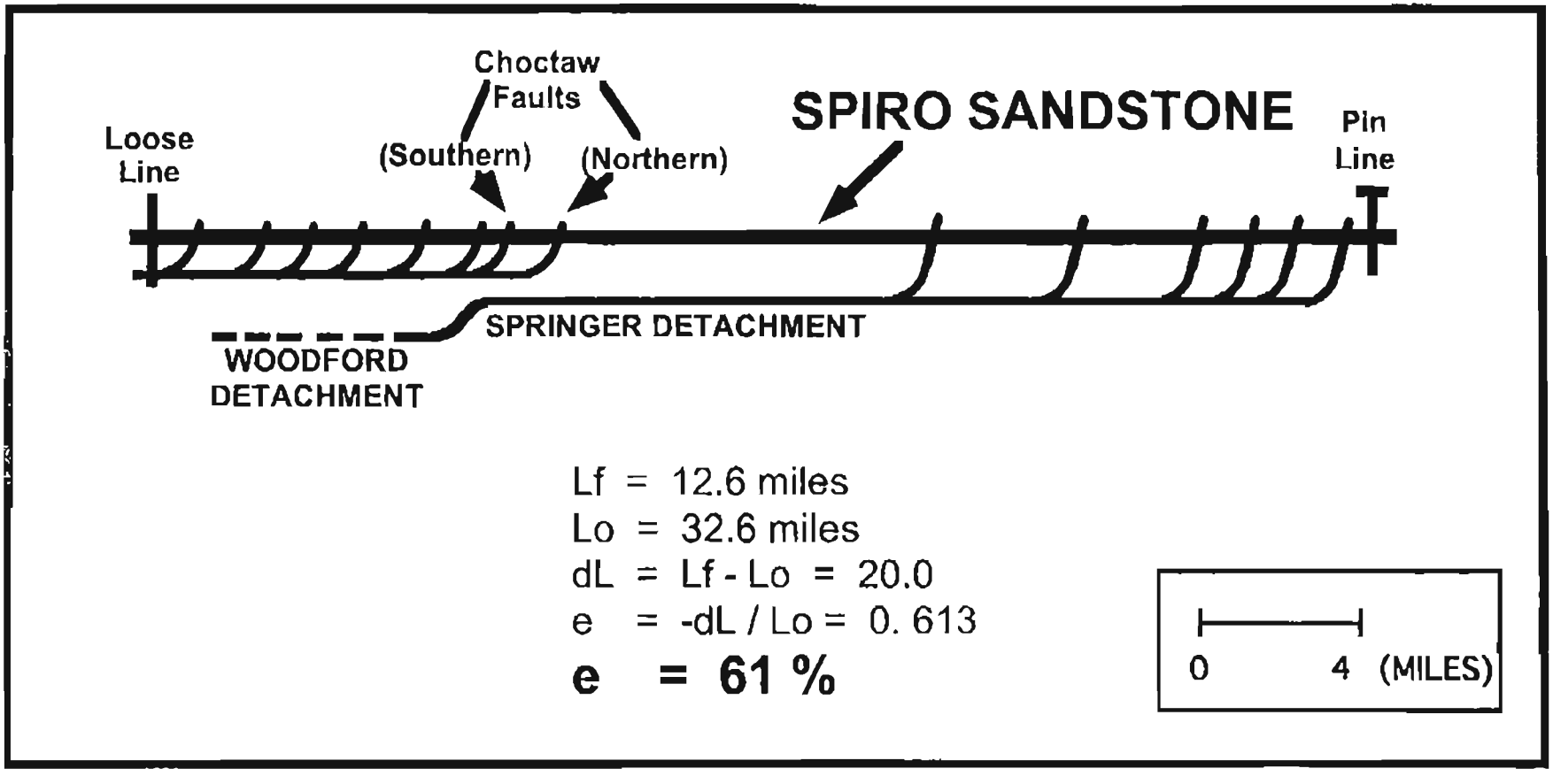

Figure 59 : Restored cross-section D-D'

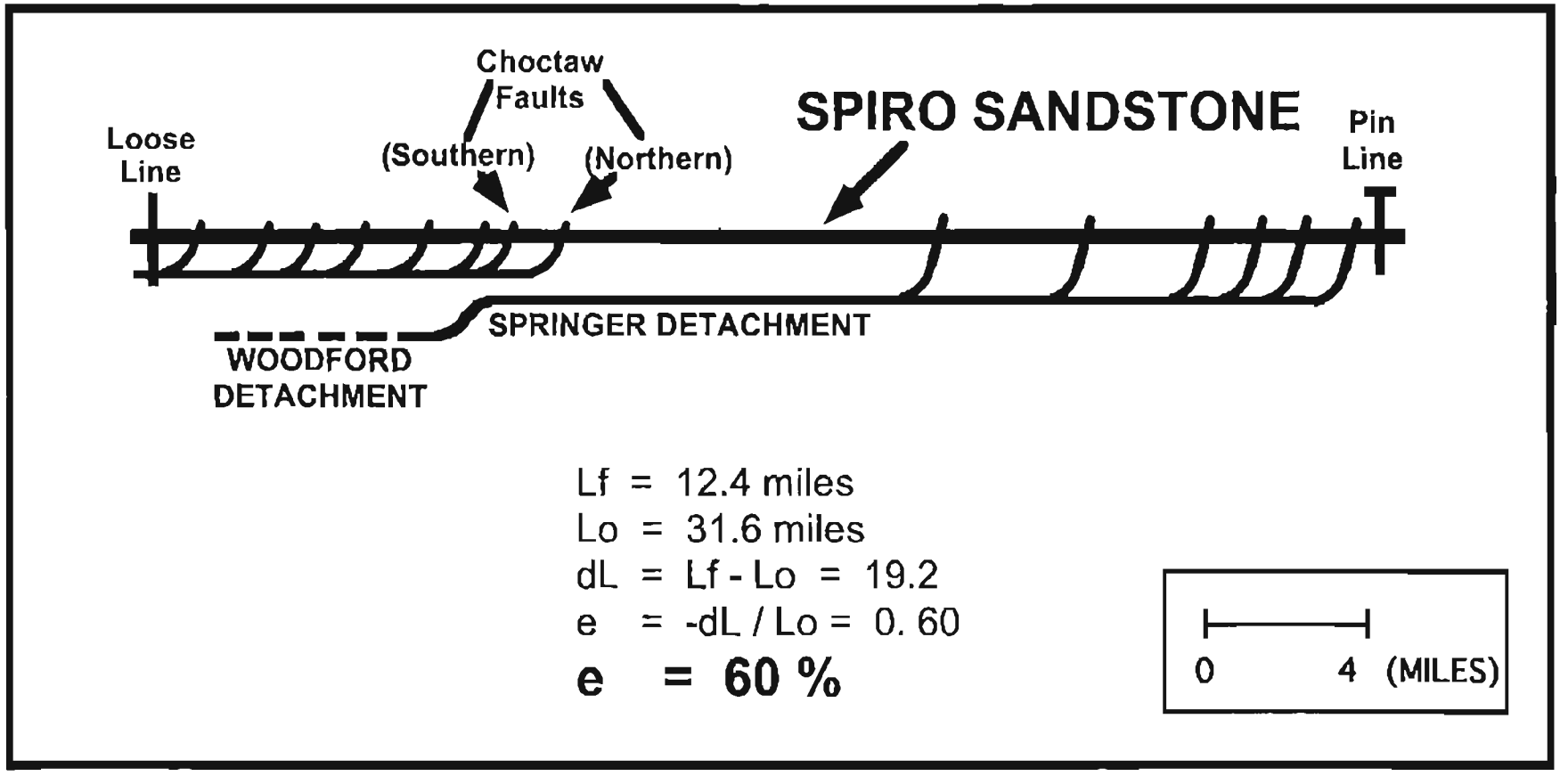

Figure 60 : Restored cross-section E – E'

CONCLUSIONS

1. The hanging wall of the Choctaw Fault is characterized by a southward-dipping imbricate fans.
2. In the footwall of the Choctaw fault, a duplex structure is observed. It is floored by the Springer Detachment.
3. The roof thrust of the duplex structure is the Lower Atokan Detachment (LAD). Horses are contained between the two detachment surfaces.
4. The transition zone is characterized by a shallow triangle zone which is flanked by the Choctaw Fault to the south, the Carbon Fault to the north, and floored by the Lower Atokan Detachment.
5. When restored to their position at the time of the Spiro deposition, by using the key-bed restoration method, the cross sections indicate about 61 % shortening in the study area.
6. The porosity within the deformation bands is almost negligible as compared to the porosity around the deformation bands and to rocks without any deformation bands.

Bibliography

Akhtar, Saleem, 1995, the Geometry of Thrust System in the Wilburton Gas Field and Surrounding, Latimer County, Oklahoma, unpublished M.S. thesis, Oklahoma State University,Stillwater, OK, 97p.

Al-Shaieb, Z., J. Cemen, A. Cleaves, 1995, Overthrusted Natural Gas Reservoirs in the Arkoma Basin, OCAST Project no. AR2-025:4859, OCAST Research and Development Programs Division, 174p.

Al-Shaieb, Z, J.W. Shelton, J. Puckette, and D. Boardman, 1995, Sandstone and Carbonate Reservoirs of the Mid-Continent, Oklahoma City Geological Society-Oklahoma State University Core Workshop; Syllabus for Short Course, Oklahoma City Geological Society, Publishers, p.59-72.

Al-Shaieb, Z., 1988, The Spiro sandstone in the Wilburton field area: Petrology, Diagenesis, Sedimentology, Porosity and Reservoir Quality: unpublished report, 139p.

Arbenz, J.K., 1989, Ouachita Thrust Belt and Arkoma Basin: in Hatcher, R.D,, Jr., Thomas, W.A., and Viele, G.W., eds., The Geology of North America, vol. F-2, The Appalachian-Ouachita Orogeny in the United States, Geological Society of America, Boulder, Colorado, p. 621-634.

Buchanan, R.S., and Johnson, F.K., 1968, Bonanza Gas Field-a model for Arkoma Basin Growth Faulting. In Cline, L.M., ed., Geology of the Western Arkoma Basin and Ouachita *Mountains*: Oklahoma City Geol. Society Guide, p. 75-85.

Boyer, S. and D.Elliot, 1982, Thrust Systems. The American Association of Petroleum Geologists Bulletin: vol. 66, no. 9, p. 1196-1230.

Butler, R., 1987, Thrust Sequences. Journal of the Geological Society, London: vol 144, p 619-634.

Camp, W.K. and Ratliff, R.A., 1989, Balanced Cross-Section Through Wilburton Gas Field, Latimer County, Oklahoma: Implications for Ouachita Deformation and Arbuckle (Cambro-Ordovician) Exploration in Arkoma Basin (abstract): AAPG Bull. v. 73, p.1044.

Cemen, I., Z. Al-Shaieb, A. Sagnak, R. Feller, and S. Akthar, 1997, Triangle Zone Geometry of the Frontal Ouachitas in the Wilburton Area, Arkoma Basin, Oklahoma: Implications for fault sealing in the Wilburton Gas Field (Abstract) AAPG Annual Convention Program with Abstracts, p. A-19.

Cemen, I., Z. Al-Shaieb, R. Feller, and S. Akthar, 1994, Preliminary Interpretation of a Seismic Profile and the Spiro Reservoir Pressure Data in the Vicinity of the Wilburton Gas Field, Oklahoma Geological Society Guidebook 29, p.249-251.

Cemen, I, Al-Shaieb, Z., Hess, F., Akthar, S., and Feller, R., 1995, Geometry of thrusting in Wilburton Gas Field and Surrounding Areas, Arkoma Basin, Oklahoma; Implications for Gas Exploration in the Spiro Sandstone Reservoirs; (Abstract): AAPG Bull. v. 79, no. 9, p. 1401.

Couzens, B.A., and Wiltschko, D.V., 1994, Some Constraints for Mechanical Models of Triangle Zones; (Abstract): Western Canadian and International Expertise. Exploration Update; A Joint Convention of CSEG and CSPG, Calgary, Alberta, 1994, p. 370-71.

Dahlstrom, C., 1969, Balanced Cross Sections. Canadian Journal of Earth Sciences, vol. 6 p. 743-757.

Evans, J., 1997, Structural Geometry of Thrust Faulting in the Baker Mountain and Panola Quadrangles, Southeastern Oklahoma: unpublished M.S. Thesis, Oklahoma State University, 99p.

Ferguson, C.A. and N.H. Suneson, 1988, Tectonic Implications of Early Penssylvanian Paleocurrents from Flysch in the Ouachita Mountains Frontal Belt, Southeast Oklahoma; in Johnson, K.S., ed., Shelf to Basin Geology and Resources of the Pennsylvanian in the Arkoma Basin and Frontal Ouachita Mountains of Oklahoma: Okla. Geol. Survey Guidebook 25, p. 49-63.

Feller, R., 1995, Characteristics of Abnormally-Pressured Gas Compartments and Potential Sealing Mechanisms in the Spiro Sandstone, Arkoma Basin, Oklahoma: unpublished M.S. thesis, Oklahoma State University, 96p.

Gross, J.S., S. Thompson, B. Claxton, and M. Carr, 1995, Reservoir Distribution and Exploration Potential of the Spiro Sandstone in the Choctaw Trend, Arkoma Basin Oklahoma and Arkansas, AAPG Bulletin, V. 79, No. 2, pp. 159-185.

Ham, W.E., 1978, Regional Geology of the Arbuckle Mountains, Oklahoma: Oklahoma Geological Survey Special Publication 73-3, 61p.

Hardie, W., 1988, Structural Styles of the Frontal Thrust Belt of the Ouachita Mountains, southern Pittsburg County, Oklahoma: Oklahoma Geology Notes, v. 48, no. 6, p.232-246.

Hemish, L.R.., 1990, Geologic map of the LeFlore Quadrangle, Latimer and LeFlore Counties, Oklahoma (unpublished): Oklahoma Geological Survey, scale 1:24000.

Houseknecht, D.W. and T.A. McGilvery, 1990, Red Oak Field, Structural Traps II, Traps Associated with Tectonics, American Association of Petroleum Geologists Treatise of Petroleum Geology, Faulting Atlas of Oil and Gas Fields, p. 201-221.

Houseknecht, D.W., 1986, Evolution of Passive Margin to Foreland Basin: The Atoka Formation of the Arkoma Basin, south-central U.S.A.: in Allen, P.A., and Homewood, eds., Foreland Basins: International Association of Sedimentologists Special Publication 8, p. 327-345.

Houseknecht, D.W. and Kacena, 1983, Tectonic-Sedimentary Evolution of the Arkoma Basin: Society of Economic Paleontologists and Mineralogists, Mid-Continent Section, v. 1, 119 p.

Hess, F. B., 1995, Sedimentology and Depositional Environments of the Lower Atokan Spiro sandstone in the Wilburton, Red Oak, and Kinta fields, Arkoma Basin, Oklahoma: unpublished M.S. thesis, Oklahoma State University, 159 p.

Jamison, W.R. 1994, Triangle Zone Evolution Mechanistic Approaches (Abstract): Western Canadian and International Expertise, Exploration Update; A Joint Convention of CSEG and CSPG, Calgary, Alberta, 1994, p. 217.

Johnson, K.S., 1988, General Geologic Framework of the field-trip area, in Johnson, K.S., ed., Shelf-to Basin Geology and Resources of Pennsylvanian strata in the Arkoma Basin and Frontal Ouachita Mountains of Oklahoma: Oklahoma Geological Survey Guidebook 25, p. 1-5.

Jones, P.B., 1994, Triangle Zone Geometry and Terminology (Abstract): Western Canadian and International Expertise, Exploration Update; A Joint Convention of CSEG and CSPG, Calgary, Alberta, 1994, p. 69-70.

Keller, G.R., and Cebull, S.E., 1973, Plate Tectonics and the Ouachita System in Texas, Oklahoma, and Arkansas: Geol. Soc. America Bull., v. 83, p. 1659-166.

Lillie, R.J., Nelson, K.D., deVoogd, Brewer, J.A., Oliver, J.F., Brown, L.D., Kaufman, S. and G. Viele, 1983, Crustal Structure of the Ouachita Mountains, Arkansas: a model based on integration of COCORP reflection profiles and regional geophysical data, American Association of Petroleum Geologists Bulletin, vol. 67, p. 907-931.

Lumsden, D.N., E.D. Pittman and R.S. Buchanan, 1971, Sedimentation and Petrology of Spiro and Foster sands (Pennsylvanian), McAlester basin, Oklahoma: AAPG Bull. 55, p. 254-266.

Mazengarb, C., 1995, Interpretation of Structure from Surface Geology, Frontal Ouachitas, Southeastern Oklahoma: in K.S. Johnson, Editor, Structural Styles in the Southern Midcontinent, 1992 Symposium: Oklahoma Geological Survey Circular 97, p.26-31.

McClay, W. M., ed., 1992, Thrust Tectonics. Chapman and Hall; London, 447p.

Mitra, S., 1986, Duplex Structures and Imbricate Thrust Systems; Geometry, Structural Position and Hydrocarbon Potential: AAPG Bull, 70, p. 1087-1112.

Morris, R.C., 1974, Sedimentary and Tectonic History of the Ouachita Mountains SEPM Special Publication 22, pp.120-142.

Nicholas, R.L. and D.E. Waddell, 1982, New Paleozoic Subsurface Data from the North-Central Gulf Coast, (abstract), Geological Society of America Abstract with Programs, no. 14, p.576.

Perry, W.J., Jr., and Suneson, N.H., 1990, Preliminary Interpretation of a Seismic Profile across the Ouachita Frontal Zone near Hartshorne, Oklahoma: Oklahoma Geological Survey Special Publication 90-1, p. 145-148

Price, R.A., 1994, "Triangle zones" as Elements in a Temporal and Spatial Spectrum of Tectonic Wedging and Delamination (Abstract); Western Canadian and International Expertise, Exploration Update; A Joint Convention of CSEG and CSPG, Calgary, Alberta, 1994, p. 208.

Ronck, J., 1996, Structural Geology of the thrust fault in the Wister Lake Area, LeFlore County, Southeastern Oklahoma: unpublished M.S. Thesis, Oklahoma State University.

Sagnak, A., 1997, Geometry of the Late Paleozoic Thrust System in the Wilburton Area: unpublished M.S. Thesis, Oklahoma State University, 101p.

Sagnak, A., Cemen, I., Al-Shaieb, Z., 1996, Geometry of Late Paleozoic Thrusting in the Wilburton-Hartshorne Area, Arkoma Basin, SE Oklahoma (Abstract): Geological Society of America, South Central Section Meeting 1996, Abstracts with Programs; p.62.

Shirley, K, 1997, Headline Gone, But Activity Goes On, AAPG Explorer, May, p. 14-15.

Suneson, N.H., 1995, Structural Interpretations of the Arkoma Basin-Ouachita mountains Transition Zone, Southeastern Oklahoma; A Review: in Johnson, K.S., ed., Structural Styles in the Southern Midcontinent, 1992 Symposium: Oklahoma Geological Survey Circular 97, p. 259-263.

Suneson, N.H., 1991, Geologic map of the Blackjack Ridge quadrangle; Latimer and LeFlore Counties; Oklahoma (unpublished): Oklahoma Geological Survey, scale 1:24,000.

Suneson, N.H. 1988, The Geology of the Ti Valley Fault in the Oklahoma Ouachita Mountains: in Johnson, K.S., ed., Shelf-to Basin Geology and Resources of Pennsylvanian strata in the Arkoma Basin and Frontal Ouachita Mountains of Oklahoma: Oklahoma Geological Survey Guidebook 25, p. 33-47.

Suppe, John, 1983, "Geometry and Kinematics of Fault-Bend Folding", American Journal of Science, vol. 283, p. 684-721.

Sutherland, P.K., 1988, Late Mississippian and Pennsylvanian Depositional History in the Arkoma Basin area, Oklahoma and Arkansas: GSA Bulletin, v. 100, no 11, p.1787-1802.

Tilford, M.J., 1990, Geological Review of the Ouachita Mountains Thrust Belt Play, Western Arkoma Basin, Oklahoma: Geology and Resources of the Frontal Belt of the Western Ouachita Mountains: Oklahoma Geological Survey Special Publication 90-1, p. 169-196.

Twiss, R., J., and E.M. Moores, 1992, Strucural Geology. W.H. Freeman and Co. 532p.

Valderrama, M., K. Neilson, G. McMechan, and Holly Hunter, 1994, Three-Dimensional Seismic Interpretation of the Triangle Zone of the Frontal Ouachita Mountains and Arkoma Basin, Pittsburg County, Oklahoma, Oklahoma Geological Survey Guidebook 29, p.

Wilkerson, M.S., and Wellman P.C., 1993, Three Dimensional Geometry and Kinematics of the Gale-Buckeye Thrust System Ouachita Fold and Thrust Belt, Latimer and Pittsburgh Counties, Oklahoma: AAPG Bulletin, v. 77, p. 1082-1100.

Woodward, N.B., Boyer, S., and J. Suppe, 1987, An Outline of Balanced Cross-Sections. University of Tennessee, Department of Geological Sciences; Studies in Geology 11, 2nd Edition.

APPENDIX - I

WELL LOG DATA

R #	4N - 21E Operator	Well	Location	Section	K.B.	Total Depth	Top Spiro
5	Arco	Ellis 1	SE SW SE	4		15900	11340/15380
6	Mobil	Peachland Creek 1-8	SE NW SE	8	1142	17798	15400
7	Ward Petroleum	Ellis -Brandt 1-20	SW SE EH	20	984	6700	NDE
8	Ward Petroleum	Sara 1-23	SE NW SE	26	1375	8239	NDE
9	Weyerhaueser	22-Jan		27	1512	9500	NDE
10	H & H Star Enregy	Lady Luck 1-28	NW NE NW	28	1072	9976	8944
11	Ward Petroleum	Secor 1-21	NW NE	28	1537	8600	NDE
12	Ward Petroleum	Lyons 1-30	NW NW NE	30	972	7905	NDE
R #	4N - 22E Operator	Well	Location	Section	K.B.	Total Depth	Top Spiro
13	Amoco	Talihina Unit 1-31	NW NW NE NW	5	781	15112	14656
R #	5N - 21E Operator	Well	Location	Section	K.B.	Total Depth	Top Spiro
14	Southland Royalty	Garner 1-2	NW EH CT	2	613	12964	12616
15	Mitchell Energy	Russel Albin 1	SW CT	3	626	13876	12940/13022
16	Pam American	J.A.Johnson Est. 1	NW EH EH	9	848	9686	NDE
17	Anadarko Petroleum	Alford A 1-15	SE NW CT	15	568	17470	10600
18	Ambassador Oil	G.W.Muncy - 1	NE SW CT	19	586	12187	10190
19	Bert Wheeler	H.T.Jennings-1	NW SE	19	579	9761	NDE
20	Ambassador Oil	Muse - 1	NW NW	22	559	11489	11194?
21	Arkla Expl.	Smith-English - 1	NE SW SW SW	25	736	10702	NDE??
22	Cities Services	Smith-English - 1	NW SE SE	36	811	14902	?????

R #	5N - 22E Operator	Well	Location	Section	K.B.	Total Depth	Top Spiro
23	Snee & Eberly	Caulfield - 1	SE NE NW	4	566	7250	NDE
24	Amoco Prod.	Blackjack Ridge 1-17	SW SW SW NE	8	1222	12987	12162
25	Amoco Prod.	Mings Unit - 1	SW NE SW SW	16	600	12644	12140
26	Mustang Fuel Corp	Borden 1-20	SE NW SW	20	592	11500	???
27	Mustang Fuel Corp	Borden 1-20	SE NW SW	20	592	11090	???
28	Amoco Prod.	Ingle - 1	NW SW NE SE	21	528	13490	11342/12344
R #	6N - 21E Operator	Well	Location	Section	K.B.	Total Depth	Top Spiro
29	Amoco Prod.	Gallagher - 2	SE NW NE NW	13	640	12150	11806
30	D-Pex Operationg	Coy - 1	NW SE NW	13	647	2000	NDE
31	Amoco Prod.	Gallagher - 3	NW EH EH EH	13	663	8150	NDE
32	Amoco Prod.	Gallagher - 4	NE SE NW	13	650	8120	NDE
33	Amoco Prod.	Gallagher WDW - 1	SW NE NW	13	624	2200	NDE
34	Amoco Prod.	Gallagher - 1	NW SE SH	13	634	12038	11951
35	Midwest Oil	Gallagher - 1	NW SE SH	13	617	12038	11870
36	Sun Exploration	Gallagher - 2	SW NH NH	14	631	12775	11974
37	ORYX Energy	Dallas James - 1	NW NE NE NE	14	707	1928	NDE
38	ORYX Energy	William Gallagher - 3	NW CT	14	697	7959	NDE
39	J.M.C. Exploration	Gallagher - 4	SE NW SW NW	14	621	7988????	NDE
40	ORYX Energy	WM Gallagher - 1	NE SW SE	14	665	12077	11938
41	Sun Oil Co.	WM Gallagher - 1	NW SW SE	14	665	12077	?????
42	Midwest Oil	Booth - 1	SE W NE	15	649	12228	12065
43	Amoco Prod.	Booth - 2	NW SE NW	15	654	12455	12050
44	Amoco Prod.	Booth unit - 2	NW SE NW	15	654	12455	12050
45	Amoco Prod.	Booth unit - 2	NW SE NW	15	654	12455	12050
46	Amoco Prod.	Booth unit - 3	NE CT	15	690	8010	NDE
47	Amoco Prod.	Booth unit - 4	SW CT	15	690	8100	NDE

R #	6N - 21E Operator	Well	Location	Section	K.B.	Total Depth	Top Spiro
48	Amoco Prod.	Circle Ranch - 1	SW SE NW	15	603	1850	NDE
49	Amoco Prod.	Booth unit - 5	NE EH EH	15	685	8020	NDE
50	Amoco Prod.	Brewer unit - 2	NW SE NW	16	664	12636	12636??
51	Amoco Prod.	Brewer - 3	NE WH EH	16	645	8128	NDE
52	Amoco Prod.	Brewer - 4	SW NE NW	16	620	8000	NDE
53	Midwest Oil	Brewer - 1	SE NE NW	16	644	12333	12083
54	Midwest Oil	Sentry Royalty - 1	SE NW NE	17	659	12600	????
55	Harry Zucker	Old Mack Coal	SE CT	17		6512	NDE
56	LeFlore County	Cutler - 1	SE NE NW	17		2673	NDE
57	Amoco Prod.	Sentry Royalty - 2	SW NE NW NW	17	680	12675	12480
58	Amoco Prod.	Sentry Royalty - 2	SW NE NW NW	17	680	12675	12480
59	Amoco Prod.	Sentry Royalty - 3	NW NW NE SW	17	699	9141	NDE
60	Amoco Prod.	Sentry Royalty - 4	NE CT	17	660	8137	NDE
61	Amoco Prod.	Sentry Royalty - 5	NW CT	17	683	7460	NDE
62	Amoco Prod.	White - 2	NW SE SW	18	690	???	???
63	Amoco Prod.	White - 3	NE SW NE NE	18	691	9130	NDE
64	Amoco Prod.	White - 4	NW EH WH	18	700	9171	NDE
65	Amoco Prod.	White - 5	NE SE NW	18	675	7500	NDE
66	Amoco Prod.	White - 6	NW EH EH	18	681	7645	NDE
67	Amoco Prod.	White - 1	SE NE SW	18	666	12940	12640
68	Midwest Oil	White - 1	SE NE SW	18	666	12940	12637
69	Humble Oil	Foster Jr - 1	NE NW SE	19	694	8450	NDE
70	Mustang Prod.	Foster Exxon 1 - 19	NE NW SE	19	696	12740	12640
71	Mustang Prod.	Gillespie 1 - 20	NW CT	20	699	8927	NDE
72	Mustang Prod.	Strother 1 - 20	SW SH CT	20	1539	13450	13252
73	Mustang Prod.	Gillespie 2 - 20	NW NW CT	20	677	12715	12453
74	Midwest Oil	Noah - 1	NW NE SE	21	626	12495	12300
75	Arco Oil & Gas	Noah - 2 - 21	SE NE SW	21	620	12460	12253
76	Amoco Prod.	Loui SE Noah - 1	NW SE EH	21	624	2050	NDE
77	Humble Oil	John Oxley - 1	NE NE SW	22	611	7913	NDE

R #	6N - 21E Operator	Well	Location	Section	K.B.	Total Depth	Top Spiro
78	Exxon Corp.	John Oxley - 2	NE SW SW	22	608	12877	12050
79	J.M.C. Exploration	Oxley - 3	NE NE SW	22	618	12306	12135
80	Amoco Prod.	Oxley - 4	NW NE EH	22	613	7850	NDE
81	Humble Oil	Erwin - 1	NE WH CT	23	605	12100	11967
82	Samson Resources	Opal - 1	NW SH NH NH	23	603	12134	12074
83	Pan American Petr.	Cecil - 1	NW EH WH	24	597	11950	11735
84	Arco Oil & Gas	Cecil - 2	NE NW SE	24	575	7500	NDE
85	Amoco Prod.	Cecil - 3	NW SE NW NW	24	600	7515	NDE
86	Amoco Prod.	Cecil - 4	NE SW NW	24	615	7678	NDE
87	Pan American Petr.	Knauer - 1	NW SW EH CT	25	902	13311	13127
88	Texas Oil & Gas	Gallagher - 1	NW NW CT	26	1000	12700	12488
89	Mustang Prod.	Lyons 1 - 27	SW SW NE	27	???	12300	12134/12234
90	Mustang Prod.	Smallwood 1 - 28	SW CT	28	628	12848	12181
91	Mustang Prod.	Noah 1 - 28	NW NW CT	28	770	13000	11607
92	Whitmar Expl.	Mary Corcoran 1- 29	NW NH	29	1540	14000	13214
93	Whitmar Expl.	Mary Corcoran 1- 29	NW NH	29	1540	14000	13214
94	Whitmar Expl.	Mccreery 1 - 30	NE EH WH	30	1670	14218	13392
95	Pan American Petr.	Melone - 1	SE NW NW	31	704	13362	12570
96	Cleary Petroleum	Cannon 1 - 33	NW SH SH	33	631	13131	????
97	Sarkeys Inc.	Thrift 1 - 33	NE WH WH	33	616	12421	12206
98	Mustang Prod.	Judd 1 - 35	SE NW SW	35	576	13265	13025/13052

R #	6N - 22E Operator	Well	Location	Section	K.B.	Total Depth	Top Spiro
99	Midwest Oil	Rider - 1	SE NW NW	17	560	12130	11943
100	Amoco Prod.	Rider - 2	NW SE NW	17	588	11852	11546
101	Amoco Prod.	Rider - 2	NW SE NW NW	17	588	11852	11546
102	Amoco Prod.	Rider - 3	NE NW SE SE	17	580	7967	NDE

R #	6N - 22E Operator	Well	Location	Section	K.B.	Total Depth	Top Spiro
103	Amoco Prod.	Rider - 4	SW NE NW	17	560	7100	NDE
104	Amoco Prod.	Rider - 5	NW SE NW	17	575	6177	NDE
105	Oryx Energy	Hulsey - 2	NW SW	18	613	12530	11723
106	Sun Expl & Prod.	Hulsey - 2	NW SW CT	18	613	12530	11722
107	Oryx Energy	Hulsey - 3	NE CT	18	617	7950	NDE
108	J.M.C. Expl.	Hulsey - 4	SW NE SW	18	609	7100	NDE
109	Oryx Energy	Hulsey - 1	SE NW NW	18	597	12453	11660
110	Sun Expl & Prod.	Husley - 1	SE NW NW	18	597	12451	11658
111	Amoco Prod.	Kent - 2	NE WH EH	19	1000	12508	12232
112	Amoco Prod.	Kent - 3	NE WH WH	19	633	7802	NDE
113	Pan American Petr.	Kent - 1	NW NE SH	19	585	12160	11956
114	Amoco Prod.	Kent - 1	NW NE SH	19	585	12160	11956
115	Pan American Petr.	Martin C - 1	NW NE SE	20	615	12500	12297
116	Amoco Prod.	Martin C - 1	NW NE SE	20	613	12500	12295
117	A & A Tank Truck	Martin C - 2	NE CT	20	600	2600	NDE
118	Amoco Prod.	Martin C - 2	NE CT	20	591	2600	NDE
119	Amoco Prod.	Martin C - 4	NE NE SW	20	583	7809	NDE
120	Amoco Prod.	Martin C - 3	NW NW SE	20	600	7850	NDE
121	Dyco Petroleum	Steele - 1	NW CT	29	823	12786	12718
122	Amoco Prod.	O.P.Brewer - 1	SW NE SE	29	780	12600	12220
123	Chaparral Energy	Brewer 1 - 29	SW NE SE	29	764	5655	NDE
124	Mustang Prod.	Fields 1 -31	NW SH SH	31	661	12353	12266/12303

Plates I, II, III, IV, and V.

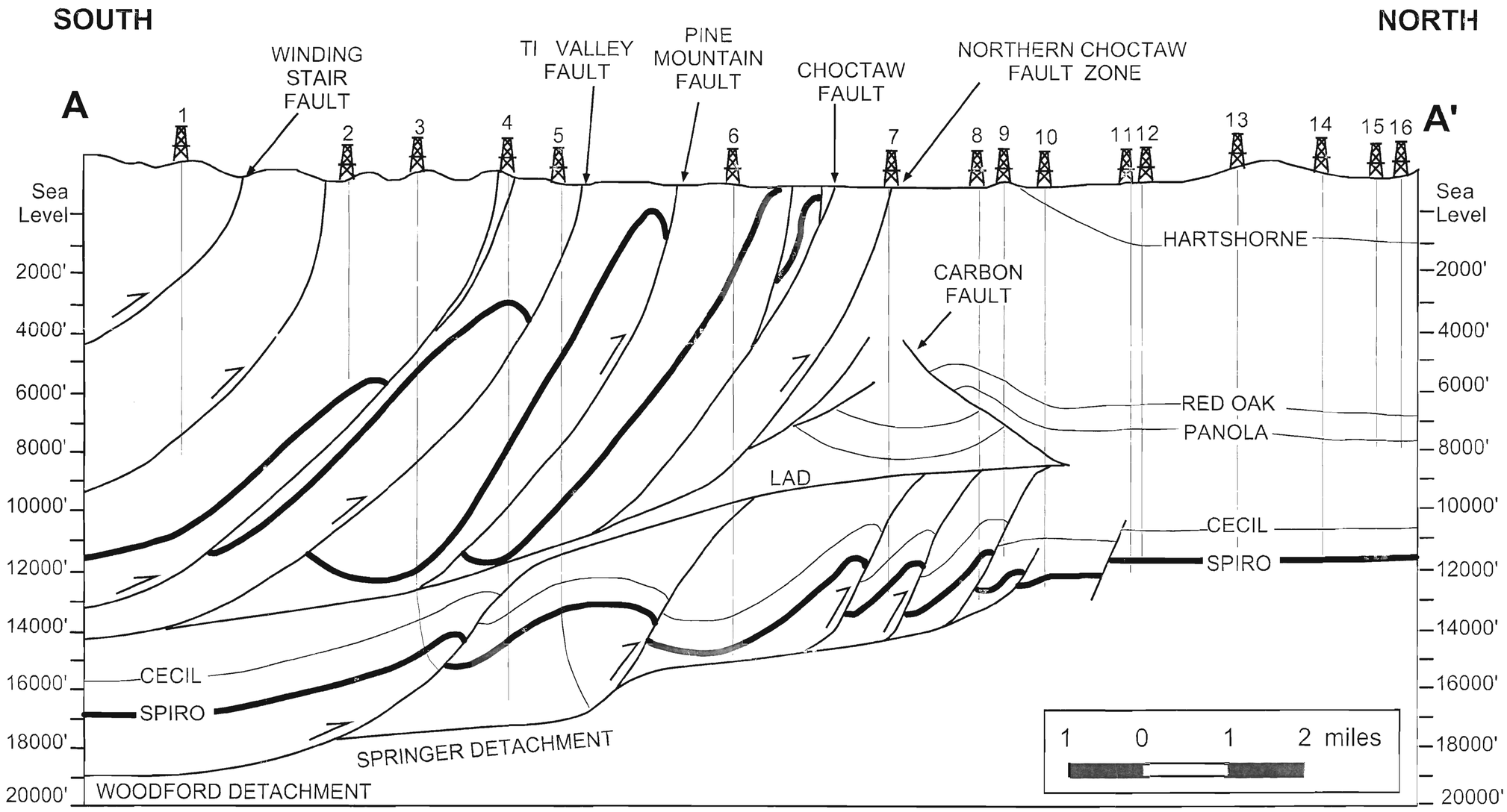

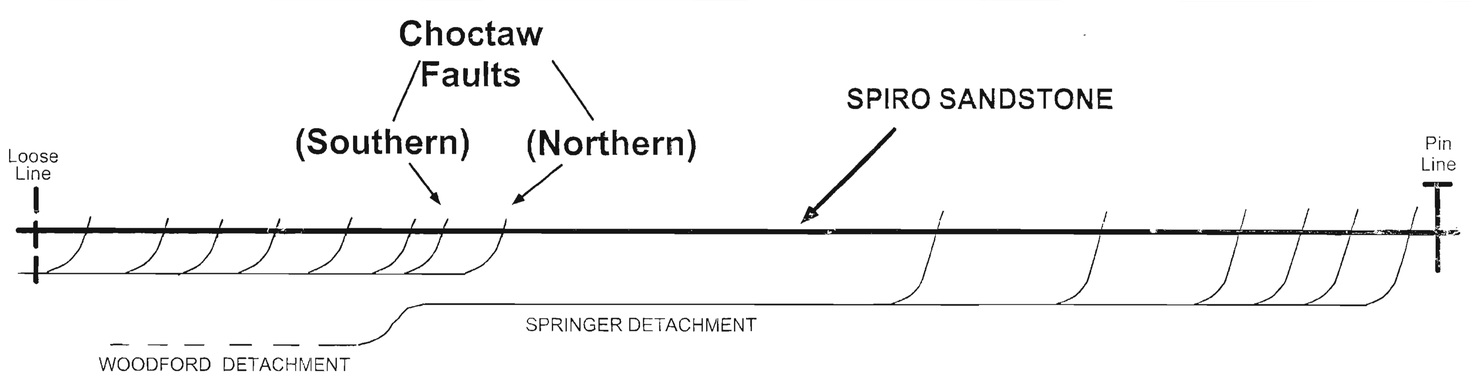

Lf = 12.6 miles
Lo = 33.2 miles
dL = Lf - Lo = 20.6
e = -dL / Lo = 0. 62
e = 62 %

0 4 (MILES)

SOUTH - NORTH

BALANCED AND RESTORED

CROSS SECTION A - A '

Arkoma Basin Plate I

Syed Y Mehdi M.S. 1998

SOUTH

B

NORTH

B'

WINDING STAIR FAULT

TI VALLEY FAULT

PINE MOUNTAIN FAULT

MAIN CHOCTAW FAULT

NORTHERN CHOCTAW FAULT ZONE

1 2 3 4 5 6 7 8 9 10 11 12 13 14 15 16 17 18 19

Sea Level

2000'

4000'

6000'

8000'

10000'

12000'

14000'

16000'

18000'

20000'

HARTSHORNE

CARBON FAULT

RED OAK

PANOLA

LOWER ATOKAN DETACHMENT

Loose Line

Pin Line

CECIL

SPIRO

SPRINGER DETACHMENT

WOODFORD DETACHMENT

1 0 1 2 miles

Choctaw Faults

(Southern) (Northern)

SPIRO SANDSTONE

Loose Line

Pin Line

SPRINGER DETACHMENT

WOODFORD DETACHMENT

Lf = 12.9 miles

Lo = 33.0 miles

dL = Lf - Lo = 20.1

e = -dL / Lo = 0. 61

e = 61 %

0 4 (MILES)

SOUTH - NORTH

BALANCED AND RESTORED

CROSS SECTION B - B '

Arkoma Basin Plate II

Syed Y Mehdi M.S. 1998

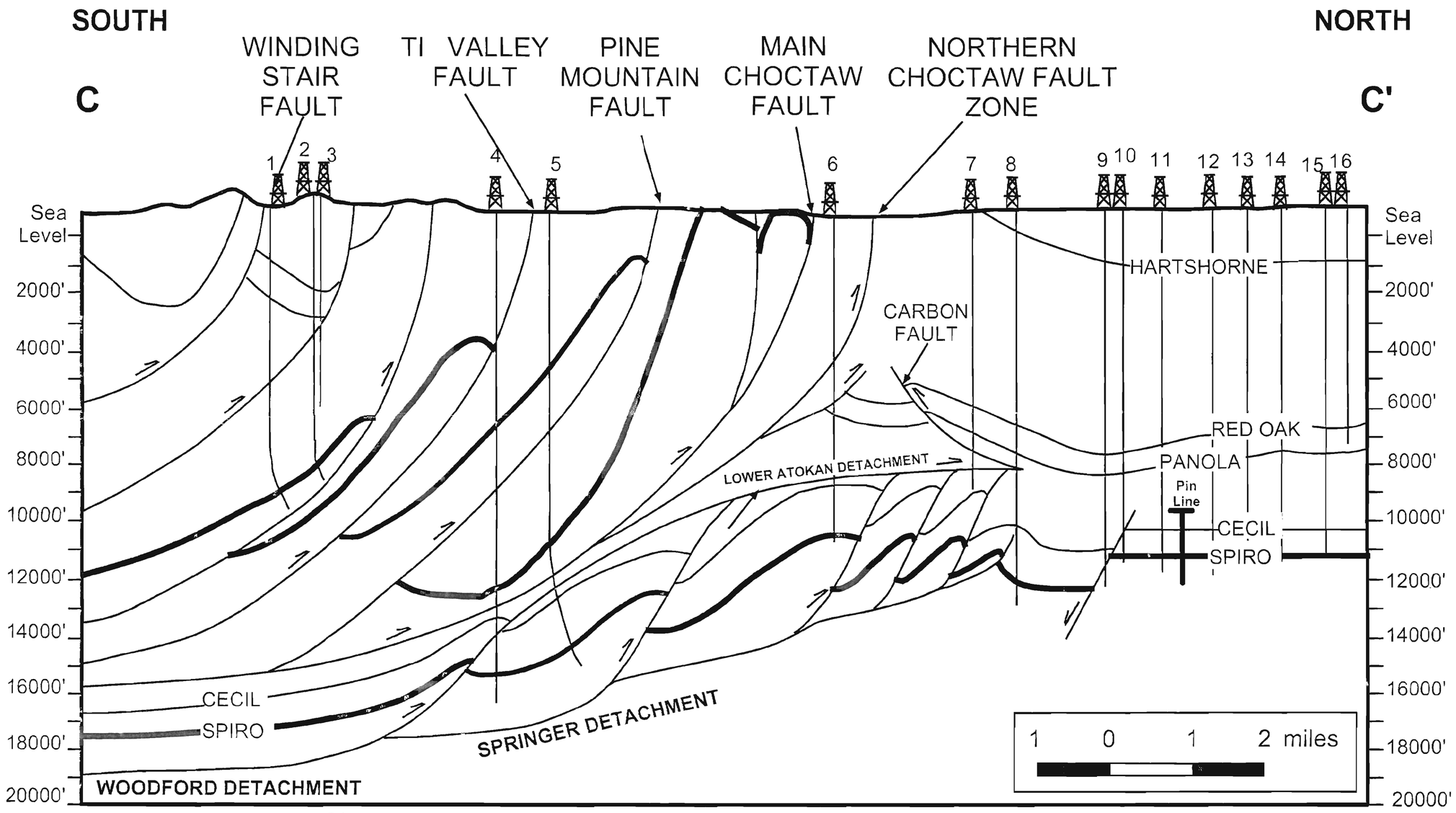

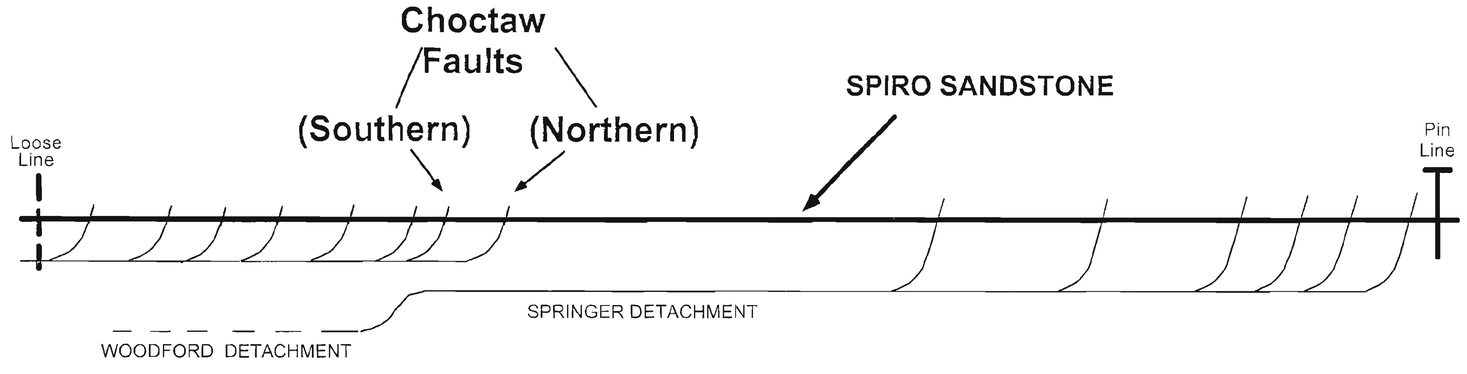

Lf = 12.7 miles
Lo = 32.8 miles
dL = Lf - Lo = 20.1
e = -dL / Lo = 0. 61
e = 61 %

0 4 (MILES)

SOUTH - NORTH

BALANCED AND RESTORED

CROSS SECTION C - C '

Arkoma Basin	Plate III
Syed Y Mehdi	M.S. 1998

SOUTH

NORTH

D

D'

WINDING STAIR FAULT

TI VALLEY FAULT

PINE MOUNTAIN FAULT

CHOCTAW FAULT

NORTHERN CHOCTAW FAULT ZONE

1 2 3 4 5 6 7 8 9 10 11

Sea Level

2000'

4000'

6000'

8000'

10000'

12000'

14000'

16000'

18000'

20000'

Loose Line

CARBON FAULT

HARTSHORNE

RED OAK

PANOLA

LAD

Pin Line

CECIL

SPIRO

WOODFORD DETACHMENT

SPRINGER DETACHMENT

1 0 1 2 miles

Choctaw Faults

(Southern) (Northern)

SPIRO SANDSTONE

Loose Line

Pin Line

SPRINGER DETACHMENT

WOODFORD DETACHMENT

Lf = 12.6 miles
Lo = 32.6 miles
dL = Lf - Lo = 20.0
e = -dL / Lo = 0. 613
e = 61 %

0 4 (MILES)

SOUTH - NORTH

BALANCED AND RESTORED

CROSS SECTION D - D '

Arkoma Basin Plate IV

Syed Y Mehdi M.S. 1998

SOUTH

NORTH

E

E'

WINDING STAIR FAULT

TI VALLEY FAULT

PINE MOUNTAIN FAULT

MAIN CHOCTAW FAULT

NORTHERN CHOCTAW FAULT ZONE

1 2 3 4 5 6 7 8 9 10 11

Sea Level

2000'

4000'

6000'

8000'

10000'

12000'

14000'

16000'

18000'

20000'

HARTSHORNE

CARBON FAULT

LAD

RED OAK

PANOLA

CECIL

SPIRO

SPRINGER DETACHMENT

WOODFORD DETACHMENT

1 0 1 2 miles

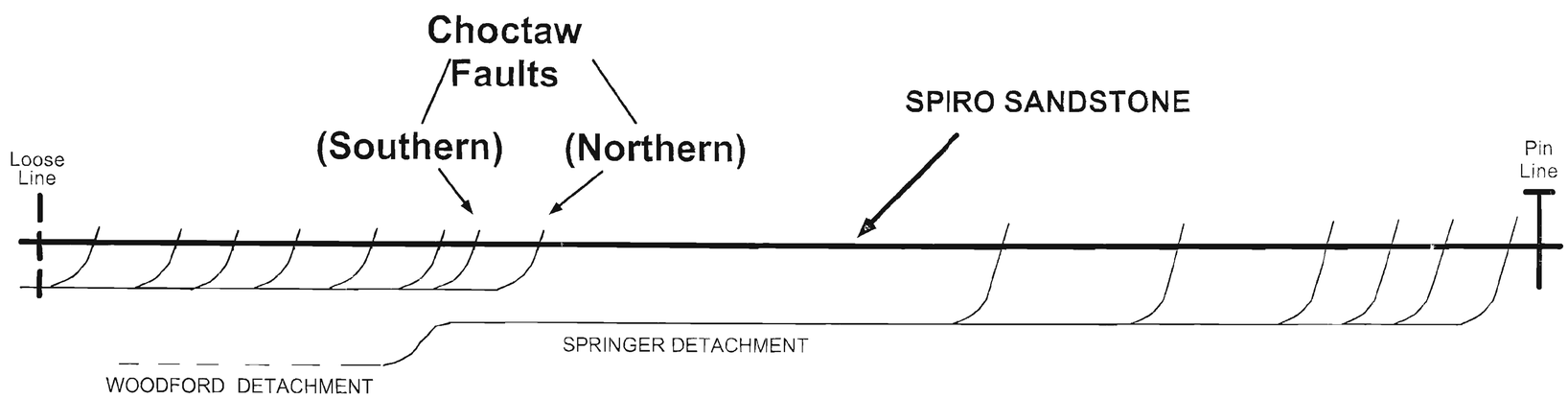

Lf = 12.4 miles
Lo = 31.6 miles
dL = Lf - Lo = 19.2
e = -dL / Lo = 0. 60
e = 61 %

0 4 (MILES)

SOUTH - NORTH

BALANCED AND RESTORED

CROSS SECTION E - E '

Arkoma Basin Plate V

Syed Y Mehdi M.S. 1998

VITA

Syed Yawar Mehdi

Candidate for the Degree of

Master of Science

Thesis: STRUCTURAL GEOMETRY OF THRUST SYSTEMS IN THE RED OAK AND TALIHINA QUADRANGLES, LATIMER AND LEFLORE COUNTIES, ARKOMA BASIN, SOUTHEASTERN OKLAHOMA

Major Field: Geology

Geographical:

Personal Data: Born in Karachi, Pakistan, August 03, 1967, the son of Syed Saeed Akhtar Payami and Razia Bano.

Education : Received Bachelor of Science in Geology from University of Karachi, Pakistan in 1989; received Master of Sceince degree in Geology from University of Karachi, Pakistan in 1991. Completed the requirements for the Master of Science degree at Oklahoma State University in May 1998, with a major in Geology.

Professional Experience: Research and Teaching Assistant, School of Geology, Oklahoma State University, January 1996 to present; Junior Geologist, Geological Survey of Pakistan, February 1993 to October 1994; Seismologist, Seismograph Service Limited (SSL), April 1991 to January 1993.

Professional Memberships: Member American Association of Petroleum Geologists, Member Geological Society of America, Member Oklahoma Geological Survey, Member Oklahoma City Geological Society.